LUND UNIVERSITY

Cryogels as Solid Supports in Bioprocessing

Jespersen, Gry

2014

Cryogels as solid supports in bioprocessing

Gry Ravn Jespersen

LUNDS UNIVERSITET

DOCTORAL DISSERTATION
March 2014

Academic dissertation which, by due permission of the Faculty of Engineering, Lund University, Sweden, will be defended on Friday 21st of March, 2014 at 1.30 p.m. in lecture hall B at the Centre of Chemistry and Chemical Engineering, Sölvegatan 39, Lund, for the degree of Doctor of Philosophy in Engineering.

Faculty opponent

Professor James M. Van Alstine, General Electric Healthcare, Uppsala, Sweden

Organization	Document name
LUND UNIVERSITY Faculty of Engineering, Department of Chemistry, Division of Biotechnology	DOCTORAL THESIS
	Date of issue 25 March 2014
Author(s)	Sponsoring organizations
Gry Ravn Jespersen	The Danish Agency for Science, Research and Innovation. Novo Nordisk A/S.

Title and subtitle: Cryogels as solid supports in bioprocessing

Abstract

In recent years the market for biopharmaceutical products has been increasing rapidly as a result of an increased demand for new and efficient treatments of various indications. Biopharmaceuticals are distinguished from chemical drugs by being derived from a biological origin and are hence, frequently constituting biological macromolecules. With the emergence of recombinant DNA technology, today most biopharmaceutical products are produced in recombinant cell lines, an advance which has led to the development of some of today's most important therapeutics such as insulins, human growth factors and monoclonal antibodies.

Industrial downstream bioprocessing is concerned with the isolation and purification of biopharmaceutical products, ensuring a high purity and quality of the manufactured product. As recombinant cell technology has enabled vast increases in production efficiencies, this has put pressure on downstream processes to keep up with this pace. Hence, industrial downstream bioprocessing faces two major challenges. Firstly, an increased demand for method improvements which can contribute to decreasing processing time and –cost. Secondly, an increasingly strict government regulation for equipment sanitation is challenging the current re-use of materials, which has prompted the industry's interest in the use of disposables.

Cryogels is a type of porous materials, which frequently constitute biocompatible solids cast in a one-block format. Characteristic to cryogels is their extremely open porous structure which allow for unhindered passage of viscous fluids or even whole cells, and due to this feature these materials have been considered as solid supports in downstream bioprocessing. Cryogels are potentially in-expensive materials, which can be easily prepared under environmentally friendly conditions and on this basis they have been considered suitable as disposable materials.

This dissertation concerns studies on cryogels utilized as solid supports in various downstream bioprocessing applications. One study focuses on the application of a cryogel as a solid support for the fast, qualitative analysis of an antibody. The use of a cryogel in this context enables easy preparation of a customized solid support, which can be used for specific detection of antibody in a cell harvest. In another study it is demonstrated that a cryogel can be used as a solid phase agent for the chemical modification of a biopharmaceutical. In this connection the use of a cryogel constitutes a process improvement in terms of being a cost-efficient, high capacity material which could be implemented into an existing process. Chemical modification of biopharmaceuticals can also be performed by enzymes and in yet another study an enzyme was immobilized on a cryogel for the purpose of modifying an antibody. The advantage of having the enzyme immobilized on a solid support is avoiding the subsequent removal of enzyme from the product as well as the potential reusability of the enzyme.

Cryogels constitute a type for solid supports that are very versatile, which is reflected by the vast amount of literature on their many different applications within downstream processing. The studies presented in this dissertation demonstrate some new applications of cryogels and emphasize the need for a further systematic work approach on developing cryogels towards taking on their own niche as biocompatible, disposable materials in downstream bioprocessing.

Key words: Downstream processing; cryogel; solid support; biomacromolecules; chromatography

Classification system and/or index terms (if any)

Supplementary bibliographical information	Language English
ISSN and key title	ISBN 978-91-7422-346-0
Recipient's notes	Number of pages 136 / Security classification / Price

Signature Gry Ravn Jespersen Date 5/2 - 2014

Cryogels as solid supports in bioprocessing

Gry Ravn Jespersen
Division of Biotechnology
Department of Chemistry
Faculty of Engineering
Lund University
2014

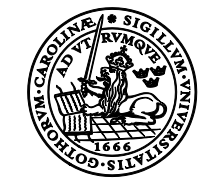

LUNDS UNIVERSITET

Cover photo by Torben Strøm

Faculty of Engineering, Department of Chemistry, Division of Biotechnology
ISBN 978-91-7422-346-0

Printed in Sweden by Media-Tryck, Lund University, Lund 2014

Popular summary

Biopharmaceuticals are modern medicines designed to treat a wide variety of diseases and chronic conditions, such as cancers or diabetes. Most frequently such biopharmaceuticals are proteins that are produced in genetically engineered cell lines. On an industrial scale these cells are cultivated in tanks, which can contain very large volumes of culture liquid.

Many biopharmaceutical drugs are administered to humans by direct injection into tissue or the bloodstream. It is therefore extremely important that the drug is pure and free from contaminants which can give rise to potentially dangerous side effects. Following its production, the biopharmaceutical must therefore be isolated in its pure form, which means that it should be separated from cells and other constituents of the cell culture which produced it.

Biopharmaceuticals are under strict governmental regulation making comprehensive requirements to procedures and documentation with regard to drug purity. Due to this, currently the major cost drivers of biopharmaceutical productions are the processes related to isolation and purification of the products. In order to meet the market demands for new and cost efficient treatments, the biopharmaceutical industry is focusing on developing new technologies for product purification, which can reduce the production time and expense.

Solid materials are commonly used in the purification of proteins – remember that biopharmaceuticals are often proteins. One method of choice within industrial scale purifications is termed *liquid chromatography*. This method is based on the selective binding of the target protein on a solid material. Most often the solid material comprises small bead-shaped particles, which are filled into a cylindrical column. Then the culture liquid of the cell production can be pumped through the column and the solid material will selectively bind the target protein, letting all other constituents pass through.

Liquid column chromatography is a very efficient method for purification of proteins. However, one major limitation is that if particulate matter is not removed from the culture liquid, the column will clog and liquid chromatography cannot be

performed. Therefore, the use of liquid chromatography with a traditional bead-shaped solid material requires preceding purification steps to clarify the culture liquid.

To try and overcome such limitations, a new type of solid materials for liquid chromatography is emerging. Instead of being bead-shaped these materials have the form of one, continuous cylinder – in other words, they fill the chromatography column as one large, single piece of material. These materials are called *cryogels*, and they are defined by containing a network of extremely large, interconnected pores. When cell culture liquid is applied at the top of a cryogel-filled column it will flow through the cryogel by passing through these pores. The pores are large enough for particulate matter to pass unhindered and therefore for protein purification the culture liquid does not have to be clarified prior to application to the cryogel. In this sense, using a cryogel will circumvent preceding, otherwise required purification steps. Other attractive features of cryogels are that they are cheap materials, which can be prepared under environmentally friendly conditions - and therefore could be considered as disposable materials.

The research presented in this dissertation focuses on the use of cryogels as materials in different applications related to the purification of biopharmaceuticals. In one study a cryogel was used as a solid material in liquid chromatography and it was shown that a target protein could be purified from a complex mixture of biological constituents. Compared to the traditional process, the use of a cryogel for this application permitted the circumvention of several preceding preparation steps. Three other research studies presented demonstrate other examples of the use of cryogels in processes related to protein drug purification.

The selection of a solid material for protein purification processes is to a large extent done case-by-case. In this respect cryogels make up a type of solid materials which in some cases can be considered as attractive alternatives to the existing, commercial materials. However, cryogels also have certain drawbacks and therefore before these interesting materials can be successfully implemented in industrial scale purification processes they must be further developed.

Abstract

In recent years the market for biopharmaceutical products has been increasing rapidly as a result of an increased demand for new and efficient treatments of various indications. Biopharmaceuticals are distinguished from chemical drugs by being derived from a biological origin and are hence, frequently constituting biological macromolecules. With the emergence of recombinant DNA technology, today most biopharmaceutical products are produced in recombinant cell lines, an advance which has led to the development of some of today's most important therapeutics such as insulins, erythropoietins and monoclonal antibodies.

Industrial downstream bioprocessing is concerned with the isolation and purification of biopharmaceutical products, ensuring a high purity and quality of the manufactured product. As recombinant cell technology has enabled vast increases in production efficiencies, this has put pressure on downstream processes to keep up with this pace. Hence, industrial downstream bioprocessing faces two major challenges. Firstly, an increased demand for method improvements which can contribute to decreasing processing time and –cost. Secondly, an increasingly strict government regulation for equipment sanitation is challenging the current re-use of materials, which has prompted the industry's interest in the use of disposables.

Cryogels is a type of porous materials, which frequently constitute biocompatible solids cast in a one-block format. Characteristic to cryogels is their extremely open porous structure which allow for unhindered passage of viscous fluids or even whole cells, and due to this feature these materials have been considered as solid supports in downstream bioprocessing. Cryogels are potentially in-expensive materials, which can be easily prepared under environmentally friendly conditions and on this basis they have been considered suitable as disposable materials.

This dissertation concerns studies on cryogels utilized as solid supports in various downstream bioprocessing applications. One study focuses on the application of a cryogel as a solid support for the fast, qualitative analysis of an antibody. The use of a cryogel in this context enables easy preparation of a customized solid support,

which can be used for specific detection of antibody in a cell harvest. In another study it is demonstrated that a cryogel can be used as a solid phase agent for the chemical modification of a biopharmaceutical. In this connection the use of a cryogel constitutes a process improvement in terms of being a cost-efficient, high capacity material which could be implemented into an existing process. Chemical modification of biopharmaceuticals can also be performed by enzymes and in yet another study an enzyme was immobilized on a cryogel for the purpose of modifying an antibody. The advantage of having the enzyme immobilized on a solid support is avoiding the subsequent removal of enzyme from the product as well as the potential reusability of the enzyme.

Cryogels constitute a type for solid supports that are very versatile, which is reflected by the vast amount of literature on their many different applications within downstream processing. The studies presented in this dissertation demonstrate some new applications of cryogels and emphasize the need for a further systematic work approach on developing cryogels towards taking on their own niche as biocompatible, disposable materials in downstream bioprocessing.

List of papers

I. Jespersen, G.R., Nielsen, A.L., Matthiesen, F., Andersen H.S., Kirsebom H. (2013) Dual application of cryogel as solid support in peptide synthesis and subsequent protein capture, Journal of Applied Polymer Science, 130 (6), 4383-4391.

II. Jespersen, G.R., Matthiesen, F., Pedersen, A.K., Andersen, H.S., Kirsebom, H., Nielsen, A.L. (2014) A thiol functionalized cryogel as a solid phase for selective reduction of a cysteine residue in a recombinant human growth hormone variant, Journal of Biotechnology, 173, 76-85.

III. Jespersen, G.R., Yun, J., Matthiesen, F., Nielsen, A.L., Andersen, H.S., Kirsebom, H. Evaluation of a new poly(ether amine) cryogel as solid support for immobilized enzyme applications. (Manuscript)

IV. Yun, J., Jespersen, G.R., Kirsebom, H., Gustavsson, P-E., Mattiasson, B., Galaev, I.Y. (2011) An improved capillary model for describing the microstructure characteristics, fluid hydrodynamics and breakthrough performance of proteins in cryogel beds. Journal of Chromatography A, 1218 (32), 5487-5497.

My contribution to the papers

I. I performed all the experimental work, participated in planning of the work in cooperation with the other authors and I wrote the first draft of the paper.

II. I performed all the experimental work, except the RP-HPLC analyses, participated in the planning of the work in cooperation with the other authors and wrote the first draft of the paper.

III. I performed all the experimental work, participated in the planning of the work in cooperation with the other authors and wrote the first draft of the manuscript.

IV. I participated in the experimental work concerning cryogel preparation and characterization as well as chromatographic testing with regard to lysozyme. I participated in writing the experimental part in the manuscript concerning my work and I revised and commented on the full manuscript.

Abbreviations

CIP	Cleaning in place
SEC	Size exclusion chromatograpy
AffC	Affinity chromatography
IMAC	Immobilized metal affinity chromatography
IDA	Iminodiacetic acid
IEX	Ion exchange chromatography
HIC	Hydrophobic interaction chromatography
RPC	Reversed phase chromatography
HCP	Host cell proteins
APS	Ammonium persulfate
TEMED	*N,N,N',N'*-tetramethylethylenediamine
AAm	Acrylamide
DMAAm	Dimethylacrylamide
HEMA	2-Hydroxyethyl methacrylate
AGE	Allyl glycidyl ether
MBAAm	Methylenebiacrylamide
PEGDA	Poly(ethylene glycol) diacrylate
PVA	Poly(vinyl alcohol)
SEM	Scanning electron microscopy
ESEM	Environmetal scanning electron microscopy
CLSM	Confocal laser scanning microscopy
HETP	Height equivalent to a theoretical plate
RTD	Residence time distribution
IgG	Immunoglobulin G
ConA	Concanavalin A

Contents

1. Introduction

1.1 Downstream processing of pharmaceutical biotechnology products

In recent years the market for biopharmaceutical products has been growing rapidly as a result of an increased demand for new and efficient treatments of various indications[1]. Biopharmaceuticals are distinguished from chemical drugs by being derived from a biological origin and are most often macromolecules such as proteins or viruses. Originally, biopharmaceuticals were isolated directly from their natural source, being humans or animals. However with the emergence of recombinant DNA technology, today most biopharmaceutical products are produced in recombinant cell lines. Recombinant DNA technology is one of recent time's most important biotechnology advances as it has led to the development of some of the most important therapeutics such as insulins for treatment of diabetes[2], monoclonal antibodies[3] for treatment of cancers and autoimmune diseases and erythropoietins[4] to stimulate production of red blood cells.

The first step in producing a recombinant therapeutic protein is the identification of the genetic code of that particular protein. Then the DNA sequence is isolated in its functional form by the assembly of individual DNA segments, which is followed by replication. The DNA segment, coding for the protein, is then introduced into a cell host, which translates it into the production of the protein, often in large quantities[5]. Subsequent to its production in a recombinant cell line, the biopharmaceutical is harvested and subjected to multiple purification steps including virus inactivation and formulation[6]. Hence, the manufacturing process for the production of a biopharmaceutical product consists of several unit operations, which can be divided into processes related to the production (upstream processing) and the purification (downstream processing) of the product (Figure 1.1).

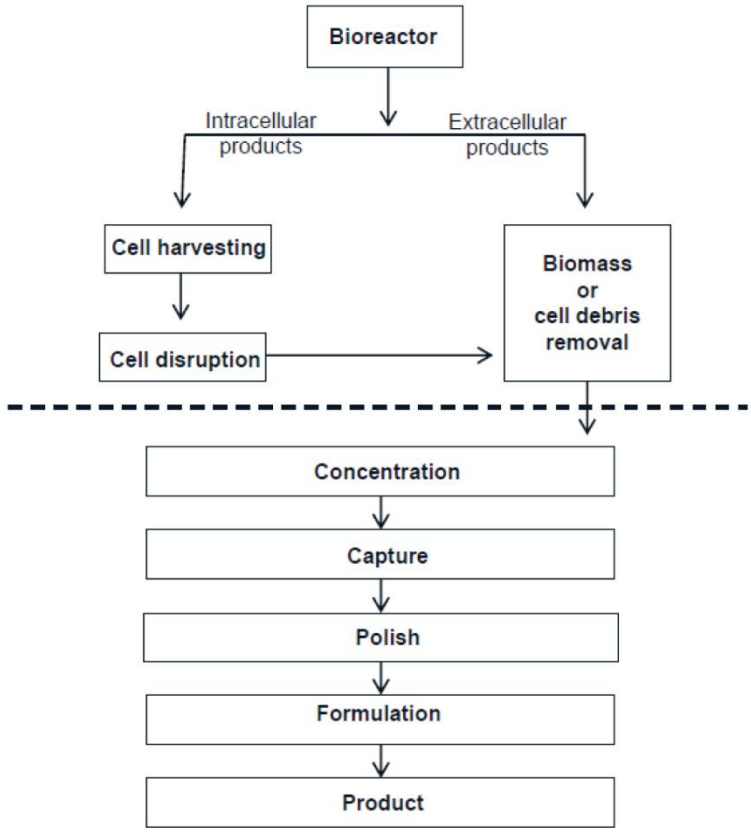

Figure 1.1: Overview of unit operations involved in the manufacturing of a biopharmaceutical product. Unit operations placed above the stippled line are related to upstream manufacture processes and unit operations placed below the dashed line are related to downstream processes.

Recent years' advances in upstream processes have led to improvements in cell culture productivity and hence, downstream processing has in many cases turned into a bottleneck in terms of increasing production volume[6]. This development has prompted the industry to focus on downstream technology improvements in terms of high throughput process development and decreasing the number of unit operations, with the gain of increased productivity[7]. Another issue is the increasingly strict government quality- and documentation regulation of biopharmaceutical manufacturing, which requires comprehensive cleaning in place (CIP) procedures of production equipment. Such demands have led to an increased awareness of the advantages of using disposable materials in downstream processing[8].

Liquid chromatography is regarded as the workhorse of industrial downstream purification, providing a set of highly effective methods for isolating and purifying biomacromolecules[9]. In traditional chromatography a cylindrical column is packed with beaded, porous particles constituting a stationary phase. Due to different physical or chemical interaction principles the target biomacromolecule is retained on the solid support, whilst various contaminants are eluted from the column[6]. However, despite their high resolution power and binding capacities, traditional beaded stationary phases are challenged in terms of productivity. In this respect productivity can be defined as amount of product processed per unit time and per unit volume of stationary phase[10]. At high flow rates packed bed columns are exposed to devastatingly high back pressures and resolution and capacity are seriously impeded by insufficient mass transfer due to diffusional limitations[6, 11].

Monoliths are continuous stationary phases cast as one-block porous materials, as opposed to the porous beads constituting conventional stationary phases[12]. In the 1990's commercial methacrylate monoliths were introduced as a new solid support format for downstream bioprocessing applications[13]. One primary characteristic of monoliths is that their relatively large pores provide mass transport by means of convection, rendering high selectivity and dynamic binding capacities, which are virtually independent of flow rate[14]. Hence, monoliths are beginning to find their place in downstream bioprocessing as alternative stationary phases in analytical as well as preparative applications, offering improved process productivity[15, 16].

Cryogels constitute a special class of monoliths, comprising of polymeric, hydrophilic gels characterized by a distinct and extremely open porous structure consisting of supermacropores[17]. According to the IUPAC classification, pore sizes are divided into pores with diameters $d_{micro} < 2$ nm $< d_{meso} < 50$ nm $< d_{macro}$ μm, corresponding to micro-, meso- and macropores, respectively[18]. In the following discussion, pores with diameters larger than 1 μm will be referred to as supermacropores.

The unique pore morphology of cryogels is derived from their preparation, which proceeds under solvent freezing conditions, where the crystalized solvent serves as porogen in the forming polymer[17]. The cryogels' internal network of interconnected supermacropores (10-200 μm) conveys mass transport by convection and allows for the unhindered passage of viscous fluids containing cell debris or even whole cells[19, 20]. These are features which are appealing in terms of minimizing process time and decreasing the number of unit operations. Furthermore, cryogels can be prepared from inexpensive monomeric precursors

under environmentally friendly conditions, which make them suitable as candidates for future disposable materials in downstream bioprocessing applications. On this background, cryogels have been studied as solid supports in a variety of biotechnological applications spanning from solid supports in downstream bioprocessing[21-23] over bioreactor applications[24-26] and tissue engineering[27, 28].

1.2 Aim and objectives

The aim of the research described in this Ph.D. dissertation was to investigate cryogels as solid supports in different bioprocessing applications as well as discuss the potential role of these matrices in downstream bioprocessing. The research was carried out as an industrial Ph.D. project at the Chemical Centre, Lund University and at Novo Nordisk A/S and therefore emphasis has been on bioprocessing applications with potential industrial relevance.

In **paper I**, a cryogel was prepared for the combined application as a solid phase for direct synthesis of a peptide affinity ligand and as a stationary phase for the affinity capture of an antibody. The concept of utilizing the same solid support in two consecutive applications represents a solution to reduce the time and cost related to the process of producing the column. It was shown that the cryogel was capable in selectively capturing antibody from a complex mixture at a high flow velocity offering the possibility of using such a cryogel for customized analytical applications.

In **paper II** a cryogel was prepared with a thiol functionalized surface for the selective reduction of a cysteine residue in a recombinant human growth hormone variant. This method turned out to be the basis for a patent application on the novel use of a cryogel as a solid phase reducing agent. The use of a cryogel in this context offered mild reducing conditions as well as an economic alternative to the existing process. Furthermore, the cryogel offered the possibility of performing the reduction as a column step, enabling easy integration with consecutive downstream processing operations.

Paper III deals with the preparation and characterization of a poly(ether amine) cryogel with immobilized enzyme for biocatalysis applications. As a model enzyme papain was chosen because of its use in the preparation of Fab fragments by selective proteolytic cleavage of antibodies. The concept of using an enzyme

immobilized on a cryogel offers the advantage of avoiding the subsequent removal of enzyme as well as being a cost-efficient, reusable biocatalyst.

Paper IV demonstrates the use of a mathematical model to describe the porous structure and flow properties of a cryogel. The use of mathematical models in predicting chromatographic performance constitutes a valuable tool in the planning of downstream purification processes, with regard to choice of chromatographic media for different applications.

The papers presented in this Ph.D. dissertation demonstrate that cryogels are a versatile class of materials, which can be customized to fit very different bioprocessing applications. In the following sections, selected literature on cryogels and their applications will be reviewed and discussed with respect to their potential role as solid supports in industrial downstream processing of biotechnology products.

2. Solid supports in downstream bioprocessing

Industrial downstream bioprocessing mainly involves recovery and purification of biopharmaceutical molecules, vaccines or other biologics – but it also includes product modifications in terms of chemical modifications. With regard to separation of biomolecules, chromatography is regarded a powerful separation technique, which is based on solid phase extraction of a product or an impurity from a liquid phase. Hence, solid supports are frequently employed for the separation of biomolecules utilizing a variety of different interaction principles, depending on the product and solution characteristics. This chapter provides an insight into the characteristics of target molecules, the principles of common target-solid phase interactions, as well as a discussion of solid supports available for bioprocessing.

2.1 Biomolecules, their chemistry and structure

Proteins

Proteins constitute a large group of biopolymers, which represents great variation within size and structure. Generally, proteins are complex macromolecules characterized by having a primary, secondary, tertiary and, in some cases, quaternary structural organization. There are 20 naturally occurring amino acids which comprise the initial building blocks of proteins and are linked together by peptide bonds. Each amino acid has its own chemical characteristics, however at physiological pH they can be grouped as either hydrophobic, polar uncharged, acidic or basic in their chemical nature[29]. The primary structure of a protein is defined by the amino acid composition of the peptide chain, whereas the secondary structure comprise the spatial organization of the peptide chain into well-defined structures of α-helices, β-sheets and loops. The secondary structure is stabilized by intramolecular hydrogen bonds of the peptide chain backbone. The three-dimensional arrangement of the tertiary structure involves bringing together

elements of the secondary structure and it is stabilized primarily by hydrophobic interactions and disulfide bridges, hence at this structural level distant parts of the primary structure are brought together. The quaternary structure of a protein involves the bonding of individual peptide chains into a super-structure, thus consisting of up to several polypeptide sub-units. The quaternary structure can be stabilized by hydrophobic interactions, hydrogen bonding or disulfide bridges and maintaining integrity at this structural level is often essential for the protein's biological function[29].

Many proteins may be post-translationally modified, meaning that certain amino acid residues in the polypeptide chain are chemically altered either by addition or elimination of chemical or molecular entities. Such post-translational modifications are highly dependent on the production cell line and the condition of the cells during upstream production steps. Due to this, pharmaceutical proteins often have a high degree of heterogeneity resulting in a collection of isoforms with potentially varying biological and chemical characteristics[10].

Polynucleotides

DNA and RNA are polynucleotides, which encode and transmit the genetic information of cells. The building blocks of these elongated macromolecules are nucleotides, which contain a phosphate group, a sugar group and a nitrogenous nucleoside group. DNA, which attains a double stranded, helical structure, contains four different nucleotides each differing in their nucleoside base. RNA is single stranded and is built from the same three nucleotides as DNA, but differs with regard to the fourth. Due to the phosphate groups, DNA and RNA are hydrophilic and carry a strong negative charge[29]. Different forms of DNA and RNA occur in very different sizes and physical forms and can therefore be separated individually and from other cellular constituents by size. From a biopharmaceutical point of view, polynucleotides can be either contaminants or constitute the product, e.g. both plasmid DNA and virus RNA for gene therapy and vaccines are products, which must be isolated and purified. Chromatography is the preferred technology for polynucleotide purification and in this respect a combination of separation by size and molecular charge is often effective[30]. Conversely, in the manufacture of pharmaceutical proteins, the polynucleotides constitute contaminants which must be removed.

Endotoxins

Bacterial endotoxins are macromolecules produced by gram negative bacteria, such as *E. coli*, in which they constitute an integral part of the outer membrane. These macromolecules are extremely toxic to humans and must be removed from biopharmaceutical products[31]. Endotoxins are lipopolysaccharides composed of three distinct chemical moieties, namely a hydrophobic lipid moiety, an oligosaccharide core region and a heterosaccharide region. Due to a partial phosphorylation of the core region, endotoxins attain a net negative charge at neutral pH. The molar mass of individual molecules ranges between 10 and 20 kDa, however due to their amphipathic nature endotoxins tend to form micelles or even vesicles with high molecular masses and diameters up to 0.1 μm[32]. Depending on the biopharmaceutical product being purified, endotoxin levels may be reduced by any purification step or alternatively they can be specifically removed by negative chromatography, capturing endotoxins due to solid support interactions. Most often endotoxins can be separated from the product based on size difference or molecular net charge[31]

2.2 Target-solid support interactions

Chromatographic separations encompass a number of different macromolecule-solid phase interactions, of which the most common are described in this section.

Steric interaction

Size exclusion chromatography (SEC), or gel filtration, is based on the principle of steric interaction. In SEC the solid support should be chemically inert and hydrophilic to avoid any interactions with the solutes being separated. A SEC solid support typically constitutes a beaded resin containing pores within a specified size range and the separation is thus based on the fraction of pores available to the individual solutes[33]. Basically, small solutes will have a larger porous area available for diffusion and will therefore be retained longer on the column than larger molecules. SEC is particularly useful with regard to separating mixtures where the product and the contaminants differ considerably in size or in connection with desalting buffer change[33]

Affinity interaction

Affinity chromatography (AffC) is based on the specific interaction between the target molecule and a ligand immobilized on the solid support. The affinity ligand can be either natural or synthetically derived and is characterized by having high specificity towards binding of a given target molecule or class of target molecules[34]. Due to the high specificity the affinity interaction, AffC is often applied as a primary capture step in a chromatographic purification process. One of the most utilized natural affinity ligands is protein A, which is derived from *Staphyloccocus aureus* and recognizes the Fc part of immunoglobulin G[35, 36]. Synthetic affinity ligands are commonly short peptides, which fall into the category of pseudo-specific ligands also comprising other types of ligands such as dyes, protein domains and metal chelates[37], the latter is described below.

Complexation interaction

Immobilized metal affinity chromatography (IMAC) is based primarily on the interaction between the amino acid histidine situated at the protein's surface and a metal ion chelated to a matrix immobilized ligand. Such ligands are bi-, tri- or multidentate hence, capable of forming complexes with metal ions making them available to amino acid interactions[38]. A commonly utilized IMAC ligand is iminodiacetic acid (IDA), which is bi-dentate and chelates the following ions with decreasing stability Cu(II) > Ni(II) > Zn(II) ≥ Co(II) >> Ca(II), Mg(II)[33]. An enhanced binding to the IMAC ligand is observed when proteins contain surface clusters of histidines or have been recombinantly altered to contain a tag consisting of a short chain of histidines, commonly referred to as a His-tag[39].

Electrostatic interaction

Ion exchange chromatography (IEX) is based on electrostatic interactions between a given target protein and ionic groups on the surface of the solid support. Based on their amino acid composition all proteins attain a net charge, which changes with varying pH. In this sense proteins are characterized by their isoelectric point (pI), which is the pH at which the proteins net charge is zero. At pH values below the pI, the protein carries a net positive charge and at pH above the pI it carries a net negative charge[33]. Hence, chromatography supports are designed as anion exchangers, carrying positively charged ligands for the binding of negatively charged targets or as cation exchangers carrying negatively charged groups for interaction with positively charged proteins. Furthermore, ion exchange ligands are categorized as weak or strong ion exchangers depending on their degree of

protonation at different pH values, thus strong ion exchangers are charged at all operational pH values whereas charge of weak ion exchangers depends on the given pH[10].

Hydrophobic interaction

Hydrophobic interaction chromatography (HIC) is based on the interaction between hydrophobic patches on a protein's surface and hydrophobic ligands immobilized onto the surface of a solid support.

The nature of a hydrophobic interaction is driven by the entropy associated with the organization of water molecules around the hydrophobic moieties. In the absence of salt, water is organized in a cage-like structure around the hydrophobic patch – this is an entropically unfavourable arrangement. By addition of salt, the water molecules arranged around the hydrophobic moieties will preferably interact with salt ions and this drives the hydrophobic moieties to bind together by a mechanism referred to as *salting out*[33]. In HIC proteins are thus applied to the solid support in high salt concentrations to promote hydrophobic interaction, and they are eluted by decreasing the ionic strength. Another mode of hydrophobic chromatography is reversed phase (RPC) where the protein is applied to the solid support under polar conditions and eluted by applying a gradient of organic modifier. Due to the denaturing conditions of the organic modifier as well as interaction with the solid support, RPC is mainly utilized for purification of smaller proteins that withstand the organic solvents[40, 41] or within analytical applications.

Mixed mode interaction

Within the last decade resins with both charged and hydrophobic ligands have been made available. These resins represent a new tool for purification of macromolecules, which combines the effects of at least two kinds of interactions between the stationary phase and the target[42]. The most common interaction combination is hydrophobic/charge and currently a number of such ligands are commercially available. Mixed mode chromatography has been demonstrated efficient both as a capture step[43], replacing AffC, and as a polishing step in the purification of proteins[44].

2.3 Types of solid supports

The solid support has a major influence on the overall performance of a downstream processing step, whether it is for chromatography or molecular modifications of the target. Generally, when working with biomolecules a hydrophilic, biocompatible support with low non-specific adsorption is desirable. Furthermore, it should be sufficiently mechanically stable in order to withstand the physical handling mode (e.g. liquid flow and pressure) and it should contain functional groups available for derivatizations. Finally, it should be compatible with different solvents, as well as a wide range of pH and conductivities[10]. For porous supports, ideally there should be a proper balance between porous surface area and pore size in order to maximizing the active surface area while minimizing diffusional limitations[12]. This section will present the different types of solid supports available for downstream processing in the form of particles, membranes and monoliths (Figure 2.1) and discuss their advantages and drawbacks (Table 2.1).

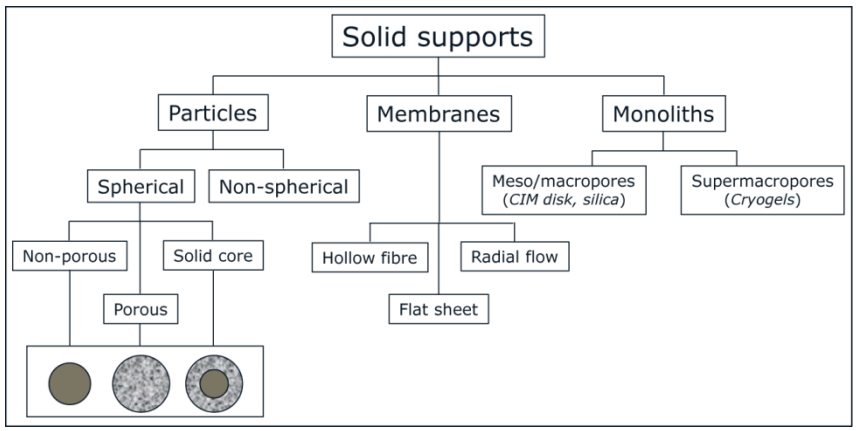

Figure 2.1. Overview of the solid supports for bioprocessing, which are discussed in this chapter.

Particle based solid supports

Traditional liquid chromatography is performed by use of a packed bed that is, a cylindrical column which is filled with tightly packed beaded particles. Such chromatography beads can be spherical or non-spherical and they can be solid, porous or porous with a solid core[12] (Figure 2.1).

The liquid flow in packed beds is primarily through the voids between the tightly packed beads and the liquid phase solutes will be accessing the porous space by

diffusion. The particle sizes applied for protein chromatography vary in the range of 2-300 µm and the pore sizes in the range of 10-100 nm[12]. Particle based supports are prepared from a variety of materials categorized as i) natural polymers, such as dextran and agarose, ii) synthetic polymers, such as polyacrylamide, polymethacrylate and polystyrene or iii) inorganic supports such as silica or hydroxyapatite[10, 12].

However, because proteins diffuse slowly conventional beaded resins are challenged in terms of resolution and capacity, when the flow rate is increased. Hence, the use of such traditional resin materials may represent a limitation with regard to optimizing the process time. To conserve resolution, ideally the time it takes the protein to travel between beads should equal the time it takes to travel through beads[34]. Approaches to solve this problem have been offered in the form of smaller and non-porous particles[45, 46] or flow-through particles which contain a bimodal system of large flow-through pores and diffusive pores[47, 48]. These solutions have offered high resolution at increased flow rates, but at the cost of decreased capacity and/or high column pressure drops. The use of particle based porous resins with large flow-through pores have received considerable commercial success and is referred to as perfusion chromatography[49]. The pore diameters of such supports are in the range 600-800 nm for the flow-through pores and 80-150 nm for the diffusive pores[50]. Between the particles and in the flow-through pores mass transport is conveyed by convection, i.e. the solutes are carried with the liquid phase, and in the diffusive pores mass transport occurs by diffusion. The combination of convective and diffusive mass transport presented by perfusion resins contributes to improved mass transfer within the resin enabling reduction of separation times which is desirable both from an analytical and preparative perspective[49, 50].

Membranes

Membranes can be regarded as porous barriers allowing for the size selective crossing of solutes in a mixture. In downstream processing membranes are primarily used as filtration devices. In the purification of proteins especially pressure driven *ultra-* and *microfiltrations* have gained success as useful techniques in size selective separation and concentration of proteins[51].

A somewhat less common use of membranes in downstream purifications is as chromatography adsorbents, a technique which has been named membrane chromatography[52]. Due to the large pore size, the mass transport through

membranes is solely conveyed by convective flow, hence eliminating diffusional mass transfer limitations. Compared to particle based supports, the advantages of using membranes in chromatography applications are high operating flow rates, a low pressure drop and easy process scale-up[53]. There are three types of membranes used for protein separations, namely flat sheet-, hollow fibre- and radial flow membranes. Flat sheet membranes are by far the most widely used and they are commercially available both as adsorbents and for size separations[52]. However, due to their physical design, comprising of thin supermacroporous sheets, chromatography membranes represent a low surface area and a concomitant low binding capacity compared to particle based chromatography supports. On the other hand, large volumes of dilute feedstreams can be processed within very short times using these membranes. Hence, in terms of protein chromatography, membrane technology is best suitable for purification of targets occurring in low concentrations[52] however, it is highly effective as a filtration device with regard to pressure driven size selective removal of impurities[54].

Monoliths

Monoliths are highly porous, polymeric materials cast as a single contineous block, often in a cylindrical shape. Due to their relatively large pore sizes, which are 1-5 μm, mass transport is conveyed by means of convection rendering high resolutions and binding capacities which are unaffected by flow rate[15, 16]. Various monoliths have been prepared through a wide range of techniques and by using different precursors, of which the most successful have undoubtedly been the methacrylate monoliths, which have been commercialized in the form of disks and cylinders[55]. Due to their convective pores and high porosity monoliths are endowed with features that render them suitable as solid supports in downstream bioprocess applications. The main advantages of monoliths are i) their high resolution power, ii) binding capacities unaffected by flow rate[56], iii) low column back pressures[57] and, iv) a relatively high binding capacity towards very large macromolecules[58].

Monoliths have been employed as solid supports in both analytical and preparative downstream processing applications. Examples of analytical applications are the very fast monitoring and quantitation of IgG antibodies from human serum[59] and crude cell supernatant[60], analytical chromatography of PEGylated proteins[61] and in-process control of the production of virus (adenovirus type 5)[62]. In terms of preparative downstream processing applications monoliths have been found

suitable especially for the purification of large biomolecules and nanoparticles, such as large proteins, plasmid DNA and viruses[63, 64].

With regard to plasmid DNA, which has a hydrodynamic diameter between 100 and 250 nm, it has been shown that the pores of conventional beaded resin are inaccessible to plasmid DNA[65], resulting in low dynamic binding capacities. Conversely, for monoliths flow independent, and relatively high dynamic binding capacities for plasmid DNA were found due to the accessible space of the macropores[66].

The generally low binding capacity towards macromolecules, combined with favourable flow properties, has prompted the use of monoliths for negative chromatography, hence for the removal of high molecular mass, low abundant contaminants. In this context it was shown that a strong anion exchange monolith could be used in the removal of bacteriophage, host cell proteins (HCP) and DNA at high flow rates[67].

Tabel 2.1. Advantages and disadvantages of particel based-, membrane and monolithic solid supports.

Solid support	Advantages	Disadvantages
Particle based support	High capacity and resolution	Mass transport by diffusion
	Highly developed technique	Limited operational flow rates
	Widely used on industrial scale	Incompatible with large biomacromolecules and particulate containing fluids
Membrane support	High throughput	Low binding capacity
	Easy scale-up	Risk of fouling
Monolithic support	High throughput	Low binding capacity
	High capacity for very large macromolecules	New technology, not developed
	High resolution	
	Low column pressure	

Table 2.1 provides an overview of advantages and disadvantages of the three types of solid supports when used in chromatography. Currently, porous beaded resin is the support of choice for many industrial chromatography unit operations because of its high capacity and well established integration into existing processes. However, as discussed especially monoliths offer features which could increase process productivity by decreasing the number of unit operations or the overall process time.

3. Cryogels, their preparation and characterization

Cryogels comprise a special class of monoliths, which are characterized by their extremely large and interconnected pores ranging from 10-200 µm. The unique porous design stems from the method by which these materials are prepared. They are formed under solvent freezing conditions allowing the solvent to act as porogen during the preparation of the cryogel. This chapter describes different aspects of the preparation, chemical functionalization and characterization of cryogels.

3.1 Principle of cryogelation

Cryogelation refers to the process of polymerization of an initially dilute solution of monomers onset at a temperature below the solvent's freezing point. Under such conditions, the solvent will freeze, forming neat crystals and thus expelling the monomers and other solutes from the crystalizing phase. Ultimately this process results in the formation of a heterogeneous solvent system composed of two phases, namely a frozen, crystalline phase and a non-frozen phase containing a high concentration of solutes[68]. The non-frozen phase extents to the exact volume, which constitutes a solute concentration causing a freezing point depression just below the systems set temperature. Hence the size and dimension of this phase is determined by the given system's initial solute concentration and the temperature[69]. This process has been referred to as cryoconcentration, and in such a heterogeneous system the polymerization of highly concentrated monomers will proceed in the non-frozen liquid phase surrounding the frozen solvent crystals [70].

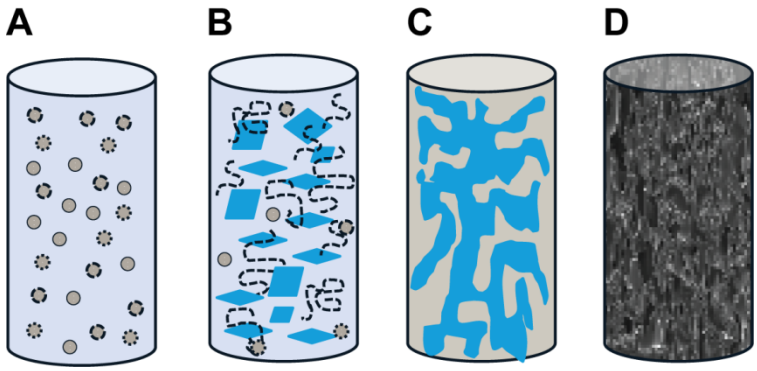

Figure 3.1. Schematic presentation of the principle of cryogelation. A: An initially dilute solution of monomers and solutes is cooledbelow the solvents freezing point. B: The solvent begins to crystalize and monomers polymerize. C: As the solvent freezes the monomers are concentrated in a non-frozen phase where the polymerization proceeds. D: When the polymerization is complete the system is thawed, rendering a cryostructurated polymeric material, also known as a cryogel.

Resulting from the cryocopolymerization of monomers is the formation of a macroporous polymeric network. As the polymeric phase has been molded around the solvent crystals the macroporous pattern of the material reflects the original freezing regime of the solvent system, hence it is cryostructurated (Figure 3.1). The pores of such a material have a high degree of interconnectivity which can be attributed to the fact that during cryopolymerization the main fraction of solvent will be in the form of crystals, which due to the confined space of the mold will grow together during freezing. The principle of cryostructuration forms the basis of the preparation of a class of macroporus, polymeric materials known as Cryogels.

3.2 Cryogels

Cryogels can be prepared either as polymeric gels by the freeze-thawing technique described in Section 3.1 or they can be prepared by a freeze-drying technique, which renders rigid, porous materials[71, 72]. This discussion focuses on the former type of cryogels, namely cryogels prepared by the freeze-thawing technique.

A polymeric gel can be defined as a solid, comprising a network of cross linked polymers, which by weight mainly consists of liquid solvent[73]. In such a system the liquid solvent is confined within the polymeric network where flow is restricted, but diffusion of solvent molecules takes place[74].

Hydrogels are hydrophilic polymer networks, which contain pores in the nano-scale range. At its equilibrium swelling level a hydrogel can contain large amounts of water. This water will be present in two states, namely bound to the polymer network or in the pores of the gel, where it is free to diffuse[75]. The preparation of cryogels by freeze-thawing involves the freezing of an initially dilute mixture of monomers at the on-set of polymerization. This technique renders cryogels highly porous, encompassing a system of interconnected supermacropores in the size range of 10-200 µm surrounded by thin and very dense polymeric pore walls (Figure 3.2)[76].

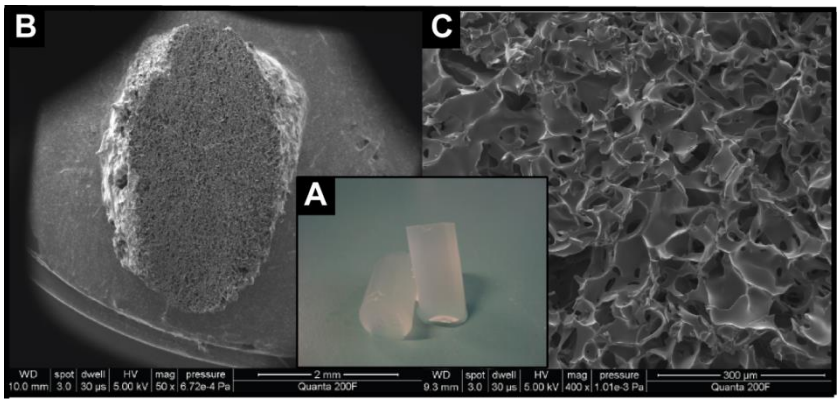

Figure 3.2. Images of a cryogel at different magnifications. A: Hydrated cryogel samples prepared with 5 mm diameter. B: Scanning electron microscopy (SEM) image of cryogel sample at 50x magnification. C: SEM image of cryogel sample at 400x magnification.

In association with cryogels, the solvent, which is usually water, can be found in two major forms, namely i) closely associated with the polymer network (i.e. in mesopores or polymer bound) and ii) as bulk liquid in the supermacropores of the cryogel. Due to the presence of solvent in these two forms cryogels have been described as heterophase systems as opposed to monophase hydrogels[76].

3.3 Polymerizations and monomers

Cryogels prepared by the freeze-thawing technique have primarily been produced as hydrogels by free radical polymerization[77, 78] or chemical cross-linking reactions[79, 80] of hydrophilic monomers. A few examples of reversible addition fragmentation chain transfer polymerizations have also been presented in the literature[81, 82].

Free radical polymerizations are chain polymerizations of unsaturated monomers, i.e. vinyl monomers, which are instigated by the addition of a small amount of initiator in the form of a substance which will readily break down into two free radical species. The breakdown of initiator into free radicals can be onset by heating, irradiation of by the addition of a reducing species, known as an activator [83]. For the preparation of freeze-thawed cryogels mainly redox initiation has been employed and the most utilized initiator/activator couple has been ammonium persulfate (APS) and *N,N,N',N'*-tetramethylethylenediamine (TEMED). Such an initiator/activator couple holds the advantage of being able to initiate the radical polymerization reaction without heating, which is crucial in cryopolymerizations where any form of heating may affect the end product. However, cryogels have also been prepared by free radical polymerizations instigated by UV-activation of a photoinitiator[84, 85].

A majority of studies with focus on the application of cryogels within bioseparations have used co-polymerizations of acrylamide (AAm) [86, 87], dimethylacrylamide (DMAAm) [70, 88], 2-hydroxyethyl methacrylate (HEMA) [89, 90], allyl glycidyl ether (AGE) [86, 87] with methylenebisacrylamide (MBAAm) or poly(ethylene glycol) dicarylate (PEGDA) as cross linkers. In the studies presented in this dissertation all cryogels were prepared by free radical polymerization using APS/TEMED as initiating system and monomers were chosen with respect to obtaining hydrophilic, biocompatible cryogels with functional groups available for derivatizations.

In **papers I** and **II** cryogels were prepared as N-(3-aminopropyl)methacrylamide-*co*-DMAAm-*co*-PEGDA (Figure 3.3 structures 1, 2 and 3) with varying co-monomer compositions. The functional co-monomer N-(3-aminopropyl)methacrylamide was chosen for these studies in order to obtain cryogels with varying degrees of primary amine loadings. In **paper III** cryogels were prepared from a blend of a mono- and diacrylated poly(ether amine) monomer (Figure 3.3 structures 6 and 7), which featured high hydrophilicity combined with the functionality of the primary amine end group and in **paper IV** a HEMA-*co*-AGE-*co*-PEGDA cryogel (Figure 3.3 structures 4, 5 and 3) was studied.

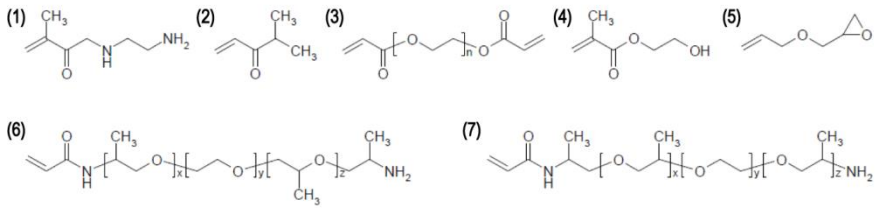

Figure 3.3. Monomers used for the preparation of cryogels in this dissertation. 1: N-(3-aminopropyl)methacrylamide, 2: DMAAm, 3: PEGDA, 4: AGE, 5: HEMA, 6: Poly(ether amine)acrylamide, MW ≈900 g/mol, (x+z)≈6, y≈12.5, 7: Poly(ether amine)acrylamide, MW ≈2000 g/mol, (x+z)≈6, y≈39.

Another method of choice for cryogel preparation has been by chemical cross linking of macromonomers and in this respect a diverse variety of monomeric entities carrying nucleophile functional groups have been utilized. Examples of such entities are poly(vinyl alcohol) (PVA)[91, 92], chitosan[93, 94], proteins[95] or even bacterial cells[96].

3.4 Synthesis conditions

The porous structure of cryogels can be controlled by the freezing temperature, the concentration of monomers in the initial reaction mixture and the type and content of the cross linker.

In this respect it has been found that increasing the initial monomer concentration results in the formation of cryogels with thicker pore walls and smaller pores, thus rendering a decreased supermacroporous porosity of the cryogel[97]. These observations can be regarded as an effect of cryoconcentration of monomers during freezing of the initial monomer solution (Section 3.1). At a given freezing temperature the monomers will be concentrated to a set level, which is defined by the freezing point depression. Therefore, at higher initial monomer concentrations the volume of the unfrozen liquid phase, where the polymerization proceeds, will be larger, rendering thicker pore walls and smaller pores[69]. Another aspect to this is, that increasing the hydrophilic character of the cross binder has been shown to increase the pore wall thickness, and at the same time increase the total swelling of the cryogel, indicating a less dense polymer phase containing more polymer bound water[97].

The freezing temperature and the concentration of initiator/activator are factors which have also been shown to affect the porous morphology of cryogels.

Increasing the concentration of APS/TEMED from 1.2% (w/w) to 5% (w/w) resulted in the formation of cryogels with impaired flow properties and significantly deviating pore morphology[98]. By increasing the initiator/activator concentration, the polymerization rate increased, which resulted in a setup where the on-set of gelation occurred before freezing of the solvent. Due to this, forming solvent crystals could not grow together and porous interconnectivity was not established in the resulting cryogel. This result emphasizes the importance of freezing before gelation for the formation of cryogels with an interconnected supermacroporous system[98].

In the case of freezing temperature, it has been shown that at lower freezing temperatures, i.e. higher freezing rates, smaller pores are formed[98, 99]. This phenomenon has been assigned to the freezing regime of water. At high freezing rates, i.e. lower freezing temperatures, more crystallization nucleation sites will be created, generating more and smaller ice crystals molding the pores of the cryogel[99]. At lower freezing temperatures the pore walls were also found to be denser, which was a result of a temperature dependent decrease of the volume of the non-frozen liquid phase[69]. In addition freezing temperature also affected the reaction rate of free radical cryopolymerization during cryogel formation. It was shown that polymerization at -10°C proceeded at a higher rate than at -20°C, albeit the monomer concentration in the non-frozen liquid phase was higher for the latter[69, 99].

In **paper III** the influence of reaction temperature, initiator/activator concentration, initial monomer concentration and reaction time on the polymerization yield of cryogels prepared from poly(ether amine)acrylamide macromonomers was investigated. Of these temperature, time and monomer concentration were found to be of significance. In accordance with other studies it was found that at -12°C polymerization proceeded at a higher reaction rate than at -20°C. During the course of cryopolymerization the reaction rate is affected by opposing factors, namely i) the low system temperature, which promotes a decreased reaction rate, ii) the increased viscosity of the non-frozen liquid phase, which limits diffusivity of monomers and hence decreases the reaction rate, and iii) the increased concentration of monomers in the non-frozen liquid phase, which increases reaction rate. As system reactivity was found to be decreased by lowering the temperature, apparently factors i and ii have a higher impact than factor iii on the overall polymerization kinetics of the co-monomer system investigated.

The elucidation of how synthesis conditions may affect the pore morphology of cryogels offers the possibility of customizing the porosity of cryogels to suit certain applications. On this basis studies have demonstrated how cryogels with tailored pore morphologies can be prepared by manipulating synthesis conditions. The preparation of cryogels with an aligned pore structure was carried out by unidirectional freezing of the polymerization mixture. By gradually submerging the monomer mixture into liquid nitrogen it was possible to control the orientation of templating ice crystals hence, rendering a uniform and aligned pore morphology of the cryogels[100-102]. The solvent composition has also been used as a tool in modifying the pores of cryogels. In this respect it has been shown that the addition of small inert solutes in the form of acetone or NaCl affected the thickness and polymer density of the pore walls[103]. The addition of a porogen in the form of poly(methylmethacrylate) fractionated particles has also been demonstrated as a means to decrease the pore wall density by the controlled introduction of small closed pores[101, 102]

3.5 Matrix functionalizations and derivatizations

In order to provide cryogels with functional groups available for derivatizations and ligand attachment different approaches have been employed. One direct approach has been the co-polymerization of a monomer with the desired chemical functionality. For this purpose, incorporation of epoxide groups by AGE has mainly been used[77, 86, 104].

To provide cryogels with primary amine functionalization **papers I** and **II** describe preparation of N-(aminopropyl)methacrylamide-*co*-DMAA-*co*-PEGDA cryogels with varying content of the primary amine functionalized co-monomer N-(3-aminopropyl)methacrylamide (Figure 3.3, structure 1) . In **paper II** it was shown that when increasing the proportion of N-(3-aminopropyl)methacrylamide in the co-monomer blend, this unit was quantitatively incorporated into the cryogel polymeric matrix. The subsequent thiol functionalization was performed by reaction with N-acetyl homocysteine thiolactone and was optimized with respect to pH, time and equivalents of thiolating reagent, rendering a cryogel thiol loading which approached full conversion of matrix primary amines (Figure 3.4).

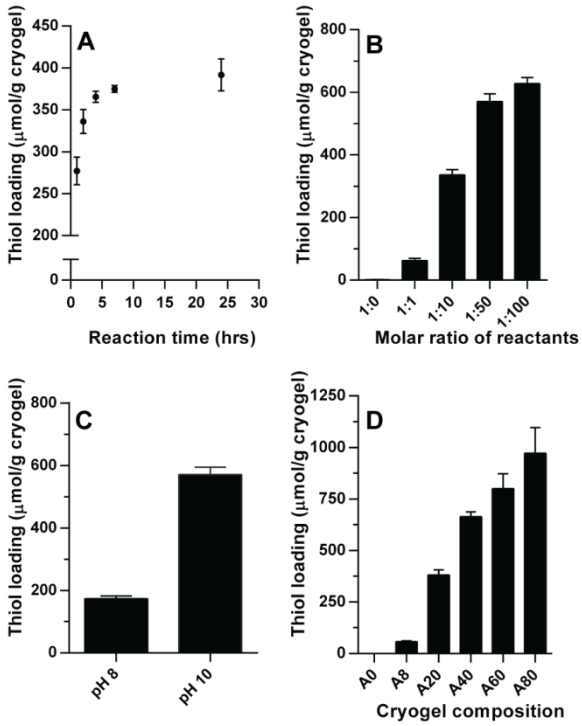

Figure 3.4. Results of optimization experiments for the thiol functionalization of N-(3-aminopropyl)methacrylamide-co-DMAA-co-PEGDA cryogel. A: Reaction time. B: Equivalents of thiolating reagent. C: pH. D: Cryogel primary amine loading (**Paper II**).

In **paper I** the primary amines of a N-(3-aminopropyl)methacrylamide-*co*-DMAA-co-PEGDA cryogel were used as anchoring points for the direct synthesis of peptides of different sizes. Hence the cryogel served as solid phase in an automated peptide synthesis application. In this connection it was shown that the product yield was in the same range as when synthesized on a conventional resin, but the purity of crude product was markedly reduced when prepared on the cryogel. These findings were attributed to the distinct porous composition of the cryogel, which encompasses supermacropores as well as micropores of the pore walls. In such a heterogeneous porous matrix reacting species are likely to have a more uneven access to anchored groups than in a more homogeneous synthesis resin, thus resulting in a poorer purity of the crude peptide.

In **paper III** an amine functionalized poly(ether)acrylamide monomer was used to prepare cryogels, which were subsequently aldehyde derivatized. The chemical route towards this derivatization was by the activation of 4-carboxybenzaldehyde

with O-(benzotriazol-1-yl)-N,N, N',N'-tetramethyluronium tetrafluoroborate (TBTU) followed by reaction of the active ester with cryogel primary amine, all performed *in situ* in the presence of the cryogel. This synthetic strategy circumvented the use of expensive reagent, succinimidyl p-formylbenzoate (SFB) and was shown to render full conversion of matrix primary amines.

Immobilizations of various proteins on cryogels have primarily been achieved by coupling to matrix epoxide or aldehyde groups. Both approaches rely on coupling to protein primary amines, which are located either at the N-terminus or in surface lysines. As the lysine content in proteins may vary, targeting primary amines in protein immobilizations makes it difficult to control the orientation of the matrix bound protein. In **paper III** an incomplete cleavage of antibody by immobilized papain was observed. An explanation for this result could be that immobilized papain has a spatial orientation which makes the active site inaccessible to antibody, rendering incomplete cleavage.

Immobilization of proteins onto solid surfaces requires mild reaction conditions, as reducing- or harsh pH or solvent conditions may disrupt the protein's native structure. In this respect, so called 'click' chemistry offers the advantage of being quantitative as well as it proceeds under mild conditions[105]. In an interesting study on the functionalization of a poly(HEMA) cryogel it was shown how matrix hydroxyls could be converted to alkynes, which were subsequently utilized in a copper(I)-catalyzed Huisgen azide-alkyn coupling strategy and hence, it was demonstrated that 'click' chemistry is compatible with cryogels[106]. Such a coupling strategy could also be applied for the immobilization of proteins, as it would allow for the controlled orientation of the protein.

Another popular approach to the derivatization of cryogels has been grafting of polymer chains with different functionalities onto the matrix. This method has been employed as a means to increase the functional group loading and binding capacity towards different targets. Hence anionic, cationic as well as hydrophobic and stimuli-responsive monomers have been attached to cryogels by graft polymerization[107-110].

3.6 Characterization

The practical application of cryogels within different areas of biotechnology depends on structural characteristics such as cryogel geometry, overall porosity, average pore size and pore size distribution, surface area, interconnectivity of

pores as well as mechanical and chemical stability. As described, the porous morphology of cryogels stems from the freezing of the reaction mixture prior to polymerization. The freezing of complex mixtures is a random process and therefore each cryogel monolith will have its own porous fingerprint, resulting in unique physical properties. In this perspective each cryogel should be considered as a separate batch and optimally should be characterized accordingly with non-invasive techniques. Regrettably, such non-invasive techniques are a shortcoming within the field of polymeric soft gel characterizations as will be discussed in this section.

Mechanical testing

The mechanical properties of a polymeric material are important parameters with regard to its application. These properties describe how strong and elastic the material is and therefore how much applied pressure it will tolerate without collapsing.

One commonly applied method for evaluating mechanical properties of polymers is tensile testing[83]. However, this method involves measuring the tensile force of the polymer stretched out between two grips, an experiment which is difficult to perform on cryogels due to their monolithic nature. Instead compression test has been frequently used to examine the mechanical properties of cryogels[96]. A common parameter derived from this test has been the Young's modulus of elasticity which is given in pressure units (kPa) and is a measure of the stiffness of the material within the linear region of stress and strain[111] – in other words, it is a measure of the tendency of a substance to deform, when a force is applied to it. Cryogels have been shown to possess high mechanical stability towards compression[112] a feature which seems to be dependent on the thickness and microstructure of the pore walls[103].

Visualizing the pore morphology

As the porous structure of cryogels is highly determining for their application, many studies have focused on visualizing the pore morphology by use of various microscopy techniques. For this purpose the most widely used technique has been scanning electron microscopy (SEM), which allows for visualization at very high resolutions enabling study of the pore wall microstructure[113]. One major drawback of this technique is the requirement for dry samples, which means that it does not permit study of cryogels in their highly hydrated in situ state. Additionally,

samples under study must be chemically fixated and metal coated prior to analysis, which introduces the risk of sample deformation.

Environmental scanning electron microscopy (ESEM), on the other hand, is a technique which allows for the visualization of hydrated samples, but at the expense of a reduced resolution[114]. Studies comparing the porous structure of a dry and wet AAm cryogel utilizing SEM and ESEM, respectively have shown that the porous structure is not markedly deformed by drying or sample treatment in connection with SEM analysis[77, 97]. This observation is attributed to the unique structural properties of cryogels, where the thin and very dense pore walls swell only to a limited degree[98]. However, keeping in mind that the pore morphology and pore wall structure depend on the applied synthesis conditions and monomer system[97-99], this feature should not be regarded as a general rule. In ESEM studies of the pore structure of the poly(ether amine) cryogel presented in **paper III** (Figure 3.3, structure 6), the pores were slightly decreased and pore wall thickness slightly increased by increasing the chamber humidity from 32% to 77% (Figure 3.5), which indicates that for this cryogel some deformation takes place during dehydration.

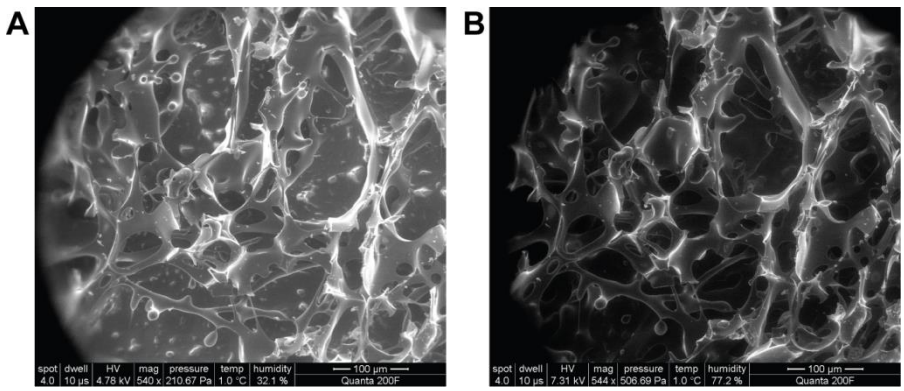

Figure 3.5. ESEM visualization of poly(etheramine) cryogel in different hydration states. A: Cryogel at 32% humidity. B: Cryogel at 77% humidity.

Another microscopy technique which has been employed in visualizing the pore structure and distribution of functional groups on the pore surfaces of cryogels is confocal laser scanning microscopy (CLSM)[115, 116]. CLSM is a light microscopy technique, which provides high resolution images by scanning the focal plane of a fluorescent stained surface and with the use of image processing software 2-D and 3-D images of the specimen can be generated[117]. The advantage of CLSM is that it

permits the study on cryogels in their *in situ* state, hence providing a more realistic basis for the analysis of cryogel pore morphology than SEM[118]. Savina and co-workers have studied the porous deformation by drying in a HEMA-*co*-AGE cryogel by comparing CLSM images of the fluorescein isothiocyanate stained sample in its wet and freeze dried state. A small diminution of pore size and wall thickness was observed on this ground, which was attributed to shrinkage of pore walls upon dehydration[119].

Porosity, pore size distribution, and specific surface area

Porosity is a parameter used to describe the void volume in a solid material. In the case of cryogels, the porosity has frequently been determined as the volume of the macropores. However, cryogels comprise two distinct pore systems, namely that of the supermacropores and that of the pore walls comprising micropores[120]. Therefore, a complete description of the porosity of a cryogel involves determination of the porosity of both these pore systems. Water contained in a cryogel has different activities depending on its degree of association with the polymer and this is reflected by its freezing temperature[120]. Such differences in cryogel bound water activity can be studied by low temperature ^{1}H-NMR – a technique, which has been used to measure the fraction of water held in the porewalls[69, 70, 103, 121]. Other methods utilized to determine the porosity of the supermacropores have been weighing of the water mechanically removed from the supermacropores[122] and cyclohexane uptake in the supermacropores of a dry cryogel[97, 103].

Microscopy analyses have been used to determine important structural parameters of cryogels such as average pore size[119, 123], pore size distribution[119, 121] and porosity[119]. In **papers I-IV**, the average pore size of cryogels was estimated from SEM images by the use of ImageJ software. Based on CLSM stacked images and by the use of image processing software Savina and co-workers have determined the specific surface area, mean pore and wall thickness as well as pore and pore wall distributions in HEMA-*co*-AGE cryogels prepared under varying synthesis conditions[119].

The specific surface area of a solid support is determining for the adsorption capacity of the material and is therefore an important parameter to consider. Due to their supermacroporous structure, cryogels are known to possess a low surface area available for macromolecular interactions compared to other porous solids. The surface area of a porous material can be determined by intrusion methods such

as mercury porosimetry or nitrogen adsorption[124, 125] and such methods have been employed in the determination of cryogels's specific surface area[126, 127]. However, these methods are destructive and they require dry sample specimens, why the measurements are not necessarily representative for the actual surface area of the cryogel in its *in* situ, hydrated state.

Liquid chromatography characterization

Cryogels have been applied in a number of studies as monolithic columns for chromatographic separations of various biomacromolecules and their performance as such has been characterized and evaluated accordingly[77, 78, 86, 122, 128].

In these studies the pore size distribution, the pressure drop and column efficiency at different flow rates, as well as the adsorption capacity have been investigated. Cryogels are known to exhibit very low hydraulic flow resistance even at high flow rates. This has been estimated by the measurement of water flow velocities through the cryogel column at a hydrostatic pressure of 0.01 MPa[77, 86] or as the water permeability calculated from the flow rates of water passing through the cryogel column at different hydrostatic pressure drops[122, 128]. The permeability of different cryogels have been found to be in the range of ($3.43\cdot10^{-11}$-$8.27\cdot10^{-13}$ m^2)[88, 122, 128, 129], which is considered as high compared to other organic polymeric monoliths ($1.11\text{-}7.2\cdot10^{-14}$ m^2)[57, 130]. In **papers III** and **IV** permeability of the cryogels was tested and found to be ($6.5\text{-}9.9\cdot10^{-13}$ m^2) and ($5.58\text{-}8.45\cdot10^{-12}$ m^2) for poly(ether amine)- and HEMA-based cryogels, respectively.

The column efficiency, which is defined as the degree to which ideal chromatography conditions are approached, is frequently described in terms of the hight equivalent to a theoretical plate (HETP)[10]. The HETP reflects the band spread, which ideally should be minimal, and therefore high efficiency chromatography columns are defined by a small HETP. In the case of cryogels, HETP has been determined from the residence time distribution (RTD) or breakthrough curves of different size tracer molecules injected on the cryogel column at different flow rates under non-binding conditions. In this respect, the HETP for different cryogel columns has been found to be in the range of 0.1-0.2 cm for applied flow rates of 1-10 mL/min[86, 87, 104, 128, 129]. To put this into perspective, in the same flow rate interval HETP for a commercial methacrylate monolith was determined to 0.001-0.002 cm as evaluated by bovine serum albumin pulse injections under non-binding conditions[131].

Mathematical models as characterization tools

A cryogel's suitability for a given biotechnology application is determined by its physico-chemical characteristics. Hence, characteristics of the porous structure and –interconnectivity as well as the surface chemistry are factors determining for important chromatographic parameters such as column efficiency and adsorption capacity. As already described, the matrix chemistry can be controlled by the choice of monomers and subsequent derivatization strategy (Section 3.3) and the physical characteristics such as pore morphology, pore wall thickness and pore size distributions can be controlled by the synthesis conditions (Section 3.4).

Methods available for the investigation of physical characteristics, such as pore size distribution and specific surface area are mainly destructive and therefore alternative non-destructive methods have been called for. One set of methods to characterize the microstructure of porous media and predict chromatographic behavior is based on the use of mathematical models[10].

Only a few studies have focused on the modelling of cryogel microstructure and -chromatographic characterization. Persson and co-workers[88] have proposed a capillary based model to characterize a cryogel matrix and predict its chromatographic behavior in order to evaluate its suitability for specific separation tasks. In this model all capillaries were assumed to have equal length, equivalent to the length of the cryogel column. The authors argue that despite the actual interconnectivity of cryogel pores, the capillary description can be justified because in a convective flow regime the path representing the lowest flow resistance is always chosen and hence resembling a bundle of capillaries. The model was found successful in predicting important features of the cryogel such as pore size distribution and flow rate dependence as well as experimental breakthrough curves.

In **Paper IV** another capillary model is presented as a method of describing the microstructure characteristics, fluid hydrodynamics and breakthrough performance of proteins in cryogel columns. The proposed model is distinguished from previous work[88, 132] by considering the tortuosity of pores and the axial dispersion coefficient to give a better description of the fluid hydrodynamics through the cryogel column (Figure 3.6).

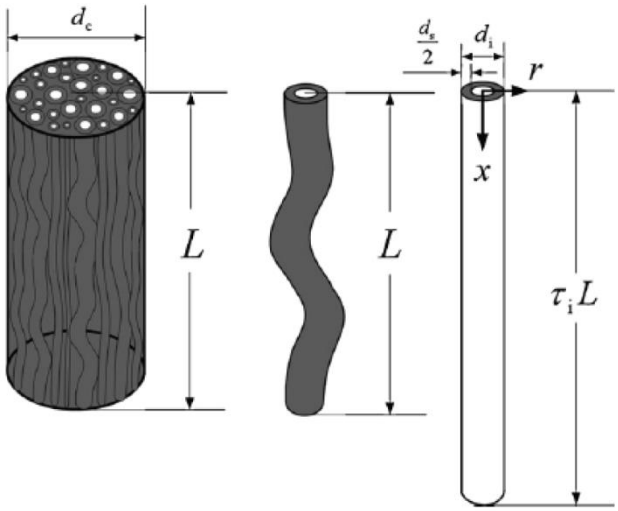

Figure 3.6. Schematic diagram of a cryogel made up of tortuous capillaries as described by the model proposed in **paper IV**.

By fitting physical parameters of the cryogel, i.e. column diameter and -length, porosity, permeability and breakthrough curves, the successful determination of pore size distributions, number of capillaries, capillary tortuousness and pore wall thickness was achieved. A further proven use of the model was demonstrated by its capability of predicting cryogel flow performance and breakthrough behaviour.

4. Cryogels in bioprocessing

Due to their easy preparation, hydrophilic character and supermacroporous structure cryogels constitute a type of solid supports, which have been considered for a range of biotechnology applications. This chapter focuses on the application of cryogels as solid supports for downstream processing of bioparticles and –molecules and within biocatalysis. Additionally, reported studies on different formats and scale-up of cryogels are described and discussed.

4.1 Cryogels as solid supports for separation of biomolecules

Cryogels are distinguished from other polymeric solid supports by their extremely open porous structure. Due to this feature cryogels constitute low pressure chromatographic supports, but with a coherent low surface area of the supermacropores. The supermacroporosity allows for bindings capacities minimally affected by flow rate and the direct loading of crude or even particulate solutions to the cryogel column without the risk of fouling or clogging of pores[86]. Due to these feature the use of cryogel based columns in certain analytical- or preparative applications, where the target molecule is present in scarce quantities, could be regarded as a process improvement in terms of time and economy.

Cryogels have been studied for their use as solid supports in a number of chromatographic separations of macromolecules and bioparticles such as proteins[21, 133], virus[134], DNA[135] and cells[20]. Chromatographic applications of cryogels have mainly focused on affinity chromatography utilizing biospecific affinity ligands or pseudoaffinity ligands, IMAC ligands. Bioparticles and large macromolecules are characterized by a slow diffusion and due to their large size the porous surface area of a conventional beaded resin is not available for binding[65]. In these cases the surface area presented by a monolith, such as a cryogel, may actually be considered as high compared to a conventional chromatography resin.

Affinity chromatography

Ahlqvist and co-workers[21] have demonstrated the application a poly(AAm-*co*-MBAAm-*co*-AGE) cryogel coupled with either protein A or the pseudospecific ligand sulfamethazine for the isolation of immunoglobulin G (IgG)-labeled inclusion bodies directly from a fermentation broth. Both cryogels performed well for this isolation and were suggested as tools in the analytical monitoring of large macromolecules production. Elaborating on this concept poly(AAm-*co*-MBAAm-*co*-AGE) cryogels coupled to protein A or with a phenyl ligand for hydrophobic chromatography were prepared to fit in the wells of a 96-well plate. In this format, the protein A cryogel was demonstrated to function as a monitoring tool for the production of inclusion bodies[136]. In this context the application of the phenyl cryogel as a solid support for enzyme-linked immunosorbent assay (ELISA) in the quantification of inclusion bodies immobilized on the cryogel was demonstrated[137].

Dainiak and co-workers[138] also prepared cryogels in a 96-well format for the purpose of screening for cell chromatography conditions. Poly(AAm-*co*-AGE) cryogels were prepared, coupled with affinity ligand concanavalin A (ConA) and used for the model separation of *Saccharomyces cerevisiae* from *Escherichia coli*. The study showed that *S. cerevisiae* could be effectively separated from *E. coli* by adsorption to the ConA-cryogel column. The subsequent elution was performed by compression of the cryogel which caused complete detachment of bound cells. Such mechanical elution was possible due to the cryogel's elastic and sponge-like morphology and circumvented the use of harsh elution conditions[138].

Cryogel based affinity chromatography using peptide affinity ligands has been demonstrated, but in an unconventional fashion, namely by the immobilization of peptide displaying bacteriophages, which constitute large filaments (up to 1000 nmx6 nm dimension)[139, 140]. Peptide ligands derived from phage libraries are more effective binders when displayed on the phage than in their isolated form. Therefore, Noppe and co-workers immobilized bacteriophages carrying affinity peptides selected from a phage library on the supermacropore surface of a cryogel and demonstrated that this cryogel could be used in the isolation of human lactoferrin from milk and von Willebrand factor from blood[139, 140].

Another interesting chromatographic application of a cryogel was presented as *chromato-panning*[141]. In this application a cryogel column with an immobilized affinity target was used as solid support for the selection of bacteriophages carrying peptides with affinity for the target. After application of the phage library

sample, the unbound samples could be washed out followed by elution and hence isolation of the affinity active phages. Additionally, it was shown that infection of *E. coli* with the selected phages could be performed on-column, i.e. by loading *E. coli* onto the cryogel with bound bacteriophages. This circumvented the elution of bacteriophages prior to infection. By using the chromato-panning procedure time could be saved, the cryogel column could be re-used several times and the phages could be eluted under mild conditions compared to conventional bio-panning methods [141].

Such a dual application of a cryogel was also demonstrated in **paper I**. In this study it was demonstrated that the same cryogel could be utilized, first as solid support for automated synthesis of a peptide ligand and then, for the chromatographic isolation of the target antibody. The binding capacity of the cryogel was found to be low (Figure 4.1), but the selectivity was high as shown by the specific capture of the target antibody from a cell harvest. Therefore, for analytical applications this cryogel could be considered. The concept of using the same cryogel for ligand synthesis as well as antibody capture allowed for the circumvention of several preparation steps and therefore posed an improvement to the conventional procedure of preparing peptide affinity chromatography columns.

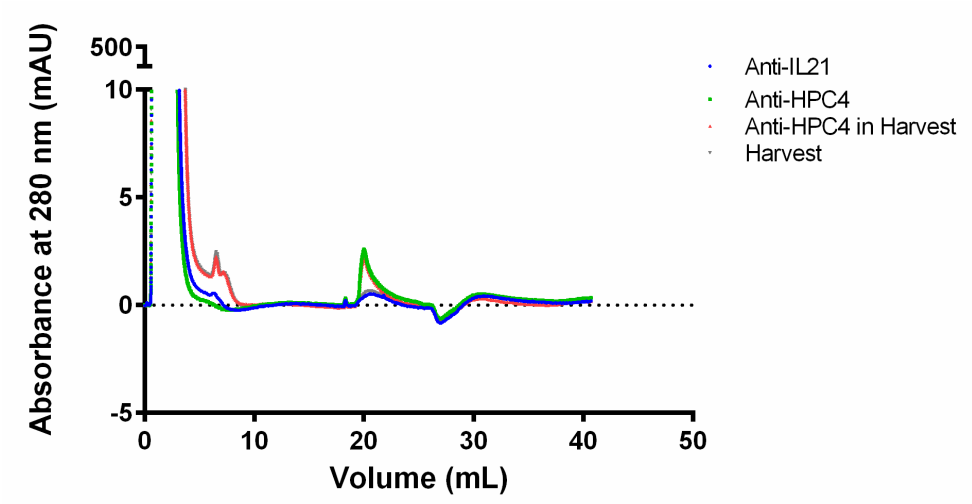

Figure 4.1. Chromatographic capture of target antibody on a cryogel with directly synthesized peptide affinity ligand, HPC4. The overlay of four chromatograms illustrates how target antibody (anti-HPC4) is captured from a buffer solution (green line) and as component in a cell harvest (red line) and that there is no non-specific binding of an alternative antibody (blue line) or from a cell harvest components (grey line) – the weak signal detected in this connection is from EDTA in the elution buffer (**Paper I**).

Plasmid DNA is another type of macromolecule, which due to its large size and viscosity, can be challenging to isolate using conventional chromatography. The application of a cryogel for isolation of plasmid DNA was demonstrated by the use of a histidine, pseudo-specific affinity ligand introduced to the poly(HEMA) cryogel by co-polymerization of N-methacryloyl-(L)-histidine methyl ester (MAH). This cryogel was successfully used to isolate plasmid DNA from a crude cell homogenate and it was found to have a binding capacity exceeding a beaded resin, which it was compared to[90].

Another example of a pseudo-specific affinity ligand used in connection with a cryogel is the dye ligand Cibacron Blue F3GA, which was used to isolate human interferon from a crude cell extract[142] and human serum albumin from blood serum[89]. Also boronate ligands were used for the isolation and separation of egg white glycoproteins[143] and the isolation of yeast cells and RNA from a bacterial crude homogenate[144].

Immobilized metal affinity chromatography

Due to its low cost and simple preparation IMAC has been the chromatography mode of choice in many studies of cryogels, where the bidentate ligand IDA has been used in the coordination with Cu^{2+}, in the form of which it binds the aromatic amino acid histidine. This feature has been exploited in the capture of macromolecules either carrying a recombinant His-tag or naturally exposing aromatic moieties at their surface[39].

In this respect, the use of IDA-cryogels for the direct capture of His-tagged proteins from crude cell homogenates has been demonstrated in a column mode[86] as well as in a 96-well plate screening format[22, 145]. Chromatography of cells by the use of IDA-cryogels has also been demonstrated[20, 78].

Cheeks and co-workers[134] conducted a study evaluating an IDA-cryogel for the purification of His-tagged lentil virus. The cryogel was compared to a commercial methacrylate monolith with IDA ligand and it was found that the latter support was superior with respect to binding capacity, elution efficiency and concentration of product in elution fraction. However, the cryogel was less prone to non-specific adsorption and it offered reduced process time, simple column regeneration, low cost and the option to process unclarified feeds.

Molecular imprinted polymer technique

Molecular imprinting is a relatively new technology, which has been applied for molecular separations. The technique involves polymerization of monomers in the presence of a target molecule, which acts as a template leaving a specific target recognition site imprinted in the polymer[146].

Molecular imprinting has also been utilized in connection with cryogels with emphasis on either isolation of various proteins from crude mixtures or small compounds occurring in low concentrations e.g. waste water pollutants. With regard to proteins, molecular imprinted cryogels have been used for the isolation of insulin[147], human serum albumin[148], cytochrome c[149], lysozyme[150] and antibody[151]. In protein isolations, generally molecularly imprinted cryogels showed high selectivity and column re-usability but for all targets binding was flow-dependent, which was regarded as a combined effect of macromolecule slow diffusivity and -binding kinetics.

For low molecular weight targets molecular imprinting on cryogels has amongst others been demonstrated for arsenic[152] and 17β-estradiol[153] from waste water and β-blockers from blood serum.[79] For these low molecular targets dynamic binding capacities were not significantly affected by flow rate and no fouling or clogging of the cryogel columns occurred even when processing large volumes of unclarified solution.

Ion exchange chromatography

IEX is another chromatography interaction mode, which has been exploited in connection with cryogels. Ion exchange groups have mainly been introduced by graft polymerization into the matrix of an already formed cryogel and targets have been various proteins, such as bovine serum albumin[154, 155] for anion exchange chromatography and lysozyme[128], lactoferrin and lactoperoxidase[156] for cation exchange chromatography.

Generally, IEX cryogels for isolation of proteins show low binding capacities, but successful efforts have been made to increase the surface area and binding capacity by preparing composite cryogels incorporating polymer particles[155] and increasing matrix ionic concentration[154]. Low molecular weight compounds have also been separated on IEX grafted cryogels, amongst others adenosine trisphosphate (ATP) which was isolated in high purity on an anion exchange cryogel exhibiting flow independent binding[129, 157].

An interesting application of an IEX cryogel was demonstrated by Hanora and co-workers, who used these matrices for negative chromatography of bacterial endotoxins[158]. In this study poly(AAm-*co*-AGE-*co*-MBAAm) cryogels were prepared and coupled with three different anion exchange ligands, namely i) polymyxin B, a cyclic anionic decapeptide antibiotic, ii) polyethyleneimine, a highly branched amine containing polymer and, iii) lysozyme. All three ligands were found to bind bacterial endotoxins at neutral pH and they were efficiently eluted with high concentration of NaCl. In terms of binding capacity, in comparison to conventional beaded resin at flow rate of 1 mL/min cryogels could not compete. However, at 10 mL/min cryogels maintained their binding capacities whereas the beaded resin could not be processed at this velocity. The cryogels all exhibited high selectivity for endotoxin binding under acidic conditions, even when *E. coli* lysate was directly applied, and the authors suggest that these matrices could be used in the cleaning of waste water[158].

As presented in the preceding sections, cryogels have been used as chromatographic matrices in a wide range of protein- and small compound separations utilizing a number of different ligands and interaction modes. As chromatographic solid supports the strength of cryogels are their supermacroporosity allowing the unhindered passage of particulates as well as their generally flow independent binding capacities. These features can in some cases make up for the intrinsic low porous surface area and hence, low binding capacities. Especially in negative chromatography applications concerned with removal of a low abundant pollutant, cryogels could excel over conventional solid supports. Such applications have been demonstrated with respect to removal of endotoxin[158], or various small compounds from waste waters [79, 152, 153]. Chromatography of cells is another application where the low supermacroporous surface area of cryogels does not necessarily convert into a low binding capacity compared to conventional beaded resin and where the hydrophilic character and elasticity of these materials protects cell viability[20, 78, 159].

In analytical and screening applications, there is also indications that cryogels can represent a cheap and easy format as an alternative to commercial columns (**paper I**)[22, 137, 138, 145]. However, the intrinsic low surface area available for macromolecule interactions continues to be a challenge with regard to the general application of cryogels in chromatography. Several studies have demonstrated how binding capacity can be increased by preparing composite cryogels[91] or developing the ligand chemistry[109, 160] and these approaches may contribute to finding a proper balance between binding capacity and flow properties.

4.2 Cryogels as solid supports in biocatalysis

Catalysis is essential to many biochemical reactions, as it involves the increase of the rate of reactions, which would normally proceed at a slow pace under physiological conditions. Catalysis is promoted by a catalyst, which participates in the chemical reaction by increasing the kinetics, but without being consumed by the reaction itself. Hence, catalysts are characterized by their reusability during the course of a bulk reaction and therefore they need only be present in minute amounts compared to the reagents[29].

Enzymes are biocatalysts and catalyze a large variety of biochemical reactions, which result in the transformation of various organic compounds including proteins and other biomacromolecules[29]. The use of enzymes in biocatalysis applications of industrial relevance often involves conditions (e.g. pH, temperature, organic solvents) that differ from the enzyme's natural environment and therefore jeopardizes its stability and catalytic activity. In this connection, the immobilization of enzyme onto solid supports has proven to be a method, which can be used to physically stabilize the given enzyme. This makes it more resilient towards harsh chemical conditions and prolongs its working life[161]. Additional advantages of immobilized enzymes are circumvention of the subsequent need to separate enzyme from product after the reaction and reusability of the enzyme[161]. On this basis, immobilized enzymes have found their use within industrial applications such as production of high fructose corn syrup[162], antibiotic modification[163] and trans-esterification of food oils[164].

Immobilized proteases

Cryogels have been considered as solid supports in enzyme immobilizations and due to their hydrophilic character PVA cryogels have frequently been chosen over other monomers. PVA cryogels have been prepared with different immobilized enzymes such as various proteases[165-167], lipase[168], and laccase[169].

One area of focus has been the preparation of cryogels with immobilized proteases for peptide synthesis in water poor media. Chemical peptide synthesis involves a number of undesirable features such as risk of racemization resulting in low purity and yield of product as well as the obligatory use of protection groups involving harsh synthesis conditions. Proteases, which under aqueous conditions catalyze the hydrolysis of peptide bonds, will in a water restricted environment catalyze the reverse reaction, namely the formation of peptide bonds[170]. Compared to chemical peptide synthesis, the use of enzymes gives the advantage of an enantioselective

reaction and avoidance of the need for protection groups, hence permitting milder synthesis conditions[171].

Cryogels have been utilized as carriers for enzymes involved in peptide synthesis. This application was demonstrated by the covalent immobilization of the proteases subtilisin-72 and thermolysin on beaded PVA-cryogel supports. The immobilized enzymes were shown to be active with respect to the synthesis of short peptides in different compositions of organic media[165, 167]. However, for both enzymes, the immobilization resulted in a reduction of activity compared to free enzyme, which was evident even when enzyme inhibitors were present during immobilization to protect the active site. On the other hand, immobilization onto the PVA-cryogels increased the enzymes' storage life as well as their tolerance towards aprotic solvent in high proportions. The latter was attributed to the enzymes' multipoint interaction with the PVA cryogel as well as the stabilizing effect of donation of water from the hydrophilic polymer[167].

Proteases immobilized on cryogels have also been utilized for the enantioselective hydrolysis of a Schiff's base in an amino acid derivative[166] and for the degradation of protein by hydrolysis of peptide bonds[23]. In this respect, Belokon and co-workers[166] demonstrated that α-chymotrypsin could be immobilized on PVA-cryogel and used for the enantioselective hydrolysis of an amino acid derivative in mixtures of water and acetonitrile. The immobilization of α-chymotrypsin resulted in a higher tolerance of the enzyme towards the presence of acetonitrile as well as an increased shelf life. The α-chymotrypsin-cryogel also proved to be superior to Sephadex G-75 with immobilized α-chymotrypsin, as the latter support collapsed in acetonitrile containing media and gave lower yield and enantiomeric purity of product.

Hedström and co-workers[23] prepared a hen albumin/chitosan cryogel with the covalently co-immobilized alkaline proteases savinase and esperase. This cryogel-based biocatalyst was shown to enable fast and continuous degradation of the protein *staphylococcal* enterotoxin B, when it was pumped through the cryogel column. The immobilized enzymes showed enhanced stability as they maintained more than 70% of their activity over seven days stored at 40°C.

In **paper III** hydrophilic, poly(ether amine) cryogels were prepared from macromonomers of two different chain lengths. Subsequently, the cysteine protease papain was covalently immobilized on the aldehyde-activated supports resulting in two cryogels with papain located on spacers with different lengths, i.e. in different distance from the pore wall.

The immobilized papain's activity towards hydrolysis of a low molecular substrate, N-benzoyl-L-arginine 4-nitroanilide (L-BAPNA), was shown to be in highly when operated in a continuous flow mode. This indicated that immobilization on the poly(ether) spacers resulted in unrestricted enzyme availability towards L-BAPNA. Furthermore, increasing the length of the spacer seemed to improve papain's availability when evaluated in a continuous flow mode.

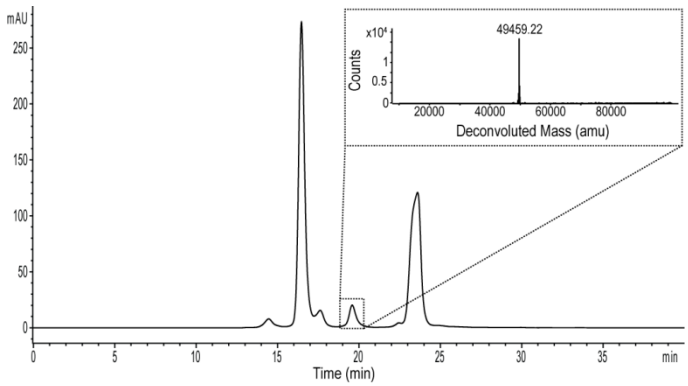

Figure 4.2. $F(ab)_2$ fragment generated by cleavage of antibody by papain immobilized on cryogel.

When tested towards a macromolecular substrate in the form of an antibody, immobilized papain was shown to hydrolyze a peptide bond in one specific position, $F(ab')_2$ fragments in low yields (Figure 4.2). This finding indicated that immobilized papain was to some degree restricted in its availability to the antibody, which resulted in incomplete hydrolysis and low yield. The findings of this study indicate that enzymes immobilized on the tested cryogels may be best suited for the conversion of low molecular substrates.

Other immobilized enzymes

Yet another enzyme which has been immobilized on cryogels is laccase. Laccase belongs to a family of oxidoreductases which catalyze the oxidation of phenolic compounds such as lignin, dyes and polyaromatic hydrocarbons.[172]

One suggested use of Laccase immobilized on cryogel is for clearance of low molecular dyes from waste waters[173]. In one study Stanescu and co-workers describe the covalent immobilization of laccase on PVA-cryogel beads through different chemical routes, namely by coupling to aldehyde, carbodimide or aldehyde-β-alanin-carbodiimide. In this study it was shown that immobilization

onto the PVA cryogel improved the pH tolerance of laccase as well as its stability when stored over time. On the other hand there was no pronounced effect of spacer or immobilization strategy[169].

In another study laccase was attached on a poly(DMAA-*co*-MBAA-*co*-AGE) cryogel through coordinative immobilization onto an IMAC ligand. As in the former study, it was seen that the immobilized enzyme had an increased shelf life as well as its pH optimum increased by one unit. The activity of the immobilized laccase was evaluated based on its activity towards oxidation of two aromatic dyes and in both cases immobilized laccase had a lower activity than free enzyme[173].

The strategy of immobilizing enzyme on cryogels through affinity interaction with an immobilized ligand was also utilized in other studies. Tüzmen and co-workers also adopted this technique for the immobilization of catalase on a poly(AAm-*co*-MBAAm-*co*-AGE) cryogel[174]. Also the glycoprotein binding ligand Con A has been used in the immobilization of inulinase and invertase onto poly(ethylene glycol dimethacrylate) cryogels[175, 176].

Another kind of solid support bioprocessing application is described in **paper II.** This study describes how a thiol functionalized cryogel was used for the selective reduction of a cysteine residue in a recombinant human growth hormone variant. In this application the thiol functionalized cryogel constituted a solid phase reducing agent for the bioconversion of growth hormone. Thiols were present on the cryogel in such high concentrations compared to the biomacromolecule that, for any practical application, thiols would never be exhausted by complete oxidation.

Interestingly in this particular application the cryogel performed as a high capacity material, contrary to the common perception of cryogels as low capacity materials. For this application, the cryogel exhibited a high reducing capacity and a mild treatment of the human growth hormone variant rendering the structural disulfides unaffected (Figure 4.3) which constituted an improved method compared to the existing utilizing a solubilized, low molecular reducing agent.

Furthermore, the apparently straight forward adaptation of the cryogel in column mode would render it easier to integrate into an existing downstream process. The novel concept of using a cryogel with an immobilized low molecular agent for bioconversions may in the described case as well as in other cases represent an improvement in terms of productivity and cost efficiency.

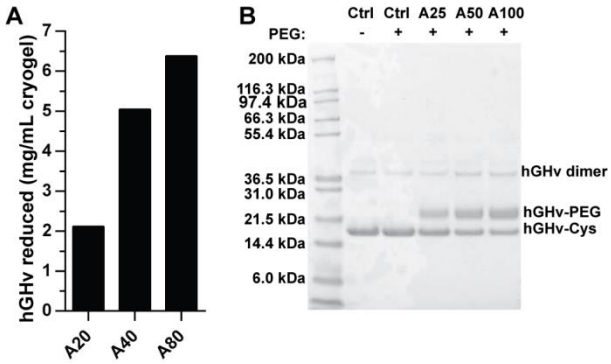

Figure 4.3. Selective reduction of a human growth hormone variant (hGHv) by cryogels with different thiol loadings. A: Amount of hGHv reduced by cryogels with increasing thiol loadings (A20→A80) after 20 hrs incubation. B: SDS-PAGE analysis of hGHv reductions after conjugation with PEG. It is seen that reduced hGHv only reacts with one molecule of PEG indicating that hGHv has been selectively reduced on the cysteine mixed disulfide leaving structural disulfides intact (**paper II**).

The use of cryogels as solid supports for enzyme immobilizations has according to the literature been shown to be a stabilizing factor, increasing the enzymes' tolerance towards pH and solvent conditions. Furthermore, it enabled reusability and storage of the enzyme. As described, cryogel based biocatalysts have been prepared with a range of different enzymes, but mainly with the purpose of low molecular substrate conversions.

Hence, not many studies have focused on applications involving macromolecular substrates. Nor are there many studies comparing cryogel based biocatalysts with conventional beaded resin or other monoliths. Operated in a continuous flow mode the cryogel could, in principle, be preferred over these formats due to its highly hydrophilic character, mechanical stability and tolerance towards organic solvents as well as its flow properties avoiding high back pressures and overcoming diffusional limitations.

4.3 Different cryogel formats and scale-up

Cryogels have been applied for a wide range of biotechnology applications, many of which pose interesting alternatives to existing solid support materials or even new solutions to technological challenges. However, in order to consider cryogels as realistic alternatives to traditional solid supports they must be presented in

proper housings making them adaptable to (automated) technology platforms within liquid chromatography and (linear) scale-up must be an option.

The scale-up of cryogels is not straight forward due to their preparation based on ice-templating for the molding of pores. The formation of pore forming ice crystals is dependent on the freezing regime, and attempts to prepare cryogels with increased column diameters would result in a varied pore distribution towards the column center, thus creating an inhomogeneous porous matrix and hampering the column to column reproducibility.

The literature does not present many studies addressing the issue of scaling up of cryogel columns, but Plieva and co-workers[177] have suggested the stacking of individual cryogels creating an elongated column. In this study dried poly(AAm-*co*-AGE-*co*-MBAAm) cryogels were stacked in a column and re-swollen directly in this. The column was closed in both ends and compressed by 25% to avoid any voids between individual cryogels. The column was connected to a fast protein liquid chromatography (FPLC) system and it was demonstrated that the stacked column showed similar properties to individual cryogels in terms of column back pressure and breakthrough profile under non-binding conditions[177]. Another approach to scale up of cryogels has been by casting them in plastic housings. This enabled the use of cryogels in a stirred tank, which could contain a large quantity of individual cryogels each cast in a plastic housing[178, 179].

Cryogels have been prepared to fit into a 96-well plate format and when operated in this cryogels were used for solid phase extraction of small polyaromatic hydrocarbons[180] and capture of proteins[22] and cells[20]. Fitting the cryogel into a 96-well plate can allow parallel processing, possibly by an automated system, and could serve as solid supports in the direct screening or analysis of unclarified, crude samples.

In **paper I** of this dissertation the cryogel was connected to an Äkta chromatography station and operated on this. The cryogel chromatography columns were prepared by swelling dried cryogels directly in the column, which resulted in a tight fitting. Compared to the packing of a column with traditional beaded resin, the handling of the cryogel was very quick, straight forward and easy. Yet another cryogel format compatible with column chromatography was developed by Yun and co-workers as they have prepared cryogels as large beaded particles[181, 182]. Such cryogel particles could find their use as packed beds or in stirred tanks.

Hence, cryogels can be prepared in a variety of formats, which can be fitted to conventional bioprocessing formats. However, the scalability of these materials may pose a challenge due to their method of preparation, which relies on the freezing regime of waters. For column applications, probably the stacking of cryogel disks poses a realistic solution to this issue. Also the concept of casting cryogels on plastic housings for the application in stirred tanks is a suggestion, which may render scale-up possible.

5. Conclusion

The biopharmaceutical industry is shifting its focus from traditional production schemes towards an emphasis on high throughput development aiming at decreasing the time and cost of downstream bioprocessing.

As a response to this, new solid support formats for downstream bioprocessing have emerged in the form of monoliths. These materials offer a new way of thinking bioprocessing in terms of productivity rather than capacity. The use of monoliths entail a relatively low binding capacity, a drawback which is however in many cases compensated by advantages such as minimized process time and decreased number of unit operations.

The literature offers numerous examples of analytical applications, where the use of monoliths have afforded process improvements, or even comprised a new method, which was not possible to perform by the use of a traditional support. Especially with respect to very large biomacromolecules, monoliths offer new and efficient means for analysis and purification. With the emergence of commercial methacrylate monoliths there is a great potential that this format can come to constitute the next new solid support within industrial scale bioprocessing.

Cryogels constitute an interesting class of monolithic supports primarily defined by their extremely large pores. The most important advantageous features of cryogels, are their easy, cost-efficient and environmentally friendly preparation as well as their capability of accommodating particulate liquids. Such qualities enable their potential use as disposable materials in downstream bioprocessing applications where sanitation is costly and cumbersome. However, drawbacks of cryogels are their extremely low binding capacities and their potentially rather large batch to batch variation. Due to their method of preparation, relying on the crystallization of water for the pore formation, cryogels are inherently prone to batch variations; especially scale-up poses a severe challenge.

Looking at the literature presented on various applications of cryogels an image is reflected of a type of solid support, which is very versatile and can be customized to fit a wide range of applications. Three novel applications of cryogels for

bioprocessing of biomacromolecules were presented in this dissertation. One interesting, and potentially promising, use of a cryogel is as a solid phase biomodifying agent. In **paper II** such an application was demonstrated by the selective reduction of a recombinant human growth variant. In this case the cryogel, offered a high loading of the reducing agent, a biocompatible, hydrophilic matrix and favourable flow properties, and represented an advantageous alternative to the existing process. A patent application was filed for the use of a cryogel based solid phase for the selective reduction of pharmaceutical proteins.

One of the strengths of cryogels is their physico-chemical solidity, which renders them compatible with very different biotechnology applications. In **paper I** such versatility was demonstrated by the use of the same cryogel as a solid phase in peptide chemistry and subsequently as a chromatography support.

Paper III provides proof of concept, that a protease can be immobilized on a highly hydrophilic cryogel support, while maintaining a high activity towards the hydrolysis of a low molecular weight substrate. By adapting a strategy for scale-up, e.g. either by stacking cryogel disks or by the use of plastic housings, the establishment of large scale, cryogel-based biocatalysts is feasible. For applications which are not relying on resolution, column heterogeneity may not be a major issue - such applications were described in **papers II** and **III.**

So forth, the evaluation of cryogels' applicability as solid supports in different areas of downstream bioprocessing has been performed empirically. However, predictive models are important tools, which can be used in the planning and elucidation of downstream processes. **Paper IV** of this dissertation describes the development and application of such a mathematical model for the description of selected cryogel parameters and properties. On order to design cryogels for specific applications in bioprocessing, in-depth understanding of the correlation between pore morphology and flow properties, is essential. Such insight can be obtained by the aid of mathematical models and therefore the development of more detailed models for the description of cryogels is needed.

Cryogels show great potential as solid supports in downstream bioprocessing. Hence, with a systematic and dedicated endeavour to develop methods for characterization, reproducible preparation, optimized surface chemistry as well as proper housings it is feasible that cryogels could fill a niche of disposable materials for applications within downstream bioprocessing.

Aknowledments

My postgraduate work has been divided between Novo Nordisk in Måløv and Department of Biotechnology in Lund and throughout my studies many people have helped, encouraged and supported me.

Firstly, I would like to thank **Finn Matthiesen** and **Dr. Harald Kirsebom** – your support has been invaluable.

Finn, I am forever grateful for your insightful supervision and encouragement. Your knowledge and enthusiasm for downstream processing and technologies have really opened my eyes towards this interesting field of science.

Harald, I cannot thank you enough for all the help and support you have provided throughout the course of this project. You are the only person whom has followed my project from its very beginning and I am grateful that you agreed to remain my supervisor even after you left Lund University.

Dr. Henrik Sune Andersen, thank you for taking over as my company supervisor when my first department was closed. Your knowledge of chemistry and enthusiasm for new technologies has been very inspiring to me.

Dr. Anders Lærke Nielsen, I am genuinely impressed with your knowledge of biotechnology and your level of productivity. I would like to thank you for our co-operations on producing scientific papers – they have been very learning to me.

Professor Bo Matthiasson, who took over as my university supervisor from 2010 to 2012. I thank you for taking me in as your student despite your busy schedule.

Professor Rajni Hatti-Kaul, who took over as my university supervisor from 2012. Even though we have not had many formal meetings, I am very grateful for your effort in terms of putting the defense together and helping me with the formalities.

Dr. Peter Szabo, thank you for attending at all our advisory meetings and showing an interest, even though the scope of my Ph.D. work is not so much within you area of research.

Dr. Igor Galaev and **Dr. Per-Erik Gustavsson**, I owe you both thanks for being my supervisors for the first part of my studies.

Dr. Junxian Yun, I am thankful for getting to know you and for having the opportunity to work with you in the laboratory in Lund on two occasions. I hope the future can bring more co-operations.

Departments 1376 and **1364** at Novo Nordisk, Måløv. Thank you all for providing a friendly and helpful atmosphere. I owe a special thanks to **Dr. Anja Kallesøe Pedersen** and **Connie Vinther** for helping me with the comprehensive RP-HPLC analyses for paper II.

Gitte and **Marianne**, thank you for some nice times at lunch and all the office chit-chats. **Henrik** and **Anne**, I have really enjoyed sharing the laboratory with you – thanks for that and for always being helpful. **Pernille**, thanks for our lonesome coffees in Måløv on the weekends and our chatting on Lync – it has been a life saver. **Line**, thanks for invaluable encouragement and a belief in my skills.

Also thanks to **Siv** and the best of luck to all past and present members of the **cryogel group** at Department of Biotechnology – especially, **Linda, Solmaz** and **Oksana**.

Above all, I am utmost thankful to my family, **Kristoffer** and **Peter**, whom have supported and believed in me through all the ups and downs. Also tremendous thanks to my **Dad** and **Annette** and **Ole** and **Else**, your help and support during these years has been invaluable.

Finally, great thanks are owed to **The Novo Nordisk STAR programme** and **The Danish Agency for Science, Technology and Innovation** which have provided the financial support to this Ph.D. project.

References

1. Walsh, G. *Nat. Biotechnol.* **2010**, *9*, 917-924.
2. Johnson, I. S. *Science* **1983**, *4585*, 632-637.
3. Nissim, A.; Chernajovsky, Y. *Handb. Exp. Pharmacol.* **2008**, 3-18.
4. Spivak, J. L. *Annu. Rev. Med.* **1993**, 243-253.
5. Behme, S. *Manufacturing of Pharmaceutical Proteins. From Technology to Economy;* Wiley -VCH Verlag GmbH & Co. KGaA: Germany, 2009; .
6. Gottschalk, U. *Biotechnol. Prog.* **2008**, *3*, 496-503.
7. Cramer, S. M.; Holstein, M. A. *Current Opinion in Chemical Engineering* **2011**, *27*.
8. Shukla, A. A.; Gottschalk, U. *Trends Biotechnol.* **2013**, *3*, 147-154.
9. Shukla, A. A.; Thoemmes, J. *Trends Biotechnol.* **2010**, *5*, 253-261.
10. Carta, G.; Jungbauer, A. *Protein Chromatography. Process Development and Scale-Up;* Wiley-VCH Verlag GmbH & Co. KGaA: Darmstadt, Germany, 2010; .
11. Stickel, J. J.; Fotopoulos, A. *Biotechnol. Prog.* **2001**, *4*, 744-751.
12. Jungbauer, A. *Journal of Chromatography a* **2005**, *1*, 3-12.
13. Svec, F.; Frechet, J. M. J. *Anal. Chem.* **1992**, *7*, 820-822.
14. Mihelic, I.; Koloini, T.; Podgornik, A.; Strancar, A. *Hrc-Journal of High Resolution Chromatography* **2000**, *1*, 39-43.
15. Jungbauer, A.; Hahn, R. *Journal of Chromatography a* **2008**, *1-2*, 62-79.
16. Subramanian, G. *Biopharmaceutical Production Technology*; Wiley-VCH Verlag GmbH & Co. KGaA: Singapore, 2012; .
17. Lozinsky, V. I. *Russian Chemical Bulletin* **2008**, *5*, 1015-1032.
18. Rouquerol, J.; Avnir, D.; Fairbridge, C. W.; Everett, D. H.; Haynes, J. H.; Pernicone, N.; Ramsay, J. D. F.; Sing, K. S. W.; Unger, K. K. *Pure & Applied Chemistry* **1994**, 1739.
19. Arvidsson, P.; Plieva, F. M.; Lozinsky, V. I.; Galaev, I. Y.; Mattiasson, B. *Journal of Chromatography a* **2003**, *2*, 275-290.
20. Dainiak, M. B.; Plieva, F. M.; Galaev, I. Y.; Hatti-Kaul, R.; Mattiasson, B. *Biotechnol. Prog.* **2005**, *2*, 644-649.
21. Ahlqvist, J.; Kumar, A.; Sundstrom, H.; Ledung, E.; Hornsten, E. G.; Enfors, S. O.; Mattiasson, B. *J. Biotechnol.* **2006**, *2*, 216-225.
22. Galaev, I. Y.; Dainiak, M. B.; Plieva, F. M.; Hatti-Kaul, R.; Mattiasson, B. *Journal of Chromatography a* **2005**, *2*, 169-175.

23. Hedstrom, M.; Plieva, F.; Yu, I.; Mattiasson, G. B. *Analytical and Bioanalytical Chemistry* **2008**, *3*, 907-912.

24. Bansal, V.; Roychoudhury, P. K.; Mattiasson, B.; Kumar, A. *Journal of Molecular Recognition* **2006**, *4*, 332-339.

25. Cheeks, M. C.; Edwards, A. D.; Arnot, C. J.; Slater, N. K. H. *New Biotechnology* **2009**, *6*, 289-299.

26. Jain, E.; Karande, A. A.; Kumar, A. *Biotechnol. Prog.* **2011**, *1*, 170-180.

27. Chang, K.; Liao, H.; Chen, J. *Acta Biomaterialia* **2013**, *11*, 9012-9026.

28. Singh, D.; Zo, S. M.; Kumar, A.; Han, S. S. *Journal of Biomaterials Science-Polymer Edition* **2013**, *11*, 1343-1359.

29. Mathews, C. K.; van Holde, K. E.; Ahern, K. G. *Biochemistry;* Addison-Wesley Publishing Company: San Francisco, U.S.A., 1997; .

30. Ghanem, A.; Healey, R.; Adly, F. G. *Anal. Chim. Acta* **2013**, 1-15.

31. Petsch, D.; Anspach, F. B. *J. Biotechnol.* **2000**, *2-3*, 97-119.

32. Anspach, F. B. *J. Biochem. Biophys. Methods* **2001**, *1-3*, 665-681.

33. Janson, J.; Rydén, L. *Protein Purification: Principles, High Resolution Methods and Applications.* Wiley-VCH: United States of America, 1998; .

34. Hatti-Kaul, R.; Mattiasson, B. *Isolation and Purification of Proteins.* Biotechnology and Bioprocessing Series; Marcel Dekker, Inc.: United States of America, 2003; Vol. 27, .

35. Hjelm, H.; Hjelm, K.; Sjoquist, J. *FEBS Lett.* **1972**, *1*, 73-&.

36. Shukla, A. A.; Hubbard, B.; Tressel, T.; Guhan, S.; Low, D. *Journal of Chromatography B-Analytical Technologies in the Biomedical and Life Sciences* **2007**, *1*, 28-39.

37. Roque, A. C. A.; Lowe, C. R. *Biotechnol. Adv.* **2006**, *1*, 17-26.

38. Cheung, R. C. F.; Wong, J. H.; Ng, T. B. *Appl. Microbiol. Biotechnol.* **2012**, *6*, 1411-1420.

39. Gaberc-Porekar, V.; Menart, V. *J. Biochem. Biophys. Methods* **2001**, *1-3*, 335-360.

40. Kroeff, E. P.; Owens, R. A.; Campbell, E. L.; Johnson, R. D.; Marks, H. I. *J. Chromatogr.* **1989**, 45-61.

41. Oliveira, J. E.; Damiani, R.; Bartolini, P.; Ribela, M. T. C. P. *Journal of Chromatography a* **2007**, *1-2*, 206-211.

42. Yang, Y.; Geng, X. *Journal of Chromatography a* **2011**, *49*, 8813-8825.

43. Schwartz, W.; Judd, D.; Wysocki, M.; Guerrier, L.; Birck-Wilson, E.; Boschetti, E. *Journal of Chromatography a* **2001**, *1-2*, 251-263.

44. Chen, J.; Tetrault, J.; Zhang, Y.; Wasserman, A.; Conley, G.; DiLeo, M.; Haimes, E.; Nixon, A. E.; Ley, A. *Journal of Chromatography a* **2010**, *2*, 216-224.

45. Unger, K. K.; Jilge, G.; Kinkel, J. N.; Hearn, M. T. W. *J. Chromatogr.* **1986**, 61-72.

46. Unger, K. K.; Jilge, G.; Janzen, R.; Giesche, H.; Kinkel, J. N. *Chromatographia* **1986**, *7-12*, 379-380.

47. Afeyan, N. B.; Gordon, N. F.; Mazsaroff, I.; Varady, L.; Fulton, S. P.; Yang, Y. B.; Regnier, F. E. *J. Chromatogr.* **1990**, *1*, 1-29.
48. Gustavsson, P. E.; Larsson, P. O. *Journal of Chromatography a* **1996**, *2*, 231-240.
49. Afeyan, N. B.; Fulton, S. P.; Regnier, F. E. *J. Chromatogr.* **1991**, *1-2*, 267-279.
50. Garcia, M. C.; Marina, M. L.; Torre, M. *Journal of Chromatography a* **2000**, *1-2*, 169-187.
51. van Reis, R.; Zydney, A. *J. Membr. Sci.* **2007**, *1-2*, 16-50.
52. Ghosh, R. *Journal of Chromatography a* **2002**, *1-2*, 13-27.
53. Thommes, J.; Kula, M. R. *Biotechnol. Prog.* **1995**, *4*, 357-367.
54. Saxena, A.; Tripathi, B. P.; Kumar, M.; Shahi, V. K. *Adv. Colloid Interface Sci.* **2009**, *1-2*, 1-22.
55. Barut, M.; Podgornik, A.; Brne, P.; Strancar, A. *Journal of Separation Science* **2005**, *15*, 1876-1892.
56. Mihelic, I.; Koloini, T.; Podgornik, A.; Strancar, A. *Hrc-Journal of High Resolution Chromatography* **2000**, *1*, 39-43.
57. Mihelic, I.; Nemec, D. A.; Podgornik, A.; Koloini, T. *Journal of Chromatography a* **2005**, *1*, 59-67.
58. Podgornik, A.; Krajnc, N. L. *Journal of Separation Science* **2012**, *22*, 3059-3072.
59. Branovic, K.; Lattner, G.; Barut, M.; Strancar, A.; Josic, D.; Buchacher, A. *J. Immunol. Methods* **2002**, *1-2*, 47-58.
60. Tscheliessnig, A.; Jungbauer, A. *Journal of Chromatography a* **2009**, *13*, 2676-2682.
61. Hall, T.; Wood, D. C.; Smith, C. E. *Journal of Chromatography a* **2004**, *1-2*, 87-93.
62. Whitfield, R. J.; Battom, S. E.; Barut, M.; Gilham, D. E.; Ball, P. D. *Journal of Chromatography a* **2009**, *13*, 2725-2729.
63. Smrekar, F.; Ciringer, M.; Strancar, A.; Podgornik, A. *Journal of Chromatography a* **2011**, *17*, 2438-2444.
64. Gerster, P.; Kopecky, E.; Hammerschmidt, N.; Klausberger, M.; Krammer, F.; Grabherr, R.; Mersich, C.; Urbas, L.; Kramberger, P.; Paril, T.; Schreiner, M.; Noebauer, K.; Razzazi-Fazeli, E.; Jungbauer, A. *Journal of Chromatography a* **2013**, 36-45.
65. Ljunglof, A.; Bergvall, P.; Bhikhabhai, R.; Hjorth, R. *Journal of Chromatography a* **1999**, *1-2*, 129-135.
66. Bencina, M.; Podgornik, A.; Strancar, A. *Journal of Separation Science* **2004**, *10-11*, 801-810.
67. Etzel, M. R.; Riordan, W. T. *Journal of Chromatography a* **2009**, *13*, 2621-2624.
68. Wolfe, J.; Bryant, G.; Koster, K. L. *Cryoletters* **2002**, *3*, 157-166.
69. Kirsebom, H.; Rata, G.; Topgaard, D.; Mattiasson, B.; Galaev, I. Y. *Macromolecules* **2009**, *14*, 5208-5214.
70. Kirsebom, H.; Rata, G.; Topgaard, D.; Mattiasson, B.; Galaev, I. Y. *Polymer* **2008**, *18*, 3855-3858.

71. Kim, J.; Taki, K.; Nagamine, S.; Ohshima, M. *Chemical Engineering Science* **2008**, *15*, 3858-3863.

72. Yamamoto, T.; Sugimoto, T.; Suzuki, T.; Mukai, S. R.; Tamon, H. *Carbon* **2002**, *8*, 1345-1351.

73. Rogovina, L. Z.; Vasil'ev, V. G.; Braudo, E. E. *Polymer Science Series C* **2008**, *1*, 85-92.

74. Osada, Y.; Kajiwara, K. *Gels handbook. Volume 1: The Fundamentals.* Osada, Y. K.,K., Ed.; Academic Press: Burlington, 2001; .

75. Hoffman, A. S. *Adv. Drug Deliv. Rev.* **2012**, 18-23.

76. Lozinsky, V. I.; Plieva, F. M.; Galaev, I. Y.; Mattiasson, B. *Bioseparation* **2001**, *4-5*, 163-188.

77. Plieva, F. M.; Andersson, J.; Galaev, I. Y.; Mattiasson, B. *Journal of Separation Science* **2004**, *10-11*, 828-836.

78. Arvidsson, P.; Plieva, F. M.; Savina, I. N.; Lozinsky, V. I.; Fexby, S.; Bulow, L.; Galaev, I. Y.; Mattiasson, B. *Journal of Chromatography a* **2002**, *1*, 27-38.

79. Hajizadeh, S.; Xu, C.; Kirsebom, H.; Ye, L.; Mattiasson, B. *Journal of Chromatography a* **2013**, 6-12.

80. Le Noir, M.; Plieva, F.; Hey, T.; Guieysse, B.; Mattiasson, B. *Journal of Chromatography a* **2007**, *1-2*, 158-164.

81. Sun, X.; He, W.; Li, J.; Li, L.; Zhang, B.; Pan, T. *Journal of Polymer Science Part A-Polymer Chemistry* **2009**, *24*, 6863-6872.

82. Sun, X.; He, W.; Pan, T.; Ding, Z.; Zhang, Y. *Polymer* **2010**, *1*, 110-114.

83. Nicholson, J. W. *Chemistry of Polymers;* The Royal Society of Chemistry: Letchworth, UK, 1997; .

84. Petrov, P.; Petrova, E.; Stamenova, R.; Tsvetanov, C. B.; Riess, G. *Polymer* **2006**, *19*, 6481-6484.

85. Petrov, P.; Petrova, E.; Tsvetanov, C. B. *Polymer* **2009**, *5*, 1118-1123.

86. Arvidsson, P.; Plieva, F. M.; Lozinsky, V. I.; Galaev, I. Y.; Mattiasson, B. *Journal of Chromatography a* **2003**, *2*, 275-290.

87. Plieva, F. M.; Savina, I. N.; Deraz, S.; Andersson, J.; Galaev, I. Y.; Mattiasson, B. *Journal of Chromatography B-Analytical Technologies in the Biomedical and Life Sciences* **2004**, *1*, 129-137.

88. Persson, P.; Baybak, O.; Plieva, F.; Galaev, I. Y.; Mattiasson, B.; Nilsson, B.; Axelsson, A. *Biotechnol. Bioeng.* **2004**, *2*, 224-236.

89. Andac, M.; Galaev, I.; Denizli, A. *Journal of Separation Science* **2012**, *9*, 1173-1182.

90. Percin, I.; Yavuz, H.; Aksoz, E.; Denizli, A. *Biotechnol. Prog.* **2012**, *3*, 756-761.

91. Hajizadeh, S.; Kirsebom, H.; Leistner, A.; Mattiasson, B. *Journal of Separation Science* **2012**, *21*, 2978-2985.

92. Plieva, F. M.; Karlsson, M.; Aguilar, M. R.; Gomez, D.; Mikhalovsky, S.; Galaev, I. Y.; Mattiasson, B. *J Appl Polym Sci* **2006**, *2*, 1057-1066.

93. Kathuria, N.; Tripathi, A.; Kar, K. K.; Kumar, A. *Acta Biomaterialia* **2009**, *1*, 406-418.

94. Berillo, D.; Elowsson, L.; Kirsebom, H. *Macromolecular Bioscience* **2012**, *8*, 1090-1099.

95. Elowsson, L.; Kirsebom, H.; Carmignac, V.; Durbeej, M.; Mattiasson, B. *Journal of Materials Science-Materials in Medicine* **2012**, *10*, 2489-2498.

96. Kirsebom, H.; Mattiasson, B.; Galaev, I. Y. *Langmuir* **2009**, *15*, 8462-8465.

97. Plieva, F. M.; Karlsson, M.; Aguilar, M. R.; Gomez, D.; Mikhalovsky, S.; Galaev', I. Y. *Soft Matter* **2005**, *4*, 303-309.

98. Plieva, F.; Xiao, H.; Galaev, I. Y.; Bergenstahl, B.; Mattiasson, B. *Journal of Materials Chemistry* **2006**, *41*, 4065-4073.

99. Lozinsky, V. I.; Vainerman, E. S.; Ivanova, S. A.; Titova, E. F.; Shtilman, M. I.; Belavtseva, E. M.; Rogozhin, S. V. *Acta Polymerica* **1986**, *3*, 142-146.

100. Wu, J.; Zhao, Q.; Liang, C.; Xie, T. *Soft Matter* **2013**, *46*, 11136-11142.

101. Dinu, M. V.; Pradny, M.; Dragan, E. S.; Michalek, J. *Carbohydr. Polym.* **2013**, *1*, 170-178.

102. Dinu, M. V.; Pradny, M.; Dragan, E. S.; Michalek, J. *Journal of Polymer Research* **2013**, *11*, 285.

103. Kirsebom, H.; Topgaard, D.; Galaev, I. Y.; Mattiasson, B. *Langmuir* **2010**, *20*, 16129-16133.

104. Yao, K.; Shen, S.; Yun, J.; Wang, L.; He, X.; Yu, X. *Chemical Engineering Science* **2006**, *20*, 6701-6708.

105. Moses, J. E.; Moorhouse, A. D. *Chem. Soc. Rev.* **2007**, *8*, 1249-1262.

106. Van Camp, W.; Dispinar, T.; Dervaux, B.; Du Prez, F. E.; Martins, J. C.; Fritzinger, B. *Macromolecular Rapid Communications* **2009**, *15*, 1328-1333.

107. Yun, J.; Shen, S.; Chen, F.; Yao, K. *Journal of Chromatography B-Analytical Technologies in the Biomedical and Life Sciences* **2007**, *1*, 57-62.

108. Yao, K.; Yun, J.; Shen, S.; Chen, F. *Journal of Chromatography a* **2007**, *1-2*, 246-251.

109. Savina, I. N.; Mattiasson, B.; Galaev, I. Y. *Polymer* **2005**, *23*, 9596-9603.

110. Savina, I. N.; Mattiasson, B.; Galaev, I. Y. *Journal of Polymer Science Part A-Polymer Chemistry* **2006**, *6*, 1952-1963.

111. *IUPAC Compendium of Chemical Terminology, 2nd ed. (The "Gold book") (1997). Online corrected version (2006-): "modulus of elasticity (Youngs modulus)",E;* .

112. Ak, F.; Oztoprak, Z.; Karakutuk, I.; Okay, O. *Biomacromolecules* **2013**, *3*, 719-727.

113. Goodhew, P. J.; Humphreys, J.; Beanland, R. *Electron Microscopy and Analysis;* Taylor & Francis: London, 2001; .

114. Stokes, D. J. *Principles and Practice of Variable Pressure/Environmental Scanning Electron Microscopy (VP-ESEM);* John Wiley & Sons: U.K., 2008; .

115. Savina, I. N.; Tuncel, M.; Tuncel, A.; Galaev, I. Y.; Mattiasson, B. *Express Polymer Letters* **2007**, *4*, 189-196.

116. Savina, I. N.; Dainiak, M.; Jungvid, H.; Mikhalovsky, S. V.; Galaev, I. Y. *Journal of Biomaterials Science-Polymer Edition* **2009**, *12*, 1781-1795.

117. Matsumoto, B. *Cell Biological Applications of Confocal Microscopy.* Methods in Cell Biology, volume 70; Elsevier: 2002; .

118. Mattiasson, B.; Kumar, A.; Galaev, I. Y. *Macroporous Polymers: Production Properties and Biotechnologiccal/Biomedical Applications.* CRC Press, Tailor and Francis Group: United States of America, 2009; pp 525.

119. Savina, I. N.; Gun'ko, V. M.; Turov, V. V.; Dainiak, M.; Phillips, G. J.; Galaev, I. Y.; Mikhalovsky, S. V. *Soft Matter* **2011**, *9*, 4276-4283.

120. Gun'ko, V. M.; Savina, I. N.; Mikhalovsky, S. V. *Adv. Colloid Interface Sci.* **2013**, 1-46.

121. Gun'ko, V. M.; Mikhalovska, L. I.; Savina, I. N.; Shevchenko, R. V.; James, S. L.; Tomlins, P. E.; Mikhalovsky, S. V. *Soft Matter* **2010**, *21*, 5351-5358.

122. Yao, K. J.; Yun, J. X.; Shen, S. C.; Wang, L. H.; He, X. J.; Yu, X. M. *Journal of Chromatography a* **2006**, *1*, 103-110.

123. Jurga, M.; Dainiak, M. B.; Sarnowska, A.; Jablonska, A.; Tripathi, A.; Plieva, F. M.; Savina, I. N.; Strojek, L.; Jungvid, H.; Kumar, A.; Lukomska, B.; Domanska-Janik, K.; Forraz, N.; McGuckin, C. P. *Biomaterials* **2011**, *13*, 3423-3434.

124. Sing, K. S. W.; Everett, D. H.; Haul, R. A. W.; Moscou, L.; Pierotti, R. A.; Rouquerol, J.; Siemieniewska, T. *Pure and Applied Chemistry* **1985**, *4*, 603-619.

125. Giesche, H. *Particle & Particle Systems Characterization* **2006**, *1*, 9-19.

126. Kumar, P. S.; Onnby, L.; Kirsebom, H. *J. Hazard. Mater.* **2013**, 469-476.

127. Zheng, Y.; Gun'ko, V. M.; Howell, C. A.; Sandeman, S. R.; Phillips, G. J.; Kozynchenko, O. P.; Tennison, S. R.; Ivanov, A. E.; Mikhalovsky, S. V. *Acs Applied Materials & Interfaces* **2012**, *11*, 5936-5944.

128. Yao, K.; Yun, J.; Shen, S.; Chen, F. *Journal of Chromatography a* **2007**, *1-2*, 246-251.

129. Yun, J.; Shen, S.; Chen, F.; Yao, K. *Journal of Chromatography B-Analytical Technologies in the Biomedical and Life Sciences* **2007**, *1*, 57-62.

130. Du, K.; Yang, D.; Sun, Y. *Journal of Chromatography a* **2007**, *1-2*, 212-218.

131. Hahn, R.; Jungbauer, A. *Anal. Chem.* **2000**, *20*, 4853-4858.

132. Yun, J.; Kirsebom, H.; Galaev, I. Y.; Mattiasson, B. *Journal of Separation Science* **2009**, *15-16*, 2601-2607.

133. Cimen, D.; Denizli, A. *Colloids and Surfaces B-Biointerfaces* **2012**, 29-35.

134. Cheeks, M. C.; Kamal, N.; Sorrell, A.; Darling, D.; Farzaneh, F.; Slater, N. K. H. *Journal of Chromatography a* **2009**, *13*, 2705-2711.

135. Ceylan, S.; Odabasi, M. *Artificial cells, nanomedicine, and biotechnology (Print)* **2013**, *6*, 376-83.

136. Dainiak, M. B.; Kumar, A.; Galaev, I. Y.; Mattiasson, B. *Proc. Natl. Acad. Sci. U. S. A.* **2006**, *4*, 849-854.

137. Ahlqvist, J.; Dainiak, M. B.; Kumar, A.; Hornsten, E. G.; Galaev, I. Y.; Mattiasson, B. *Anal. Biochem.* **2006**, *2*, 229-237.

138. Dainiak, M. B.; Galaev, I. Y.; Mattiasson, B. *Journal of Chromatography a* **2006**, *2*, 145-150.

139. Noppe, W.; Plieva, F.; Galaev, I.; Vanhoorelbeke, K.; Mattiasson, B.; Deckmyn, H. *Journal of Chromatography a* **2006**, *1-2*, 79-85.

140. Noppe, W.; Plieva, F. M.; Vanhoorelbeke, K.; Deckmyn, H.; Tuncel, M.; Tuncel, A.; Galaev, I. Y.; Mattiasson, B. *J. Biotechnol.* **2007**, *3*, 293-299.

141. Noppe, W.; Plieva, F.; Galaev, I. Y.; Pottel, H.; Deckmyn, H.; Mattiasson, B. *Bmc Biotechnology* **2009**, 21.

142. Dogan, A.; Ozkara, S.; Sari, M. M.; Uzun, L.; Denizli, A. *Journal of Chromatography B-Analytical Technologies in the Biomedical and Life Sciences* **2012**, 69-76.

143. Sun, S.; Tang, Y.; Fu, Q.; Liu, X.; Du, W.; Guo, L.; Zhao, Y. *Journal of Separation Science* **2012**, *7*, 893-900.

144. Srivastava, A.; Shakya, A. K.; Kumar, A. *Enzyme Microb. Technol.* **2012**, *6-7*, 373-381.

145. Hanora, A.; Bernaudat, F.; Plieva, F. M.; Dainiak, M. B.; Bulow, L.; Galaev, I. Y.; Mattiasson, B. *Journal of Chromatography a* **2005**, *1-2*, 38-44.

146. Kempe, M.; Mosbach, K. *Journal of Chromatography a* **1995**, *1-2*, 317-323.

147. Cavus, A.; Baysal, Z.; Alkan, H. *Colloids and Surfaces B-Biointerfaces* **2013**, 84-89.

148. Andac, M.; Baydemir, G.; Yavuz, H.; Denizli, A. *Journal of Molecular Recognition* **2012**, *11*, 555-563.

149. Tamahkar, E.; Bereli, N.; Say, R.; Denizli, A. *Journal of Separation Science* **2011**, *23*, 3433-3440.

150. Bereli, N.; Andac, M.; Baydemir, G.; Say, R.; Galaev, I. Y.; Denizli, A. *Journal of Chromatography a* **2008**, *1-2*, 18-26.

151. Bereli, N.; Erturk, G.; Tumer, M. A.; Say, R.; Denizli, A. *Biomedical Chromatography* **2013**, *5*, 599-607.

152. Onnby, L.; Pakade, V.; Mattiasson, B.; Kirsebom, H. *Water Res.* **2012**, *13*, 4111-4120.

153. Le Noir, M.; Plieva, F. M.; Mattiasson, B. *Journal of Separation Science* **2009**, *9*, 1471-1479.

154. Wang, C.; Sun, Y. *Journal of Chromatography a* **2013**, 73-79.

155. Wang, C.; Dong, X.; Jiang, Z.; Sun, Y. *Journal of Chromatography a* **2013**, 20-25.

156. Billakanti, J. M.; Fee, C. J. *Biotechnol. Bioeng.* **2009**, *6*, 1155-1163.

157. Yan, C.; Shen, S.; Yun, J.; Wang, L.; Yao, K.; Yao, S. *Journal of Separation Science* **2008**, *22*, 3879-3883.

158. Hanora, A.; Plieva, F. M.; Hedstrom, M.; Galaev, I. Y.; Mattiasson, B. *J. Biotechnol.* **2005**, *4*, 421-433.

159. Kumar, A.; Plieva, F. M.; Galeav, I. Y.; Mattiasson, B. *J. Immunol. Methods* **2003**, *1-2*, 185-194.

160. Savina, I. N.; Galaev, I. Y.; Mattiasson, B. *Journal of Molecular Recognition* **2006**, *4*, 313-321.

161. DiCosimo, R.; McAuliffe, J.; Poulose, A. J.; Bohlmann, G. *Chem. Soc. Rev.* **2013**, *15*, 6437-6474.

162. Jensen, V. J.; Rugh, S. *Methods in enzymology* **1987**, 356.

163. Chandel, A. K.; Rao, L. V.; Narasu, M. L.; Singh, O. V. *Enzyme and microbial technology* **2008**, 199.

164. Holm, H.; Cowan, D. *European Journal of Lipid Science and Technology* **2008**, 679.

165. Bacheva, A. V.; Plieva, F. M.; Lysogorskaya, E. N.; Filippova, I. Y.; Lozinsky, V. I. *Bioorganic & Medicinal Chemistry Letters* **2001**, 1005.

166. Belokon, Y. N.; Kochetkov, K. A.; Plieva, F. M.; Ikonnikov, N. S.; Maleev, V. I.; Parmar, V. S.; Kumar, R.; Lozinsky, V. I. *Appl. Biochem. Biotechnol.* **2000**, *1-3*, 97-106.

167. Filippova, I. Y.; Bacheva, A. V.; Baibak, O. V.; Plieva, F. M.; Lysogorskaya, E. N.; Oksenoit, E. S.; Lozinsky, V. I. *Russian Chemical Bulletin* **2001**, 1896.

168. Plieva, F. M.; Kochetkov, K. A.; Singh, I.; Parmar, V. S.; Belokon', Y. N.; Lozinsky, V. I. *Biotechnol. Lett.* **2000**, *7*, 551-554.

169. Stanescu, M. D.; Fogorasi, M.; Shaskolskiy, B. L.; Gavrilas, S.; Lozinsky, V. I. *Appl. Biochem. Biotechnol.* **2010**, *7*, 1947-1954.

170. Glass, J. D. *Enzyme Microb. Technol.* **1981**, *1*, 2-8.

171. Kumar, D.; Bhalla, T. C. *Appl. Microbiol. Biotechnol.* **2005**, *6*, 726-736.

172. Madhavi, V.; Lele, S. S. *Bioresources* **2009**, *4*, 1694-1717.

173. Stanescu, M. D.; Sanislav, A.; Ivanov, R. V.; Hirtopeanu, A.; Lozinsky, V. I. *Appl. Biochem. Biotechnol.* **2011**, *7-8*, 1789-1798.

174. Tuzmen, N.; Kalburcu, T.; Denizli, A. *Process Biochemistry* **2012**, *1*, 26-33.

175. Altunbas, C.; Uygun, M.; Uygun, D. A.; Akgol, S.; Denizli, A. *Appl. Biochem. Biotechnol.* **2013**, *8*, 1909-1921.

176. Uygun, M.; Uygun, D. A.; Ozcaliskan, E.; Akgol, S.; Denizli, A. *Journal of Chromatography B-Analytical Technologies in the Biomedical and Life Sciences* **2012**, 73-78.

177. Plieva, F. M.; De Seta, E.; Galaev, I. Y.; Mattiasson, B. *Separation and Purification Technology* **2009**, *1*, 110-116.

178. Onnby, L.; Giorgi, C.; Plieva, F. M.; Mattiasson, B. *Biotechnol. Prog.* **2010**, *5*, 1295-1302.

179. Plieva, F. M.; Mattiasson, B. *Ind Eng Chem Res* **2008**, *12*, 4131-4141.

180. Gupta, A.; Sarkar, J.; Kumar, A. *Journal of Chromatography a* **2013**, 16-21.

181. Yun, J.; Tu, C.; Lin, D.; Xu, L.; Guo, Y.; Shen, S.; Zhang, S.; Yao, K.; Guan, Y.; Yao, S. *Journal of Chromatography a* **2012**, 81-88.

182. Yun, J.; Dafoe, J. T.; Peterson, E.; Xu, L.; Yao, S.; Daugulis, A. J. *Journal of Chromatography a* **2013**, 148-154.

Paper I

Journal of Applied Polymer Science

Dual Application of Cryogel as Solid Support in Peptide Synthesis and Subsequent Protein-Capture

Gry Ravn Jespersen,[1,2] Anders Lærke Nielsen,[2] Finn Matthiesen,[3] Henrik Sune Andersen,[2] Harald Kirsebom[1]

[1]Department of Biotechnology, Lund University, 221 00 Lund, Sweden
[2]Novo Nordisk A/S, Department of Biopharm Chemistry, Novo Nordisk Park, DK-2760 Måløv, Denmark
[3]Novo Nordisk A/S, Department of Protein Purification Technology, Novo Nordisk Park, DK-2760 Måløv, Denmark
Correspondence to: H. Kirsebom (E-mail: Harald.Kirsebom@biotek.lu.se)

ABSTRACT: The use of a cryogel in a combined application as a solid support for automated synthesis of a peptide ligand followed by affinity chromatography of a target protein is evaluated. The advantage, of synthesizing the ligand directly on the cryogel, is the circumvention of the standard process of synthesizing a peptide on a solid support, followed by cleavage, purification, analysis, and finally immobilization on the cryogel. To demonstrate the application, a peptide affinity ligand is synthesized directly on a cryogel with a yield of 28.4 μmol g^{-1} dry polymer and purity of 45% of crude product. The affinity capture of an antipeptide antibody reveals a specific binding capacity of 0.86 mg g^{-1} dry polymer. To further elucidate the general availability of a peptide ligand to a macromolecular interaction, a trypsin substrate is synthesized on a cryogel. Trypsin cleavage of immobilized substrate is determined to 1.5 μmol g^{-1} dry polymer. © 2013 Wiley Periodicals, Inc. J. Appl. Polym. Sci. 130: 4383–4391, 2013

KEYWORDS: gels; porous materials; proteins; separation techniques

Received 24 April 2013; accepted 28 June 2013; Published online 20 July 2013
DOI: 10.1002/app.39727

INTRODUCTION

As the biopharmaceutical industry expands its portfolio of recombinant protein therapeutics, the need for new and alternative methods within analysis and purification are called for.[1] Chromatography is currently employed as a primary tool in purification and analysis of many biopharmaceutical products, based on the high separation efficiencies achieved through this technique.[2] Of the different chromatographic techniques available, affinity chromatography is highly useful in the capture of a target protein, as it is based on specific interactions between target and ligand. One well characterized affinity-pair is based on an antibody, which specifically binds in a calcium dependent manner to a short peptide termed HPC4, derived from protein C.[3] This affinity tag may be used for isolation of recombinant proteins carrying the HPC4 epitope.[4]

Within affinity chromatography the application of small peptide ligands has increased due to the development of spot synthesis, which facilitates the identification of new peptide affinity ligands.[5] Subsequently, when a suitable ligand candidate has been selected, it is produced in larger scale by solid phase peptide synthesis (SPPS), cleaved off the resin, purified and finally covalently linked onto a chromatography stationary phase.

One particular class of chromatography media are collectively termed monoliths. This term refers to the fact that these stationary phases are cast as one-block, porous materials. Monoliths are characterized by a porous structure constituted by a network of interconnected macropores. These macropores enable mass transport by means of convection and thus resolutions and binding capacities that are unaffected by flow.[6] This property of monoliths makes them ideal as stationary phases in analytical applications, as has been demonstrated in several studies.[7–11] Cryogels comprise a subclass of monoliths that are polymeric gels prepared at temperatures $<0°C$ where the solvent, typically water, freezes and by this acts as porogen in forming of the polymeric network.[12] Cryogels prepared by radical polymerization of water soluble vinyl monomers are endowed with a distinct macroporous morphology and very high mechanical stability, combined with the flexibility and general biocompatibility of a hydrogel.[12,13]

To improve the current procedure for production of peptide-functionalized affinity-chromatography stationary phases it would be a significant advantage, in terms of limiting the steps of preparation and loss of ligand, if the peptide ligand was synthesized directly on the chromatographic support. Until now, only a few studies have investigated the potential of utilizing a monolithic support in peptide synthesis followed by a

chromatographic application and these studies have all been performed on poly(glycidyl methacrylate-*co*-ethylene dimethacrylate) monoliths also known as CIM® discs.[14–16]

Cryogels are easily prepared from inexpensive monomeric precursors and, as well as other monoliths, they exhibit flow-independent binding capacities.[17] A distinct feature of cryogels is that, due to their very large macropores, it is possible to apply a crude cell homogenate directly to the column without risk of pores clogging, thus circumventing prior, otherwise mandatory, steps of centrifugation and filtration.[17] These qualities render cryogels as an attractive platform for analytical chromatography applications where speed and cost efficiency are at focus. In addition, due to the potentially low cost of manufacture, cryogels could be considered as disposable materials, as the concept of single-use materials is gaining increasing interest within biotechnology applications.

To the best of our knowledge, no prior work on synthesizing a peptide ligand directly on a cryogel for the purpose of performing protein chromatography has been published. Therefore, in this study we aim at demonstrating the feasibility of the dual application of a cryogel as solid support for the synthesis of a peptide ligand, followed by affinity capture of a target protein. To do this we utilize the HPC4 peptide-tag as the model affinity-ligand synthesized directly on a cryogel, followed by specific capture of an anti-HPC4 antibody. Simultaneously, we aim at validating the applicability of a cryogel to automated laboratory systems and therefore the synthesis of the peptide is performed using a microwave assisted automated peptide synthesizer which constitutes a considerable improvement to lab-bench peptide synthesis in terms of speed and handling. The chromatography is performed using an Äkta Avant liquid chromatography station.

To further demonstrate the application of a cryogel as solid support in SPPS, and to elucidate the general availability of a peptide ligand to macromolecular interactions, we also synthesize a trypsin substrate with varying spacer length and evaluate and compare the yield of synthesis versus the degree of subsequent trypsin cleavage.

EXPERIMENTAL

Materials

N,N′-dimethylacrylamide, poly(ethylene glycol)diacrylate ($M_n \approx 250$), ammonium persulfate (APS), 4-(2-hydroxyethyl)piperazine-1-ethanesulfonic acid (HEPES), sodium chloride, Tween®80, trypsin from bovine pancreas, diisopropylethylamine (DIPEA), ethylenediamine tetraacetic acid (EDTA), and calcium chloride were all purchased from Sigma–Aldrich. *N*-(3-aminopropyl)methacrylamide was purchased from Polysciences Europe, GmbH and tetramethylethylenediamine (TEMED) was purchased from Amresco®. All L-amino acids were purchased from either Protein Technologies, Inc. or Novabiochem®, {2-[2-(fmoc-amino)ethoxy}acetic acid (oligoethylene glycol, OEG) was purchased from Novabiochem®, N^{α}-Fmoc-N^{β}-2,4-dinitrophenyl-L-2,3-diaminopropionic acid (fmoc-Dap-(Dnp)-OH) was purchased from Bachem, 2-(Boc-amino)benzoic acid (Boc-2-Abz-OH) and 4-[(2,4-dimethoxyphenyl)(Fmoc-amino)methyl]phenoxyacetic acid (RINK amide linker) were purchased from Sigma–Aldrich. Ethyl cyano(hydroxyimino)acetate (Oxyma Pure), 1-hydroxy-7-azabenzotriazole (HoAt), and 1-hydroxybenzotriazole (HOBt) were purchased from Novabiochem®, piperidine, diisopropylcarbodiimide (DIC), and trifluoroacetic acid (TFA) were purchased from Biosolve Chimie (France), triisopropylsilane (TIPS) was purchased from Fluorochem (UK) and Tentagel® RAM resin was purchased from Rapp Polymere. The 2-propanol, formic acid, *N*-methylpyrrolidone (NMP), dichloromethane (DCM), methanol, acetonitrile, diethyl ether, and acetic anhydride were all purchased from Merck Chemicals, GmbH. Purified antibodies with specificities against interleukin-21 and HPC4, respectively as well as CHO cell harvest containing antibody with alternative specificity was obtained from Novo Nordisk A/S.

Preparation of Cryogel

Prior to polymerization, inhibitors were removed from dimethylacrylamide and poly(ethylene glycol)diacrylate by passing the respective monomer through a 2 mL column of inhibitor remover purchased from Sigma–Aldrich (product no. 306312). To prepare the cryogels, a 7% (w/w) mixture of *N*-(3-aminopropyl)methacrylmide, dimethylacrylamide, and poly(ethylene glycol)diacrylate (molar equivalents 1 : 9 : 2) in Milli-Q water was prepared. TEMED, constituting 3% (w/w) of monomers, was added and the mixture was degassed with N_2 for 15 min and then cooled on ice for 30 min. Then APS, 1% (w/w) of monomers, was added and the mixture was stirred briefly before 0.2 mL of the suspension was added to glass tubes with an inner diameter of 5 mm. The glass tubes were then quickly transferred to a Jalubo, F34-EH refrigerated circulator bath (Jalubo GmbH, Germany) with a fixed temperature of −12°C. Care was taken to ensure that the content of all glass tubes was frozen within a few minutes and they were then allowed to react in the freezing bath for 24 h. The resulting cryogels were thawed at room temperature and washed with 30 column volumes of Milli-Q purified water. The cryogels were then removed from their glass tube and stored in water at 4°C until further use.

Characterization of Cryogel

To determine the polymerization yield of the prepared cryogel, samples were lyophilized and their dry weight recorded. The polymerization yield was calculated with the use of the following equation:

$$\text{Yield}\,\% = \frac{w_1}{w_0} \times 100$$

where w_0 and w_1 are the theoretical and actual dry weights, respectively.

The degree of swelling of unmodified cryogels in water and NMP was determined by swelling dry samples in the respective solvent for a minimum of 5 h. The degree of swelling was then calculated with the use of the following equation:

$$\text{Swelling} = \frac{w_2 - w_1}{w_1}$$

where w_1 and w_2 are the dry and swollen weights of the sample, respectively.

To visualize the pore morphology of the cryogel scanning electron microscopy was used. Samples for microscopy were prepared by cutting cryogels into thin discs which were freeze dried before they were sputter coated with a mixture of gold and palladium (40 : 60). Scanning electron microscopy was performed with a JEOL JSM-80 5600 LV microscope (Tokyo, Japan). The mean pore diameter was determined by measuring the diameter of pores identified as surface pores from representative SEM images, an average pore diameter was determined on the basis of 35 measurements. Analyses of the image were conducted using the ImageJ software, version 1.47 was employed (http//imagej.nih.gov/).

Primary Amine Loading of the Cryogel

Lyophilized cryogel samples were swollen in NMP and were each added a mixture of (0.030 mmol, 10 equiv) Fmoc-glycine-OH, (0.030 mmol. 10 equiv) HoAt, (0.030 mmol, 10 equiv) DIC and (0.038 mmol, 12 equiv) DIPEA, dissolved in 1 mL NMP. Couplings were conducted for 18 h at room temperature with vigorous mixing, followed by three washes with NMP, one with DCM, one with methanol and finally three washes with DCM. Following the coupling reaction a Kaiser test was performed revealing incomplete coupling.[18] The coupling was repeated, followed by a second Kaiser test which was also positive, thus at this point all primary amines available for coupling had been reacted. Samples were then lyophilized and weighed in order to determine their dry weights. The dry samples were then immersed in 3 mL mixture of NMP with 20% (v/v) piperidine and were allowed to react with this mixture for 1 h at room temperature with rigorous mixing. The supernatants' absorbances at 290 nm were determined by use of a Nanodrop spectrophotometer (NanoDrop 1000 Spectrophotometer, Thermo Scientific). The cryogel primary amine loading was calculated based on the concentration of fulvene-piperidine adduct in the mixture by use of Lambert-Beers law and molar absorptivity 5253 M^{-1} cm^{-1}.[19]

Automated Peptide Synthesis on Cryogel

Automated peptide synthesis on cryogels was performed on a Liberty Automated 12-channel Microwave Peptide Synthesizer® (CEM Corporation). For each synthesis 30 mg dry cryogel (equivalent to ~10 μmol primary amines) was swollen in NMP for minimum 5 h and was then placed in the microwave reactor. The excess of amino acids over cryogel primary amines, used for the couplings, was 100 molar equivalents. Fmoc-deprotection was carried out using 5% piperidine in NMP and the couplings were carried out by applying a mixture of 0.3 M amino acid and 0.3 M Oxyma in NMP and DIC, all steps were carried out applying microwaves. All peptides intended to remain attached on the cryogel support were acetylated using 1 M acetic anhydride in NMP.

When cleavage of the synthesized peptides from the solid support was required, a RINK-amide linker was initially coupled to the cryogel, followed by assembly of the peptide. All couplings were carried out as described above.

For synthesis of HPC4-peptide tag the deprotection mixture was also added 0.75 mM HOBt to minimize the formation of aspartimide by-product.[20]

For peptide synthesis on a conventional resin, amino functionalized TentaGel RAM (Rapp Polymere) (0.21 mmol primary amine/g polymer) was used in a quantity equivalent to 12 μmol primary amines. For these syntheses the same method as above was applied. For bulk production of trypsin substrate a preset 0.25 mmol method, applying amino acids in fourfold molar excess to resin primary amines, was used.

Cleavage and Deprotection of Peptides

Resin or cryogel was washed several times with DCM to remove all traces of NMP. Peptides were then cleaved off and deprotected by treatment of the resin or cryogel with a mixture of (v/v) 93% TFA, 4% TIPS and 3% Milli-Q purified water for 2 h at room temperature. The supernatant was then isolated by filtration and was evaporated with N_2 to a minimal volume. The peptide was precipitated by the addition of ice cold diethyl ether and the precipitate was isolated by centrifugation.

Peptides that were not to be cleaved off cryogel were deprotected, following the same method as described above, however, after treatment with the TFA mixture the gels were washed with DCM, NMP and Milli-Q purified water before being stored at 4°C in water until further use.

Analysis of Peptides

Mass spectrometry was performed on a Waters Acquity UPLC with a Waters Acquity UPLC BEH, C-18, 1.7 μm, 2.1 mm × 50 mm column and a Waters (Micromass) LCT Premier XE detector. Solvent A consisted of milli-Q purified water with (v/v) 0.1% formic acid and the separation was performed by applying a 5–90% linear gradient of solvent B, which consisted of acetonitrile with 0.1% (v/v) formic acid. The gradient run time was 4.0 min and the total run time was 7.0 min applying a flow rate of 0.4mL min^{-1}. Column temperature was 40°C.

Peptide purity was assessed by dissolving a small quantity in 10% acetonitrile followed by analysis on a Waters Acquity UPLC system with an Acquity UPLC BEH C18 column (1.7 μm, 2.1 mm × 150 mm) and a Waters Acquity TUV detector.

Peptide quantitation was carried out using an Antek8060 Chemiluminescence Nitrogen Detector (CLND coupled to an Agilent 1200 series HPLC-system equipped with a Phenomenex Jupiter 5u C18 300Å (100 × 4.6 mm^2) column. The sample nitrogen content was quantified by relative comparison to an internal calibration standard solution of insulin aspart, containing 0.55 mg nitrogen/mL.

Chromatography

Liquid chromatography experiments were performed on an ÄktaAvant liquid chromatography station (GE Healthcare). The dry cryogel sample was inserted into a Tricorn 5/20 column (GE Healthcare) and then swollen *in situ*. The column was connected to the Äkta system and packed by applying increasing flow until the cross column pressure increased significantly, indicating that the cryogel had reached its pressure limit and the cryogel settled at the bottom of the column. The volume of the packed cryogel was 0.2 mL.

The following method was applied to all experiments: The cryogel was equilibrated with 40 column volumes of equilibration

buffer (20 m*M* HEPES, 1.0 m*M* $CaCl_2$, 100 m*M* NaCl, 0.005% (v/v) Tween80, pH 7.5) at flow rate 2 mL min^{-1}. Then it was loaded with 2 mL of one of the following (i) anti-IL21 antibody (0.2 mg mL^{-1}) in application buffer (20 m*M* HEPES, 10 m*M* $CaCl_2$, 100 m*M* NaCl, 0.005% (v/v) Tween80, pH 7.5), (ii) anti-HPC4 antibody (0.2 mg mL^{-1}) in application buffer, (iii) cell harvest with anti-HPLC4 antibody (0.2 mg mL^{-1}) and 10 m*M* $CaCl_2$, (iv) cell harvest with 10 m*M* $CaCl_2$ at flow rate 0.5 mL min^{-1}. A wash step was performed with 80 column volumes of wash buffer (20 m*M* HEPES, 1.0 m*M* $CaCl_2$, 1*M* NaCl, 0.005% (v/v) Tween80, pH 7.5) at flow rate 2 mL min^{-1} and the column was eluted by applying 30 column volumes of elution buffer (20 m*M* HEPES, 5 m*M* EDTA, 100 m*M* NaCl, 0.005% (v/v) Tween80, pH 7.5) at flow rate 1 mL min^{-1}. As a final step the cryogel was washed with 80 column volumes of equilibration buffer. Flow through and elution was collected as 0.5 mL fractions. All experiments were repeated five times.

Size Exclusion HPLC-Analysis of Elution Fractions

The relevant eluted fractions were pooled and analyzed for concentration and purity on a Bio Sep-SEC–S3000 column (Phenomenex, Denmark) connected to a Waters Alliance HPLC-system (Waters, Denmark). Running buffer (200 m*M* sodium phosphate, 300 m*M* NaCl, 10% 2-propanol (v/v), pH 6.9), flow rate 1 mL min^{-1}, column temperature 30°C. To determine the antibody concentration in the eluates, the peak area was compared to the peak area of an antibody standard of known concentration (2.8 mg mL^{-1}) and the concentration was calculated based on this.

Protein Analysis of Elution Fractions

Qualitative protein analysis of elution fractions was performed by use of Agilent 2100 Bioanalyzer® (Agilent Technologies, Denmark). Prior to analysis, elution fractions were concentrated by centrifugation to a volume of 0.3 mL using Satorius Vivaspin 6 columns (Satorius Stedium, Germany). Protein analysis was performed according to the 2100 Bioanalyzer® Agilent protein 230 Kit protocol with the one exception that for elution fractions 20 μL was added in the sample preparation instead of 4 μL (replacing water in final sample).

Trypsin Cleavage of Substrate on Cryogel

To enable conversion of the fluorescence signal, resulting from a trypsin digest of immobilized substrate, into a measure of fluorophore concentration, a standard curve based on a full trypsin digest of different substrate concentrations, in solution, was prepared. Fluorescence was read at $\lambda_{em} = 414$ nm, $\lambda_{ex} = 325$ nm by use of a SpectraMax M2e multimode microplate reader (Molecular Devices, United States) and the concentrations tested were in the range 0–0.5 m*M*. The fluorescence of fully cleaved substrate was linear with increasing substrate concentration in the range of 0–63 μ*M*. All trypsin digests were performed in triplicates.

Cryogel samples, functionalized with trypsin substrate, were placed in polypropylene vials (Nunc, Denmark) and were then each added 2.7 mL buffer (50 m*M* HEPES, 0.1*M* NaCl, 0.02% (v/v) tween80) with 0.1 μ*M* trypsin. The samples were incubated for 2 h at room temperature with gentle shaking and subsequently the fluorescence was quantified. The same experiments were performed without the addition of trypsin to measure the background fluorescence, which was deducted from the result of the trypsin cleavage. Experiments were performed in triplicates.

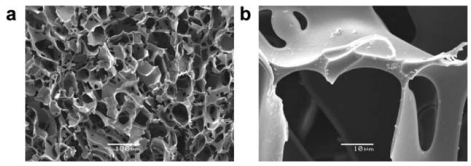

Figure 1. Scanning electron microscopy image of the macroporous cryogel morphology at 200 times (a) and 2000 times (b) magnification.

RESULTS AND DISCUSSION

Preparation and Characterization of Cryogels

A solid support suitable for peptide synthesis, as well as chromatographic applications must possess the following features (i) a uniform matrix structure, (ii) stability towards applied solvents and reagents, (iii) an appropriate functional group loading, and (iv) high swelling in appropriate solvents. The copolymerization of *N*-(3-aminopropyl)methacrylamide, dimethylacrylamide and poly(ethylene glycol)diacrylate monomers provided cryogels with reaction yields consistently around 80% indicating a straight forward and unhindered radical polymerization reaction at the applied conditions. In support of this, analysis of the pore morphology by SEM revealed a uniform macroporous matrix with pore walls that appeared smooth and with a mean pore diameter of 125 ± 34 μm (Figure 1).

The primary amine loading of the cryogel, prepared from 10% amino functional comonomer, was determined by coupling of Fmoc-protected glycine, followed by quantification of the fulvene-piperidine adduct in the supernatant after cleavage with 20% piperidine in NMP. The reactive amino loading of the cryogels was determined to 0.32 ± 0.05 mmol per gram dry polymer. This is in the same range as the amino loading of several commercial synthesis resins, and is generally considered ideal with regard to minimizing steric hindrance during synthesis.[21]

A high material swelling is desirable in SPPS, as it is synonymous with efficient distribution of solvent and reagents throughout the polymer network and thus conveys the delivery of reagents to the sites of reaction. However, monolith chromatography is based on convective flow and thus ligand–target interactions on the surface of the pore walls. Any ligands situated in the pore walls are inaccessible to the protein target and is therefore redundant with respect to chromatographic capture of target. For the specific application of using a cryogel as a solid support for ligand synthesis, followed by protein capture, it could therefore be questioned if swelling is a crucial parameter. In the present study, the swelling of the cryogel in two relevant solvents, namely water and NMP, was investigated and revealed swelling capacities of 24 mL g^{-1} dry cryogel and 19 mL g^{-1} dry cryogel, respectively. In comparison, commercial synthesis resin Tentagel S swells 3.6 mL g^{-1} dry resin and 4.7 mL g^{-1} dry resin in water and dimethylformamide, respectively,

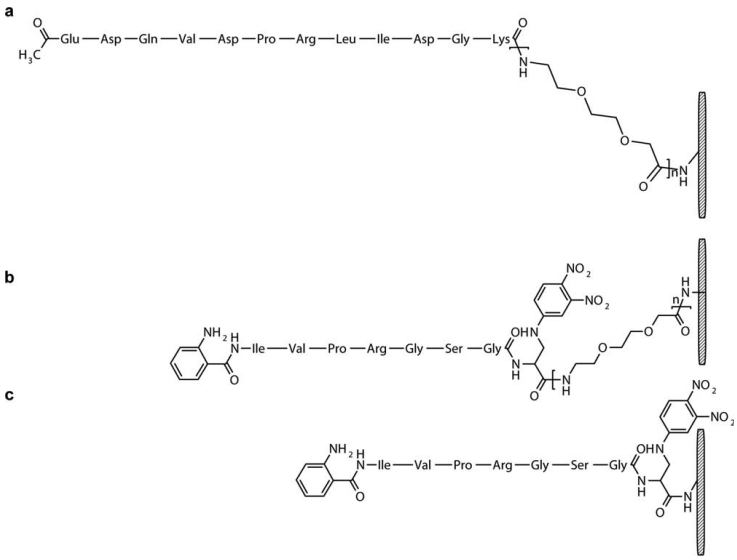

Figure 2. Structural presentation of the three peptides synthesized on cryogel. Structure a is HPC4-peptide ligand with a three OEG units spacer, b is trypsin substrate with a six (OEG)-units spacer, and c is trypsin substrate without a spacer. Flanking the trypsin substrate (b and c) is a fluorophore at the N-terminal and a fluorophore quencher at the C-terminal.

as stated by the manufacturer. The much higher swellings of the cryogel compared to Tentagel can be ascribed to the distinct porous morphology of cryogels, which typically represent porosities of >90% and therefore contain a very large fraction of the solvent in the pores.

Cryogels are macroporous, polymeric networks,[22] which in the present work were cast as cylindrically shaped monoliths. An important parameter in liquid chromatography is the mechanical stability of the stationary phase, as it must resist the pressure applied by liquid flow. To test the flow resistance the cryogel column was subjected to increasing linear flow velocities for durations of 2 min and the resulting cross column pressure was recorded. The results of this experiment showed that the cryogel column tolerated linear flow velocities up to 15 mL min^{-1} with negligible cross column pressure, while at flow rates above this, it immediately began to compress. Very high operating flow rates accompanied with low flow resistance has been reported for other cryogel systems[17] as well as for other monoliths[23] and these findings support that the macroporosity of these materials allows for the unhindered flow of water through such a column. To put this result into context, HPLC columns are typically operated in a flow rate range of 0.1–10 mL min^{-1} with concomitant very high pressures,[24] thus in this perspective monoliths could be considered as low pressure alternatives in fast flow analytical applications.

Peptide Synthesis

In this study, three different peptide constructs were synthesized on the cryogel, by the use of microwave assisted automated peptide synthesizer (Figure 2). The HPC4-peptide tag is a construct of three (OEG)-spacer units and 12 natural amino acids comprising a total of 15 sequential peptide coupling cycles. This peptide contains an Aspartic acid residue that is C-terminally linked to a Glycine residue and is thus prone to aspartimide formation during the Fmoc deprotection step. Aspartimide formation results in the loss of one molecule of water (18 g mol^{-1}) caused by a ring-closure between the β-carboxy side-chain of aspartic acid and the nitrogen of the α-carboxamide.[20,25] By addition of HOBt to the cleavage mixture the formation of aspartimide by-product was reduced to ~50% of total product. Analytical UPLC separation of the crude product revealed two large peaks comprising more than 80% of the chromatogram total peak area (Figure 3) and the mass spectrometry confirmed that the crude product consisted primarily of the product and the aspartimide by-product (Figure 4). Based on the information, provided by UPLC- and mass spectrometry analyses, it was not possible to distinguish between the HPC4-peptide tag and its aspartimide derivative. Table I displays the approximate crude product HPC4-peptide tag yield and purity which was determined to 45% and 28.4 μmol g^{-1} dry polymer, respectively.

The two trypsin substrate constructs contained a fluorophore and a fluorophore quencher, flanking a short peptide with a trypsin cleavage site located on the C-terminal side of the arginine amino residue (Figure 2). The fluorophore quencher was included to prevent the uncleaved substrate from fluorescing when tested in solution. Trypsin substrate I was synthesized directly on the cryogel matrix without insertion of a spacer,

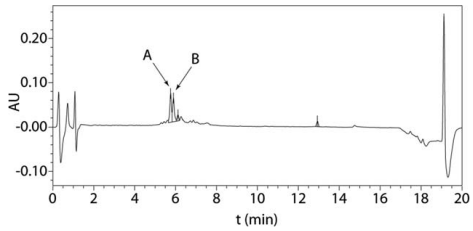

Figure 3. UPLC separation of components in the crude product of the HPC4-peptide ligand synthesized on cryogel. The two large peaks at retention times 5.8 min (arrow a) and 5.9 min (arrow b) comprise more than 80% of the total peak area and are identified as the HPC4-product and the aspartimide by-product.

whereas substrate II contained a six unit (OEG)-spacer. The two peptide constructs comprised 10 and 16 peptide couplings including the coupling of the RINK-amide linker, respectively.

UPLC analysis and nitrogen quantification of substrate I and II cleaved from cryogels showed 54 and 57% purity of crude product and 72.2 μmol and 14.4 μmol g^{-1} dry polymer, respectively (Table I). To provide a perspective on how the present cryogel performs as synthesis resin, the syntheses of substrates I and II were repeated on a conventional synthesis resin, applying the same equivalents of reagents as for the cryogels.

The synthesis on conventional resin resulted in >80% purity of the crude products and yields of 84.6 and 22.0 μmol g^{-1} dry resin for substrates I and II, respectively. The much lower purity of crude product, produced on cryogel, may be explained by the macroporous morphology of cryogel. The solute transport in the macropores is mainly driven by convection and is thus dependent on liquid flow, whereas solute transport in micropores is governed by diffusion. In the automated peptide synthesizer mixing is performed by bubbling of air through the reaction mixture and therefore we suspect that the reagents are not as evenly distributed in the cryogel and thus not as effectively delivered to the points of reaction. The TentaGel resin, on the other hand, is comprised of porous beads with a diameter of 90 μm and thus represents a combination of geometry and surface area which renders a comparably larger number of functional groups more directly available for reaction under the given automated conditions. The yield of substrates I and II produced on cryogels, as determined by nitrogen quantification was a little lower, but in the same range as the yields achieved on synthesis resin. With respect to comparison to other monoliths, Vlakh et al. have investigated the use of a CIM disc monolith as a solid support for peptide synthesis by the synthesis of a four amino acids- and an eight amino acids peptide.[14] The synthesis was performed in a flow-through mode and the purity of both peptides was found to be in the range of 80%. The fact that Vlakh et al. obtained such high product purities on a monolith can probably be attributed to their application of the flow-through mode for the synthesis. In a flow-through set-up, diffusion of reagents into the pore walls is limited and the reaction would be restricted to mainly proceed at the pore wall surface, which represents an easily accessible area with low steric hindrance. However, if it is in fact the case that reaction at the pore wall surface renders a higher purity of product, then this feature is universal to cryogels and would also be the case in the present study set-up using the peptide synthesizer, where reagents are distributed by bubbling of air through the mixture. Thus the same purity of ligand would be available to capture the target regardless of the procedure of manufacture, as ligands situated within the pore walls are inaccessible to the protein. Interestingly Vlakh et al. report to obtain the same ligand loading whether it is produced by direct synthesis or by covalent immobilization of the ligand, which supports the suggestion that application of reagents in a flow-through mode restricts the reaction to proceed solely at the surface of the pore walls.

Table I. Yield and Purity of Crude Product Produced by Automated Peptide Synthesis on Cryogel

Peptide	Yield of product (μmol g^{-1} dry polymer)	Purity of crude product (%)
$(OEG)_3$-HPC4	28.4	45
Trypsin substrate I	72.2	54
$(OEG)_6$-Trypsin substrate II	14.4	57

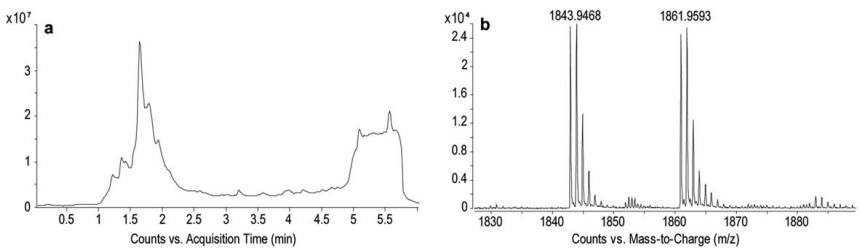

Figure 4. LC-MS analysis of crude HPC4-peptide ligand synthesized on cryogel. Image a shows the electrospray ionization TIC signal and image b is the mass spectrum. The analysis clearly shows how both HPC4-peptide (1861 g mol^{-1}) and the aspartimide by-product (1843 g mol^{-1}), which are both N-terminal acetylated, are present in the crude product.

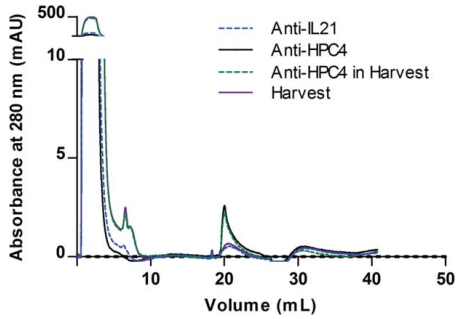

Figure 5. Overlay of chromatograms of application of anti-HPC4 antibody (dotted, blue), anti-IL21 antibody (straight, black), anti-HPC4 antibody in cell harvest (dotted, red) and cell harvest (straight, green) on HPC4-cryogel followed by elution with EDTA. Because of the high absorbance of the cell harvest, absorbances above 10 mAU are not displayed here. [Color figure can be viewed in the online issue, which is available at wileyonlinelibrary.com.]

Anti-HPC4 Antibody Binding to HPC4-Cryogel

To evaluate the binding capacity and specificity of the HPC4-peptide tag functionalized cryogels, a series of four experiments were carried out on five individual cryogels. These were mounted in commercially available columns and, connected to an Äkta Avant chromatography station. Once tightly fitted in the column and connected to the chromatography system, each cryogel was loaded with (i) anti-IL21 antibody, (ii) anti-HPC4 antibody, (iii) anti-HPC4 antibody in microfiltered cell culture broth containing antibody with alternative specificity, and (iv) microfiltered cell culture broth containing antibody with alternative specificity alone. After each application, bound protein was eluted with 5 m*M* EDTA. The HPC4-peptide tagged cryogel should have explicit specificity towards the binding of anti-HPC4 antibody and hence the applications of an anti-IL21 antibody and cell harvest served as control experiments. The 280-nm absorbance was recorded to allow comparison of loading and elution profiles of the different applications.

Comparison of the elution profiles of these four applications demonstrates the cryogel's capability of specifically capturing the anti-HPC4 antibody both in purified form and from a cell harvest (Figure 5). At the applied flow rate of 0.5 mL min^{-1} (153 cm h^{-1}), the residence time of the respective proteins in the cryogel column is 24 s, which can be regarded as very short. Figure 5 displays an overlay of chromatograms of the four different applications. At 20 mL it is very clear that anti-HPC4 antibody is eluted in a sharp peak from the application containing anti-HPC4 antibody. The sharpness of the elution peak clearly demonstrates the strong Ca^{2+} dependency of the target–ligand interaction of this system, as anti-HPC4 antibody is released from the column immediately upon addition of EDTA. The applications which did not contain anti-HPC4 antibody also show a minor UV signal at 20 mL, which is due the presence of EDTA in the elution buffer. The applications of harvest exhibit a small bump on the hind side of the application peak at ~5 mL. This is probably due to the slight retention of the cryogel column of some of the components in the harvest, which consists of a complex mixture of molecules. This retention can be elicited through either hydrophobic interactions with the cryogel matrix or by sixe exclusion effects.

The elution fractions collected from the four experiments in this study were analyzed by size exclusion HPLC to evaluate their purity and determine the binding capacities. For the application of anti-HPC4 antibody in purified form and as a component in cell harvest, the cryogels had average binding capacities of 0.86 ± 0.03 mg g^{-1} and 0.71 ± 0.10 mg g^{-1}, respectively. The slightly lower binding capacity toward anti-HPC4 antibody in cell harvest can be explained by the concomitant presence of proteins, lipids, and other cell components, which are interacting and interfering with the binding of the antibody to the peptide tag.

As mentioned, monoliths normally have binding capacities that are independent of the flow rate, a feature which most probably also applies to the present cryogel as seen by the fact that target binding is detected at a protein residence time as short as 24 s, which was the case at the conditions under study. Given that the aim of this study was to provide proof of concept that a cryogel can be used as a single solid support for the direct synthesis of ligand followed by protein target capture, no attempt was made to optimize this model affinity cryogel. A natural next step in the further development and optimization of this cryogel would be to characterize it by determining binding kinetics and evaluate how flow rate may affect binding capacity or purity of product.

To obtain an additional qualitative record of the elution fractions, they were analyzed on an Agilent 2100 Bioanalyzer (Figure 6). Prior to the analysis, it was necessary to concentrate the elution fractions, to a level above the technique's detection

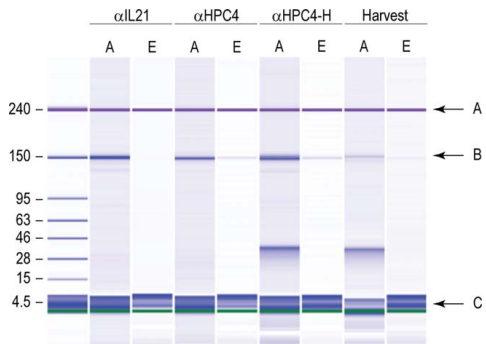

Figure 6. Bioanalyzer gel chip with application (A) and elution fractions (E) from application of anti-IL21 antibody (αIL21), anti-HPC4 antibody (αHPC4), anti-HPC4 antibody in cell harvest (αHPC4-H) and cell harvest (harvest) on HPC4-cryogel. The arrows indicate internal upper (1) and lower (3) markers and the band position at 150 kDa (2), which is the molecular weight range of antibodies. [Color figure can be viewed in the online issue, which is available at wileyonlinelibrary.com.]

limit. As the procedure of upconcentration may result in some loss of protein, the Bioanalyzer was not used for quantitation of protein contents. From the Bioanalyzer gel chip it was confirmed that the HPC4-peptide tag cryogel does not bind anti-IL21 antibody. Furthermore it can be seen that the cryogel captures anti-HPC4 antibody both in its purified form and as a component in a cell harvest. Finally it appears that the cryogel captures a faint amount of unspecified antibody present in the cell harvest (Figure 6). This binding could be due to unspecific ionic interaction with charged amino acid residues in the peptide ligand and is so minor that it could not be quantified by SE-HPLC and we therefore consider it as negligible, especially when anti-HPC4 antibody is present in the mixture.

The binding capacity of the HPC4-tag functionalized cryogel, towards the anti-HPC4 antibody, was low, especially when compared to the determined HPC4-peptide tag ligand loading (Table I). It appears that only a very small fraction of the ligands present on the cryogel were available for binding of the antibody. Studies on antibody capture using cryogels generally show markedly higher binding capacities than the ones reported here.[26–30] The binding capacity can be directly related to the surface area of the cryogel that is available for antibody interaction, and in a monolith, such as these cryogels, this is the surface area of the macropores. The size and morphology of cryogel macropores depend on the conditions applied during polymerization and therefore the area of macropores varies between different cryogel systems.[31–33] At present there is no effective method for measuring the specific area of the macropores in a soft monolith, such as a cryogel, and therefore direct comparison of macromolecule binding capacities of different cryogel systems is problematic.

Trypsin Cleavage of Substrate with Varying OEG-Spacer Synthesized Directly on the Cryogel

As shown above, we were able to manufacture a peptide ligand on a cryogel that selectively binds its target protein, but the binding capacity was unexpectedly low. Therefore, we wanted to elucidate the general availability of peptide ligands synthesized directly on the cryogel matrix and the possible effect of introducing a spacer. To do this, we utilized a trypsin substrate sequence with a C-terminal di-nitrophenyl quencher and an N-terminal 2-aminobenzoic acid fluorophore. This allowed us to monitor substrate cleavage by quantifying the amount of released fluorophore.[34] The amount of cleaved substrate was determined using a standard curve correlating the amount of cleaved substrate and the resulting fluorescence.

The amount of substrate cleaved by trypsin, determined by an end-point measurement, was 1.1 μmol g^{-1} dry polymer for the substrate with no spacer and 1.5 μmol g^{-1} dry polymer for substrate with six unit (OEG)-spacer (Table II). Comparing this to the binding capacity of the HPC4-functionalized cryogels toward the anti-HPC4 antibody, which was determined to 5.7 nmol g^{-1} dry polymer, the amount of substrate available for trypsin cleavage is ~200-fold higher. This difference in availability may be explained by two factors, namely the size difference between anti-HPC4 antibody (≈150 kDa) and trypsin (23.8 kDa) and the macromolecules' different mode of interaction

Table II. Substrate I and II Loading and Yield of Trypsin Cleavage

Substrate type	Cryogel substrate loading (μmol g^{-1} dry polymer)	Substrate cleaved by 0.1 μM trypsin (μmol g^{-1} dry polymer)
Substrate I, no spacer	72.3	1.1 ± 0.1
Substrate II, $(OEG)_6$-spacer	14.4	1.5 ± 0.2

with their targets. First, the hydrodynamic radius of a typical antibody is ~5 nm, whereas the hydrodynamic radius of trypsin is ~2 nm.[35,36] Consequently, the surface area of the cryogel macropores can accommodate more molecules of trypsin compared to the antibody. Secondly, the mode of interaction of the antibody and trypsin with their respective ligands or substrate is different. The interaction between anti-HPC4 antibody and ligand is static in the sense that, when one molecule of antibody is bound it covers a specified area, and possibly other ligands in close proximity, until it is eluted. In comparison, the trypsin-substrate interaction can be described as dynamic in the sense that it is an on/off mode of interaction, thus rendering a larger surface area and amount of ligands available.

Considering the effect of insertion of a spacer on the substrate availability to cleavage, it is seen that 1.5% of the substrate without spacer is cleaved whereas 10% of the substrate with spacer is cleaved. These results indicate that insertion of a spacer enhances the availability of substrate to trypsin cleavage, which seems logical as moving the substrate away from the pore wall surface would minimize possible steric hindrances preventing trypsin from encountering the peptide cleavage site. With regard to optimization of the cryogel for chromatography these results suggest that insertion of a spacer could be an optimization parameter for increasing the ligand availability. In this study the HPC4-ligand was attached to a six-unit (OEG)-spacer, but possibly the binding capacity of the cryogel could be increased by incorporation of an even longer spacer.

The findings in this study show a large discrepancy between the cryogel ligand loading and the macromolecule binding capacity and this indicates that the investigated cryogel encompasses two distinct porous systems; (i) a porous system consisting of micro- and possibly mesopores accessible to small molecule reactions, and (ii) a porous system consisting of highly interconnected supermacropores which is accessible to macromolecules, this can be visualized by SEM (Figure 1). This feature of cryogels has been investigated and characterized in several studies and this collected work is reviewed by Gun'ko et al. 2013.[22] The surface area of the macropores of a cryogel is vanishingly small compared to that of the nano-, micro- and mesopores which comprise more than 95% of the specific surface area of a cryogel.[20] This relationship explains the observed large discrepancy between the present cryogel's ligand or substrate loading and the availability of these for macromolecular interaction.

The low binding capacity of cryogels toward proteins has long been known and recognized, but the rather high capacity

toward small molecule reactions, as observed in this study has not been thoroughly investigated.

CONCLUSIONS

The feasibility of using a cryogel in dual applications as demonstrated in this study, where a model ligand is synthesized directly on the cryogel followed by capture of the target protein, is an improvement of the existing procedure, by circumvention of time-consuming preparation steps and consequently loss of ligand. Solid phase peptide synthesis, using a cryogel as solid support was successfully performed by the use of a microwave assisted peptide synthesizer, which is a substantial improvement to lab-bench peptide synthesis in terms of reducing time consumption and work load. Furthermore the chromatography was performed by connecting the cryogel to an automated liquid chromatography station which offers the advantages of easy handling and online monitoring of key chromatography parameters such as cross column pressure, UV, pH, and conductivity. The cryogel, which was the subject of the present study, showed binding capacities which were low, but consistently reproducible as tested by five different sample cryogels, proving that the preparation procedure outlined in this study is sound. As mentioned, cryogels offer the possibility of the direct application of crude cell homogenate without prior purification. Combined with the facts that these matrices are easily prepared, inexpensive, customizable and exhibit flow independent binding make cryogels obvious candidates as solid supports in analytical chromatography applications where speed, cost efficiency and material flexibility are desired. Examples of such applications could be within online analysis of fermentation processes or the analysis of radioactive reagents where a disposable material is needed. By following the procedure outlined in this study cryogels carrying peptide ligands for analytical chromatography can easily be prepared, but to improve the purity of ligand and binding capacity of the cryogel further optimization and chromatography characterization studies must be undertaken.

REFERENCES

1. Walsh, G. *Nat. Biotechnol.* **2010**, *9*, 917.
2. Carta, G.; JUngbauer, A. Protein Chromatography: Process Development and Scale-Up; Wiley-VCH Verlag GmbH & Co. KGaA: Germany, **2010**.
3. Stearns, D. J.; Kurosawa, S.; Sims, P. J.; Esmon, N. L.; Esmon, C. T. *J. Biol. Chem.* **1988**, *2*, 826.
4. Rezaie, A. R.; Fiore, M. M.; Neuenschwander, P. F.; Esmon, C. T.; Morrissey, J. H. *Protein Expr. Purif.* **1992**, *6*, 453.
5. Frank, R. *J. Immunol. Methods* **2002**, *1*, 13.
6. Mihelic, I.; Koloini, T.; Podgornik, A.; Strancar, A. *J High Resolut Chromatogr* **2000**, *1*, 39.
7. Neff, S.; Jungbauer, A. *J. Chromatogr. A* **2011**, *17*, 2374.
8. Zacharis, C. K.; Kalaitzantonakis, E. A.; Podgornik, A.; Theodoridis, G. *J. Chromatogr A* **2007**, *1*, 126.
9. Spross, J.; Sinz, A. *Anal. Bioanal. Chem.* **2012**, *7*, 2395.
10. Strancar, A.; Barut, M.; Podgornik, A.; Koselj, P.; Schwinn, H.; Raspor, P.; Josic, D. *J. Chromatogr. A* **1997**, *1*, 117.
11. Urbas, L.; Jarc, B. L.; Barut, M.; Zochowska, M.; Chroboczek, J.; Pihlar, B.; Szolajska, E. *J. Chromatogr. A* **2011**, *17*, 2451.
12. Plieva, F. M.; Galaev, I. Y.; Mattiasson, B. *J. Sep. Sci.* **2007**, *11*, 1657.
13. Lozinsky, V. I.; Galaev, I. Y.; Plieva, F. M.; Savinal, I. N.; Jungvid, H.; Mattiasson, B. *Trends Biotechnol.* **2003**, *10*, 445.
14. Vlakh, E.; Ostryanina, N.; Jungbauer, A.; Tennikova, T. *J. Biotechnol.* **2004**, *3*, 275.
15. Pflegerl, K.; Podgornik, A.; Berger, E.; Jungbauer, A. *J. Comb. Chem.* **2002**, *1*, 33.
16. Pflegerl, K.; Podgornik, A.; Berger, E.; Jungbauer, A. *Biotechnol. Bioeng.* **2002**, *7*, 733.
17. Arvidson, P.; Plieva, F. M.; Lozinsky, V. I.; Galaev, I. Y.; Mattiasson, B. *J. Chromatogr. A* **2003**, *986*, 275.
18. Kaiser, E.; Colescot, R. L.; Bossinge, C. D.; Cook, P. I. *Anal. Biochem.* **1970**, *2*, 595.
19. Stewart, J. M.; Young, J. D. Solid Phase Peptide Synthesis; Pierce Chemical Company: Rockford, **1984**; 2nd edn., p 176.
20. Lauer, J.; Fields, C.; Fields, G. *Lett. Pept. Sci.* **1995**, *1*, 197.
21. Chan, W. C.; White, P. D.; Hames, B. D., Eds. Fmoc Solid Phase Peptide Synthesis. Oxford University Press: United States of America, **2000**.
22. Gun'ko, V. M.; Savina, I. N.; Mikhalovsky, S. V. *Adv. Colloid Interface Sci.* **2013**, *187/188*, 1.
23. Hahn, R.; Jungbauer, A. *Anal. Chem.* **2000**, *72*, 4853.
24. Skoog, D. A.; West, D. M.; Holler, F. J. Fundamentals of Analytical Chemistry, 7th ed.; Thomson Learning: United States of America, **1996**; p 701.
25. Palasek, S. A.; Cox, Z. J.; Collins, J. M. *J. Pept. Sci.* **2007**, *3*, 143.
26. Dainiak, M. B.; Kumar, A.; Plieva, F. M.; Galaev, I. Y.; Mattiasson, B. *J. Chromatogr. A* **2004**, 1/2, 93.
27. Babac, C.; Yavuz, H.; Galaev, I. Y.; Piskin, E.; Denizli, A. *React. Funct. Polym.* **2006**, *11*, 1263.
28. Alkan, H.; Bereli, N.; Baysal, Z.; Denizli, A. *Biochem. Eng. J.* **2010**, *3*, 153.
29. Alkan, H.; Bereli, N.; Baysal, Z.; Denizli, A. *Biochem. Eng. J.* **2009**, *3*, 201.
30. Bereli, N.; Erturk, G.; Denizli, A. *Sep. Sci. Technol.* **2012**, *12*, 1813.
31. Plieva, F. M.; Karlsson, M.; Aguilar, M. R.; Gomez, D.; Mikhalovsky, S.; Galaev', I. Y. *Soft Matter* **2005**, *4*, 303.
32. Plieva, F.; Xiao, H.; Galaev, I. Y.; Bergenstahl, B.; Mattiasson, B. *J. Mater. Chem.* **2006**, *41*, 4065.
33. He, X.; Yao, K.; Shen, S.; Yun, *J. Chem. Eng. Sci.* **2007**, *5*, 1334.
34. LeBonniec, B. F.; Myles, T.; Johnson, T.; Knight, C. G.; Tapparelli, C.; Stone, S. R. *Biochemistry* **1996**, *22*, 7114.
35. Armstrong, J. K.; Wenby, R. B.; Meiselman, H. J.; Fisher, T. C. *Biophys. J.* **2004**, *6*, 4259.
36. Chiu, K.; Agoubi, L. L.; Lee, I.; Limpar, M. T.; Lowe, J. W., Jr.; Goh, S. L. *Biomacromolecules* **2010**, *12*, 3688.

Paper II

Journal of Biotechnology 173 (2014) 76–85

Contents lists available at ScienceDirect

Journal of Biotechnology

journal homepage: www.elsevier.com/locate/jbiotec

A thiol functionalized cryogel as a solid phase for selective reduction of a cysteine residue in a recombinant human growth hormone variant

Gry Ravn Jespersen[a,b], Finn Matthiesen[a], Anja Kallesøe Pedersen[a], Henrik Sune Andersen[a], Harald Kirsebom[b], Anders Lærke Nielsen[a,*]

[a] Novo Nordisk A/S, Biopharmaceutical Research Unit, Novo Nordisk Park 1, DK-2760 Måløv, Denmark
[b] Lund University, Department of Chemistry, Division of Biotechnology, Getingevägen 60, SE-221 00 Lund, Sweden

ARTICLE INFO

Article history:
Received 24 September 2013
Received in revised form
18 November 2013
Accepted 31 December 2013
Available online 18 January 2014

Keywords:
Macroporous monolith
Solid phase reducing agent
Peptide disulfide
Human growth hormone

ABSTRACT

Site selective chemical modification is a preferred method, employed to prolong the circulation half-life of biopharmaceuticals. Cysteines have been used as attachment point for such modification, however, to be susceptible for chemical modification the involved thiol must be in its reduced form. Proteins often contain disulfides, which aid to maintain their tertiary structure and therefore must remain intact. Thus, methods for selectively reducing cysteine residues, introduced through site-directed mutagenesis, are of interest. In this study a macroporous, polymeric monolith was designed for selectively reducing a single cysteine residue inserted in recombinant human growth hormone (hGH). Advantages of such a material are the circumvention of the need to remove the reducing agent after reaction, as well as milder reduction conditions and a concomitant lower risk of reducing the native disulfides. The designed monolith showed very high capacity towards the selective reduction of an unpaired cysteine residue in a recombinant hGH variant. Factors influencing the selectivity and rate of reaction were investigated and it was found that monolith thiol loading, and buffer pH had an effect on the rate of reduction, whereas hGH variant concentration and buffer conductivity influenced both rate of reduction and selectivity. The developed system constitutes the basis for the development of a scalable platform for selective reduction of a capped cysteine residue in hGH.

1. Introduction

Treatment of human diseases with biopharmaceutical agents offers a number of advantages over traditional pharmaceuticals, such as high selectivity and potency, leading to potent drug action. However, the circulatory half-life of biopharmaceuticals is often short and significant efforts have been invested in the engineering of next-generation biopharmaceuticals with increased half-life (Bailon and Won, 2009).

Human growth hormone (hGH) is one example of a biopharmaceutical product for which half-life extension is desired. hGH is a 22 kDa peptide hormone with a primary structure comprised of 191 amino acids and with a tertiary structure stabilized by two cysteine bridges. The peptide hormone is secreted by the pituitary gland and stimulates the growth of bone, cartilage and muscles (Baumann, 2004).

Recombinant hGH is presently used in the treatment of various conditions resulting from hGH deficiency. Due to its short *in vivo* half-life, it is administered daily, causing inconvenience to the patients, which are often children (Saggese et al., 1998). Owing to this, recombinant human growth hormone has been the subject of a number of studies focused on extending its half-life (Finn, 2009). One method of choice has been to utilize an unpaired cysteine residue, introduced through site-directed mutagenesis, as an attachment point for introducing half-life extending polymers (Jevsevar et al., 2010).

Recombinant proteins with unpaired cysteine residues are often secreted in a form where the unpaired cysteine is capped with

Abbreviations: DTT, dithiothreitol; TCEP, tris(2-carboxyethyl)phosphine; hGHv, recombinant human growth hormone variant with an extra cysteine residue inserted; TEMED, N,N,N′,N′-tetramethylethylenediamine; DMAA, dimethylacrylamide; PEG-DA, poly(ethylene glycol)diacrylate; APS, ammonium persulfate; GSSG, glutathione disulfide; GSH, reduced glutathione; HEPES, 4-(2-hydroxyethyl)piperazine-1-ethanesulfonic acid sodium salt; TEA, triethanolamine; EDTA, ethylenediaminetetracetic acid; DTNB, 5,5′-dithiobis-(2-nitrobenzoic acid); SEM, scanning electron microscopy; PEG-MAL, α-methoxy-ω-maleimino poly(ethylene glycol).

* Corresponding author at: Novo Nordisk A/S, Biopharmaceutical Research Unit, Novo Nordisk Park 1, C9.2.29, DK-2760 Måløv, Denmark. Tel.: +45 30 79 31 44.
E-mail address: AeLN@novonordisk.com (A.L. Nielsen).

0168-1656/$ – see front matter © 2014 Elsevier B.V. All rights reserved.
http://dx.doi.org/10.1016/j.jbiotec.2013.12.015

a thiol-containing small molecule such as cysteine or glutathione (Ostergaard and Petersen, 2008). In order to keep the production costs as low as possible, it is essential to have a high-yielding process for producing the chemically modified biopharmaceutical. One important prerequisite for a high-yielding process is the availability of a method for selectively reducing the introduced cysteine residue without reducing the native disulfides in the protein.

Today, a wide range of reducing agents are commercially available. These include the strong reducing agents such as dithiothreitol (DTT) and tris(2-carboxyethyl)phosphine (TCEP) and a number of less reactive phosphine based compounds such as *e.g.* triphenylphosphine disulfonic acid and tris(3-sulfonatephenyl)phosphine hydrate sodium salt, which are better suited for selective reductions (Burns et al., 1991; Cleland, 1964; Ostergaard and Petersen, 2008). However, the use of these soluble agents is hampered by the need for removing the reducing agent after reduction combined with the risk of unwanted reduction of native disulfides. Moreover, phosphine-based reducing agents are all relatively expensive and thus may add significantly to the cost of production. One solution could be to use a reducing agent immobilized on a suitable solid support, thereby eliminating a purification step after reduction. Moreover, restricted accessibility to native buried disulfides within the protein structure, by the immobilized reducing agent, could provide milder reducing conditions, thereby preventing unwanted reduction of native disulfides.

When selecting a solid support for such a system, scalability and manufacturing cost are important parameters, as the system should be applicable and scalable to industrial production of the biopharmaceutical, while being economically attractive, compared to the available alternatives. Due to the mode of preparation under solvent freezing conditions (Plieva et al., 2011), one class of polymeric solid phases is collectively termed cryogels. These materials are typically cast as monoliths and are characterized by a macroporous morphology, permitting mass transport through convection. Thus, the flow properties of cryogels are unaffected by diffusional limitations and high flow rates can be applied at concomitant very low column back pressures (Arvidsson et al., 2003; Plieva et al., 2011). Cryogels have been studied as solid supports in a wide range of biotechnological applications as they possess a number of desirable properties, namely, that they can be prepared with a wide range of chemical functionalities, they posses biocompatibility of hydrogels combined with compatibility with aqueous and organic solvents and they have favourable flow properties allowing for scalability (Jespersen et al., 2013; Lozinsky et al., 2003; Plieva et al., 2007, 2008, 2009). Cryogels are distinguished from other monoliths by their extremely open porous structure, which consequently renders a reduced porous surface area available for molecular interactions. However, cryogels hold a number of features of industrial relevance, such as compatibility with a wide range of different physico-chemical conditions as well as their easy, environmentally friendly and cost efficient preparation which potentially makes cryogels suited as disposable materials (Jain and Kumar, 2013; Hahn and Jungbauer, 2004). Adding to the notion of using cryogels in a disposable fashion, is the fact that these materials are very easy to handle and store. Due to their monolithic format they are easy to pack into a column and they can be dried and re-swollen, making storage until use very convenient. Based on these appealing features, a cryogel was chosen as the solid support in the present study, where a new process technology, utilizing an inexpensive solid-phase reducing agent for the selective reduction of a capped cysteine residue in a cysteine mutant, recombinant human growth hormone variant (hGHv) was developed. Cryogels with varying extents of thiol functionalization were prepared. The ability of the thiol-functionalized cryogels to act as a reducing agent was confirmed using oxidized glutathione. Subsequently it was successfully tested for selective reduction of a cysteamine capped cysteine in hGHv. An initial investigation of the influence of a number of reaction parameters, such as cryogel thiol loading, hGHv concentration and buffer pH and conductivity, was undertaken. Finally, it was demonstrated that the reduction was efficient in a setup using recirculation of the hGHv solution indicating that the process could be introduced as a column step in an industrial process.

2. Experimental

2.1. Materials

N-(3-aminopropyl)methacrylamide hydrochloride was purchased from Polysciences Inc., N,N,N′,N′-tetramethylethylenediamine (TEMED) (ultra-pure grade) was purchased from Amresco Inc., α-methoxy-ω-maleimino poly(ethylene glycol) (PEG-MAL, MW 2000 Da) was purchased from RAPP Polymere, dimethylacrylamide (99%, DMAA), poly(ethylene glycol)diacrylate (99%, average MW 258, PEG-DA), ammonium persulfate (98%, APS), 4-(2-hydroxy-1-naphthylazo)benzenesulfonic acid sodium salt (Orange II), N-acetyl homocysteine thiolactone (98%), N-acetyl cysteine (99%), L-glutathione disulfide sodium salt (98%, GSSG), pyridine (99.8%), 4-(2-hydroxyethyl)piperazine-1-ethanesulfonic acid sodium salt (99.5%, HEPES), L-cysteine (97%), sodium chloride (99.5%), triethanolamine (99%, TEA), acetic acid anhydride (98%), were all purchased from Sigma–Aldrich; ethylenediaminetetracetic acid disodium salt dehydrate (EDTA) (electrophoresis purity) was purchased from BIO-RAD, 5,5′-dithiobis-(2-nitrobenzoic acid) (DTNB) was purchased from Thermo Scientific, 1 M hydrochloric acid and 1 M sodium hydroxide were purchased from VWR; fuming hydrochloric acid (37%, 12.3 M), disodium hydrogenphosphate, sodium dihydrogenphosphate, disodium carbonate, sodium hydrogencarbonate were all of analytical grade and were purchased from Merck; trifluoroacetic acid (TFA) was purchased from Applichem; acetonitrile (HPLC grade) was purchased from Rathburn. The variant of recombinant human growth hormone (hGHv) with an extra unpaired cysteine was supplied by Novo Nordisk A/S.

2.2. Cryogel preparation

All cryogels were prepared from 7% (w/w) blends of N-(3-aminopropyl)methacrylamide and DMAA monomers in water with the following molar ratios of the two: 10:90, 25:75, 50:50, 75:25, 100:0. The gels were cross-linked with PEG-DA in a 20:80 molar ratio of PEG-DA:(N-(3-aminopropyl)methacrylamide + DMAA). In these cryogels the content of N-(3-aminopropyl)methacrylamide co-monomer comprised 0, 8, 20, 40, 60, 80% of the total co-monomers and in the following these blends will be referred to as A0, A8, A20, A40, A60, A80. Polymerization was initiated with APS and TEMED, added in a ratio of 1:99 and 3:97 to total monomer weight, respectively. The cryogels were prepared by dissolving monomers and TEMED in milli-Q water (MQ water), the mixture was degassed with N_2 for 15 min before being cooled on ice for at least 30 min. APS was added, the mixture was stirred briefly and 0.2 mL was transferred to open-ended glass tubes (Ø = 5 mm) plugged with a rubber stopper in one end. The glass tubes were placed in a pre-cooled Jalubo, F34-EH refrigerated circulator bath (Jalubo GmbH, Germany) fixed at −12 °C. After 24 h the glass tubes were thawed. The resulting cryogels were washed with at least 30 column volumes of deionized water before being removed from the glass tube and stored in deionised water at 4 °C until use.

2.3. Determination of polymerization yield and water content

The dry weights of the cryogels were determined following overnight lyophilization (Christ Gamma 1-16 LCS freeze dryer,

Martin Christ GmbH). The wet and dry weights of five replicate samples were recorded. The polymerization yield ($Y_{polym.}$) was determined using Eq. (1), where $m_{lyophil.}$ is the average dry weight of the cryogels and $m_{theoret.}$ is the theoretical dry weight at 100% polymerization yield.

$$Y_{polym.} = \frac{m_{lyophil.}}{m_{theoret.}} \times 100\% \quad (1)$$

The cryogels's water content (S_{water}) was determined from Eq. (2), where m_{wet} is the average wet weight of the replicate cryogel samples.

$$S_{water} = \frac{m_{wet} - m_{lyophil}}{m_{wet}} \times 100\% \quad (2)$$

2.4. Texture analysis

The mechanical stabilities of three replicate samples of the unmodified cryogels were determined using a texture analyser (XT2i, Stable Micro Systems, Godalming, England) with a 2 kg weight load and a cylindrical probe with a diameter of 25 mm. The cryogel samples were placed on a metal plate and the weight was applied at a test speed of 0.5 mm/s. During the test, samples were compressed to 20% of their original height and the applied force was calculated using Exponent v.5.0.9.0 software (Godalming, England). All experiments were performed at room temperature and the linear range elasticity modulus of the samples were calculated at the point of 80% of the original sample height, using the Young's modulus equation:

$$E = \frac{F/A_0}{\Delta l/L_0}$$

where E is the Young's elasticity modulus (Pa), F is the force applied (N), A_0 is the cross sectional area (m^2), Δl is the change in sample height during the compression (m) and L_0 is the sample's original height.

2.5. Scanning electron microscopy (SEM)

To visualize the pore morphology of the cryogels, thin discs were cut from the middle part of each sample. The discs were lyophilized and then sputter coated with gold/palladium (40/60). Scanning electron images were recorded using a JEOL JSM-5000LV scanning electron microscope. Mean pore diameter was determined by measuring the diameter of 25 surface pores in the SEM images, using ImageJ software version 1.46r (http://imagej.nih.gov/).

2.6. Determination of primary amine loading

4-(2-Hydroxy-1-naphthylazo)benzenesulfonic acid (Orange II) was used to quantify the primary amine loading, using a method modified from a protocol previously described (Noel et al., 2011). Three replicate cryogel samples (0.2 mL, Ø = 5 mm) of each comonomer blend were washed once with acidic solution (MQ water, pH adjusted to 3 with 1 M HCl) and then 1.5 mL of dye solution (Orange II, 14 mg/mL in acidic solution) was added. Samples were incubated for 3 h at r.t. with gentle mixing. Hereafter samples were washed extensively with the acidic solution, until no colouring of the surrounding solution was observed. The samples were then lyophilized (Christ Gamma 1-16 LCS freeze dryer, Martin Christ GmbH). Dry sample weights were recorded before Orange II was eluted from the samples by addition of 1 mL alkaline solution (MQ water, pH adjusted to 12 with 1 M NaOH) followed by incubation for 30 min at r.t. with mixing. The pH of the elution was adjusted to 2 by addition of 1% (v/v) 12.3 M HCl and the UV-absorbance at 484 nm was determined using a SpectraMax M2e multimode microplate reader (Molecular Devices, United States). The Orange II concentration was determined using an Orange II standard curve.

2.7. Thiol functionalization of amino-functionalized cryogels

Thiol groups were introduced by reacting the primary amines on the cryogel with N-acetyl homocysteine thiolactone, in all reactions the experimentally determined amine-loadings were used for the calculations. Cryogels containing the N-(3-aminopropyl)methacrylamide:dimethylacrylamide blends: 0:100, 10:90, 25:75, 50:50, 75:25 and 100:0, as previously mentioned, designated A0, A8, A20, A40, A60, A80, respectively, were reacted with 50-fold molar excess of N-acetyl homocysteine thiolactone. The reactions were performed in sodium carbonate buffer (0.1 M, 5 mM EDTA, pH 10.0) for 5 h, at r.t. Unreacted primary amines were subsequently capped by reaction with acetic anhydride containing 0.2% (v/v) pyridine for 30 min. Cryogels were then washed successively with water and sodium phosphate buffer (0.1 M, 5 mM EDTA, pH 8) until pH 8 and were then stored at 4 °C until use.

To assess the time dependency of the reaction with N-acetyl homocysteine thiolactone, three replicate A20 cryogels were reacted with 10-fold molar excess of N-acetyl homocysteine thiolactone 1 h, 2 h, 4 h, 7 h and 24 h (0.1 M sodium carbonate, 5 mM EDTA, pH 10.0) and the resulting thiol loadings were determined.

The concentration dependency of the reaction with N-acetyl homocysteine thiolactone was assessed using three replicate A20 cryogels, which were reacted for 20 h with 0, 1, 10, 50, 100-fold molar excess of N-acetyl homocysteine thiolactone (0.1 M sodium carbonate, 5 mM EDTA, pH 10.0), and the resulting thiol loadings were determined.

To investigate the pH dependency of reaction with N-acetyl homocysteine thiolactone, three replicate A20 cryogels were reacted with 50-fold molar excess of N-acetyl homocysteine thiolactone for 3 h in sodium phosphate buffer (0.1 M, 5 mM EDTA) at pH 8 or sodium carbonate buffer (0.1 M, 5 mM EDTA) at pH 10.

2.8. Determination of thiol loading on cryogel

The thiol loadings of the cryogels were quantified by the use of 5,5′-dithiobis-(2-nitrobenzoic acid) (DTNB), also known as Ellman's reagent, according to the following procedure modified from the original protocol (Ellman, 1958). Thiols were deacetylated by reaction with 0.1 M NaOH for 30 min. Samples were washed repeatedly with sodium phosphate buffer (0.1 M, 5 mM EDTA, pH 8) before the addition of 4.5 mL of DTNB (1.0 mg/mL DTNB in 0.1 M sodium phosphate, 1 mM EDTA, pH 8). Samples were incubated with this for 3 h, at r.t., with gentle mixing, and then the absorbances at 412 nm of the supernatants were recorded using a SpectraMax M2e multimode microplate reader (Molecular Devices, United States). The UV measurements where compared to an N-acetyl cysteine standard curve.

2.9. Reduction of glutathione disulfide (GSSG) using a thiol-functionalized cryogel

The functionalized cryogels were treated with 0.1 M NaOH as described above. The effect of cryogel thiol loading on the reduction of GSSG was investigated using three replicates of each A8, A20, A40, A60 and A80 cryogels. The cryogels were each added 3 mL of 7 mM GSSG in sodium phosphate buffer (0.1 M, 5 mM EDTA, pH 8). Samples were incubated with gentle mixing for 2 h at r.t. The amount of reduced glutathione (GSH) was quantified by the following procedure: 250 μL of the supernatants were mixed with 2.5 mL sodium phosphate buffer (0.1 M, 5 mM EDTA, pH 8) and 50 μL DTNB (4 mg/mL DTNB in sodium phosphate buffer) and incubated for 15 min. The absorbances were measured at 412 nm and

were recorded as described above and the UV measurements where compared to an N-acetyl cysteine standard curve.

The maximum reducing capacity of the cryogel towards GSSG was determined by the use of three replicate A80 cryogels. Each cryogel was added 3 mL of GSSG in the concentrations of 1, 2.5, 5, 10, 15 or 20 mM and were then incubated for 17 h at r.t., with mixing. The amount of GSH was determined as described above.

The reducing capacity of the A80 cryogel under flow conditions was investigated using a 1 mL (Ø = 10 mm) thiol functionalized cryogel. The cryogel was inserted into a glass column, which was connected to a peristaltic table pump (Watson-Marlow 403U/VM3, Watson-Marlow Flexicon A/S). The flow-rate was adjusted to 1 mL/min and 30 mL GSSG solution (7 mM in 0.1 M sodium phosphate, 5 mM EDTA, pH 8) was re-circulated through the cryogel. 250 μL samples were taken out at consecutive time points and the amount of GSH was determined as described above.

2.10. Selective reduction of hGHv using thiol functionalized cryogel (batch mode)

Prior to the experiments, all thiol functionalized cryogels were treated with 0.1 M NaOH for 30 min, as described above. To investigate the effect of the thiol loading on the efficiency of reduction of the cysteamine-capped hGHv, A20, A40 and A80 cryogels were each added 3 mL of 0.5 mg/mL hGHv diluted with MQ water from a stock solution of 5 mg/mL in 20 mM TEA, 100 mM NaCl, pH 7.9. The samples were incubated with mixing for 18 h, r.t.

To investigate the effect of the type of cysteine capping group, thiol-functionalized A80 cryogels were incubated with 3 mL of either cysteamine-capped or glutathione-capped hGHv (0.5 mg/mL, pH 7.9) as described above.

To investigate the effect of pH on the cryogel reduction of cysteamine-capped hGHv, the stock solution (5.0 mg/mL hGHv in 20 mM TEA, 100 mM NaCl, pH 7.9) was divided into five aliquots, which were each diluted to a concentration of 0.5 mg/mL with a buffer containing 50 mM HEPES, 150 mM NaCl and pH was adjusted to 7.0, 7.25, 7.50, 7.75 or 8.0. 3 mL of each hGHv/pH solution was added to an A60 cryogel (0.2 mL, 5 mm diameter) and was incubated with this. Samples were taken out for analysis at 1 h and 4 h. The experiment was performed in triplicates.

To investigate the effect of hGHv concentration and buffer conductivity on the reduction of cysteamine-capped hGHv a 2^2 factorial design experiment was designed and executed. Five hGHv solutions were prepared containing the following: Sample (1) hGHv 5 mg/mL in 13 mM TEA, 60 mM NaCl, pH 7.9, conductivity 6.4 mS/cm; Sample (2) hGHv 5 mg/mL in 1.3 mM TEA, 6 mM NaCl, pH 7.9, conductivity 0.6 mS/cm; Sample (3) hGHv 2.7 mg/mL in 7.1 mM TEA, 33 mM NaCl, pH 7.9, conductivity 4.0 mS/cm; Sample (4) hGHv 0.5 mg/mL in 13 mM TEA, 60 mM NaCl, pH 7.9, conductivity 6.4 mS/cm; Sample (5) hGHv 5.0 mg/mL in 1.3 mM TEA, 6 mM NaCl, pH 7.9, conductivity 0.6 mS/cm. Three mL of each solution was incubated with a cryogel (A60, 0.2 mL, 5 mm diameter), and samples were drawn for analysis at 1 h, 4 h and 20 h. All experiments were performed in triplicates and samples were analyzed in arbitrary sequences within each time block. Data were evaluated by use of the DoE section in statistical software MiniTab version14 (Minitab, Inc).

2.11. Selective reduction of hGHv using re-circulating flow

To investigate the reducing capacity of the thiol functionalized cryogel under flow conditions a 1 mL A60 (10 mm diameter) cryogel was used. The cryogel was inserted into a glass column (10 mm diameter) which was connected to a peristaltic table pump (Watson-Marlow 403 U/VM3, Watson-Marlow Flexicon A/S) and the flow was adjusted to 1 mL/min. A solution of 2.7 mg/mL cysteamine capped hGHv (7.1 mM TEA, 33 mM NaCl, pH 7.9, conductivity 4.0 mS/cm) was prepared and 15 mL of this was applied to the cryogel column by a re-circulating flow, 1 mL/min. Samples were taken for analysis at consecutive time points.

2.12. Analyses of hGHv reduction

To determine efficiency of the reduction of hGHv, the collected samples were analyzed on a RP-HPLC system (Agilent 1100 series) with an XBridge C8, 3.5 μm, 4.6 mm × 150 mm column (Waters), buffer A: 0.1% TFA in MQ water, buffer B: 0.07% TFA in acetonitrile with UV detection at 214 nm. Samples were compared to a 1.03 mg/mL hGH wildtype standard sample (Novo Nordisk).

Prior to SDS-PAGE analysis, the supernatants collected from the cryogel incubations were reacted with PEG-MAL (2 kDa) by adding the reagent to the hGHv solution in a 6.5-fold molar excess to hGHv. The reaction was allowed to proceed for 30 min at r.t., until it was quenched by addition of cysteine to a concentration of 0.15 mM. SDS-PAGE analysis was performed using a 4–12% Bis-Tris gel (Invitrogen) with MES buffer (Invitrogen) using a Mark12 protein ladder (Invitrogen), as described by the supplier.

3. Results and discussion

3.1. Cryogel preparation and physical characterization

Cryogels with varying primary amine loadings were prepared from the co-polymerization of N-(3-aminopropyl)methacrylamide (in the following referred to as "amine functionalized co-monomer"), with DMAA and PEG-DA. The loadings of the cryogels were determined by binding of the anionic dye, Orange II as described in section 2.6. To verify that no unspecific adsorption interfered with the results of this test, a cryogel prepared without amine functionalized co-monomer (cryogel A0), was subjected to the same treatment with Orange II, and no binding was detected. From Table 1, it is evident that for co-monomer blends A20, A40, A60 and A80, the measured primary amine loadings were in the same range. However, the consistently high polymerization yields (Table 1), indicate quantitative incorporation of the amine functionalized co-monomer in all cryogels. Therefore, an explanation for the observed non-linear increase in primary amine loading could be found in the method used for measuring the

Table 1
Characteristics of cryogels with varying content of amine functionalized co-monomer.

Total content of amino functionalized co-monomer	Polymerization yield (%) ($N = 3$)	Water content (g/g dry polymer) ($N = 3$)	Elasticity module (kPa) ($N = 3$)	Primary amine loading (mmol/g dry polymer) ($N = 3$)	Mean pore diameter (μm) ($N = 25$)
A8 (8%)	79 ± 4	24.2 ± 1.2	17.5 ± 0.7	0.37 ± 0.04	120 ± 36
A20 (20%)	76 ± 1	27.7 ± 1.7	20.5 ± 4.2	1.07 ± 0.30	95 ± 24
A40 (40%)	78 ± 2	32.2 ± 0.5	17.1 ± 3.7	1.21 ± 0.27	79 ± 22
A60 (60%)	78 ± 4	40.0 ± 1.5	16.3 ± 0.8	1.17 ± 0.41	69 ± 22
A80 (80%)	79 ± 2	38.7 ± 1.7	9.1 ± 0.5	0.95 ± 0.16	63 ± 21

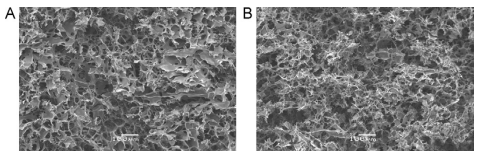

Fig. 1. Scanning electron microscopy of cryogel pore morphology at 100× magnification. Image A: cryogel A20 (with 20% amine functionalized co-monomer), image B: cryogel A80 (with 80% amine functionalized co-monomer).

primary amine loading. For cryogels with amine functionalized co-monomer contents ≥A20 it is feasible that the otherwise quantitative binding of Orange II dye is sterically hindered due to the high densities of primary amines, resulting in a lack of increase in loading between A20, A40, A60 and A80.

To determine the elasticity of the different cryogels, the Young elasticity modulus was calculated for each of the cryogels. It was found that cryogel A80 has a markedly lower elasticity than the other cryogels tested. These data indicate that addition of DMAA co-monomer has a stabilizing effect on the mechanical properties of the cryogel, possibly due to the lower hydrophilicity of the DMAA monomer, compared to the amino functionalized co-monomer. This could lead to exclusion of water from the pore walls, thereby allowing a more dense packing of the polymeric network. From the data presented in Table 1, it is also evident that an increasing primary amine content correlates with increasing water content and interestingly, a decreasing mean pore diameter (Table 1 and Fig. 1). The pore morphology of a cryogel is directly influenced by the freezing regime of water during the cryogelation process, which in turn is dependent on the type and composition of monomers (Kirsebom et al., 2010; Plieva et al., 2006). Increasing the proportion of hydrophilic, amine functionalized co-monomer could lead to a change in the freezing regime, causing the formation of smaller and more inhomogeneous ice crystals. This would result in the formation of smaller pores of the cryogel, as observed in this study. The increase in water content, correlating with an increasing proportion of amine functionalized co-monomer, is most likely due to an increased hydrophilicity of the polymeric network, allowing for a greater up-take of water into the pore walls.

3.2. Thiol functionalization of cryogels

N-acetyl homocysteine thiolactone was selected for the introduction of thiol groups in the cryogel matrix, as it is highly reactive towards primary amines and introduces a thiol on a short spacer arm (Hermanson, 2008). The applied reaction conditions were optimized with respect to pH, time and equivalents of N-acetyl homocysteine thiolactone, in order to obtain the highest possible thiol loading (Fig. 2). The highest yielding conditions were identified as pH 10 with a reaction time of 5 h and 50-fold molar excess of N-acetyl homocysteine thiolactone over the primary amine loading of the cryogels. Using these conditions, the A80 cryogel reached the highest thiol loading. The measured thiol loading of this cryogel was in the same range as the measured primary amine loading, indicating a quantitative conversion of primary amines available for reaction (Table 1 and Fig. 2).

3.3. Characterization of thiol functionalized cryogel as a reducing solid phase: reduction of a small peptide disulfide

To evaluate the capacity of the thiol functionalized cryogels for reducing a small disulfide linked molecule, GSSG was chosen as a model. Initially, the cryogels with varying monomer blends, and concomitant thiol loadings, were assessed.

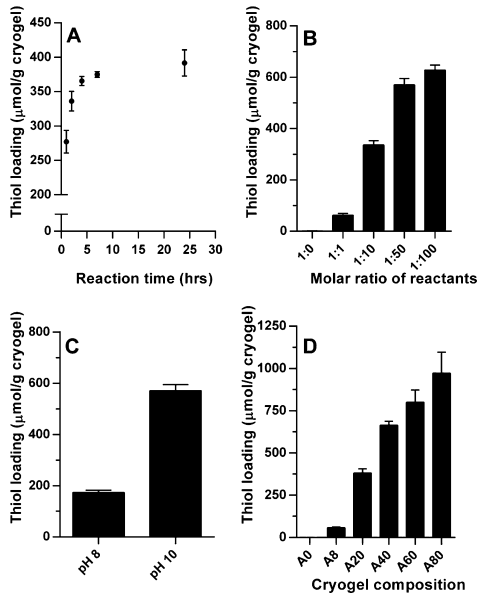

Fig. 2. Optimization of reaction conditions for thiol-functionalization of the amino-functionalized cryogels. (A) Thiol loadings resulting at different times of reaction. (B) Thiol loadings resulting from varying the excess of N-acetyl homocysteine thiolactone. (C) Thiol loadings achieved by reaction at varying pH. (D) Thiol loadings obtained for cryogels with different 3-(aminopropyl)methacrylamide co-monomer content. All data points represent the mean as SD of triplicate determinations.

The cryogels were all added the same amount of GSSG, equivalent to 5-fold molar excess of GSSG to thiols on the cryogel with the highest loading (A80), and the reaction was allowed to proceed for 2 h. The results showed that reducing capacity increased up to A40, where after it levelled off (Fig. 3A).

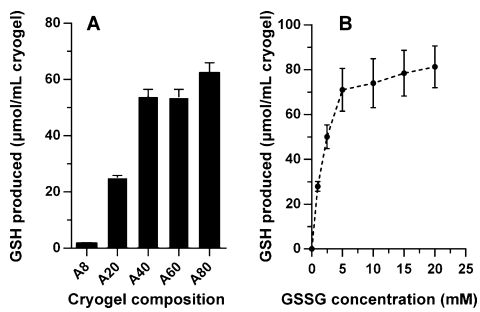

Fig. 3. Reduction of GSSG by thiol-functionalized cryogels. (A) Capacity of thiol functionalized cryogels, with varying amino functionalized co-monomer content, for reduction of GSSG, as measured by the generation of glutathione. (B) The capacity of the thiol-functionalized cryogel for reduction of GSSG at different GSSG concentrations. All data points represent triplicate determination. The dotted line is drawn to guide the eye.

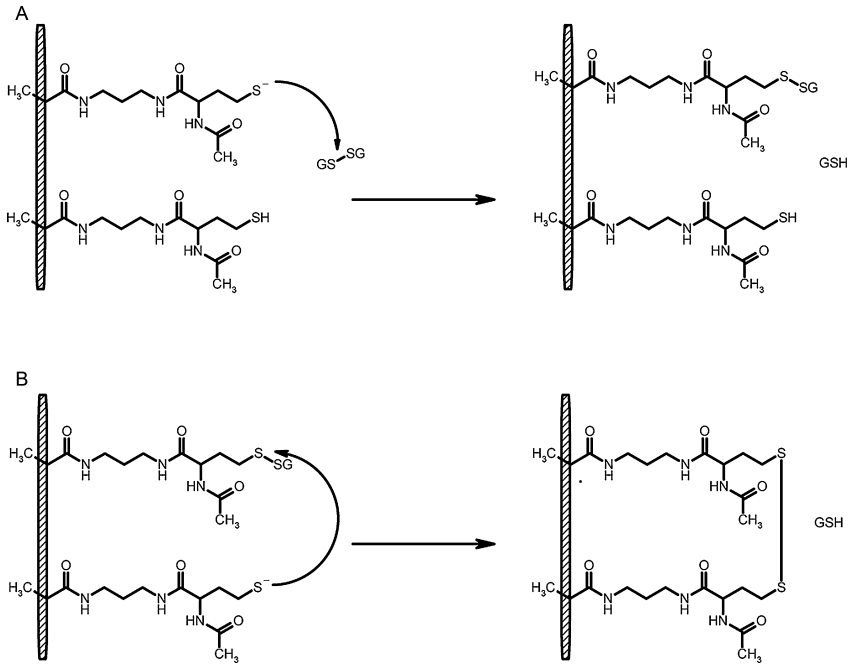

Scheme 1. Suggested mechanism for the thiol functionalized cryogel's reduction of GSSG.

An explanation to this observation could be found in the mechanism by which cryogel thiols elicit the reduction of GSSG. The disulfide exchange reaction occurs by nucleophilic attack of a thiolate ion on one of the two sulfurs of the disulfide. Such a reaction is governed by the redox potential of the reduced thiol towards the reduction of the disulfide (Gilbert, 1995). Complicating this picture is the aspect that cryogels with high thiol loadings should be regarded as two-thiol reagents, as thiols in close proximity may react with each other. Hence, the cryogel mediated thiol disulfide exchange reaction can be divided into two steps of (1) a cryogel thiol reacting with the soluble disulfide, releasing one thiol to the solution and creating a cryogel mixed disulfide, and (2) a cryogel thiol reacting with the cryogel mixed disulfide, releasing one thiol to solution and creating a cryogel intra-molecular disulfide (Scheme 1). The result of the overall reaction is a heavy cross linking of cryogel thiols, especially on high loading cryogels, which could render the remaining cryogel thiols inaccessible to reaction with the soluble disulfide.

Next, an assessment of the reducing capacity of the A80 cryogel towards different GSSG concentrations was conducted. The reaction was allowed to proceed for 17 h (Fig. 3B). It was found that the maximum reducing capacity of the cryogel was reached at GSSG concentrations of $\geq$5 mM, equivalent to approximately 2-fold excess of GSSG over measured cryogel thiols. This capacity appeared somewhat higher than the cryogel thiol loading, as measured by use of DTNB (Fig. 2D).

As mentioned, a disulfide exchange reaction is governed by the redox potentials of the participating species (Gilbert, 1995). Thus, in the system under investigation, the redox potentials of the cryogel-bound thiols and either GSSG or DTNB dictate the extent of the reduction. Additionally, time may play a role, as it is observed that GSSG reductions recorded after 17 h reaction (Fig. 3B) are much higher than reductions recorded after 2 h reaction (Fig. 3A). The thiol loading of the cryogels were determined after 3 h of reaction of DTNB with the cryogels and the reaction may therefore not have reached its maximum at this point.

To investigate the time dependency of the reducing capacity of the cryogel in flow mode, an A80 cryogel (1 mL, 10 mm diameter) was mounted in a glass column and a solution of GSSG was re-circulated through it (Fig. 4). It was found that after 5 h the maximum batch mode reducing capacity was reached (Fig. 3B and Fig. 4). Interestingly, when applying GSSG in a flow mode, a higher reducing capacity, compared to batch mode, was observed. After 20 h reaction, a reducing capacity of 132 μmol/mL cryogel was reached (Fig. 4). This is markedly higher than the measured batch mode reducing capacity, which indicates that a prolonged contact time between the cryogel and GSSG results in a faster rate–and a correspondingly higher yield of reduction.

3.4. *Thiol functionalized cryogel as a reducing solid phase: capacity towards selective reduction of hGHv*

To investigate if the thiol functionalized cryogel described in this study could be used as a solid phase in the selective reduction of a cysteine residue in a potential therapeutic protein, hGHv was used as a model compound. hGHv contains two native and one inserted, structural disulfide bridges, as well as one unpaired cysteine residue. The latter is capped as a mixed disulfide with cysteamine.

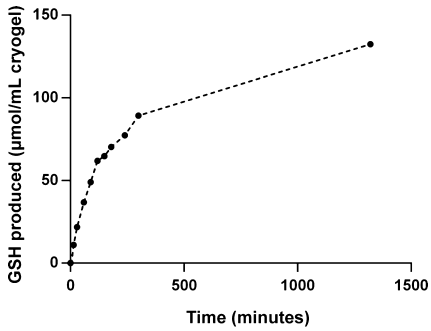

Fig. 4. GSSG reduction elicited by A100, thiol functionalized cryogel operated in flow mode. The graph shows increasing levels of GSH generated by increasing GSSG contact time with the cryogel column. The experiment was performed once, and the dotted line is drawn to guide the eye.

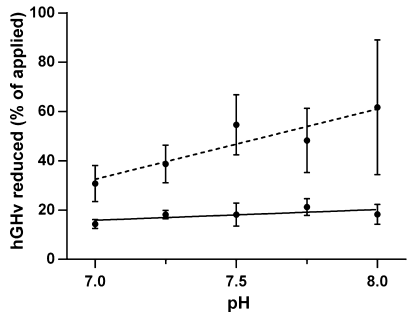

Fig. 6. Effect of increasing pH on the reduction of hGHv-cysteamine elicited by thiol A60 functionalized cryogel. The black line, linear regression is amount of hGHv reduced after 1 h reaction ($Y = 4.348X - 14.56$), the dotted line, linear regression is amount of hGHv reduced after 4 h reaction ($Y = 25.24X - 141.7$). All data points represent the mean and SD of triplicate determinations.

Initially, it was investigated if the thiol functionalized cryogel could be used in the selective reduction of the hGHv mixed disulfide. To assess the influence of the thiol loading of the cryogel on the reduction, A20, A40 and A80 cryogels were incubated with a solution of hGHv for 20 h. It was found that all cryogels were capable of reducing hGHv and that an increasing thiol loading resulted in an increasing rate of reduction as assessed by RP-HPLC (Fig. 5A). To verify that reduction had occurred exclusively on the free cysteine, the reduced hGHv was reacted with a PEG-MAL reagent (2 kDa) and analyzed by SDS-PAGE (Fig. 5B). It was found that only a single PEG moiety was incorporated in all reactions, indicating that the structural disulfide bridges were left intact.

The influence of the cysteine capping group on the rate of reduction was also investigated. A80 cryogels were incubated with hGHv capped with either cysteamine or glutathione. After 20 h incubation with the cryogels, 96% of the applied hGHv-cysteamine was reduced, whereas only 17% of the hGHv-glutathione was reduced. This is in line with the previous discussion (Section 3.3) of the dependency of the disulfide exchange rate on the redox potentials of the involved species. Moreover, steric hindrance may also play a significant role when it comes to immobilized reducing agents such as the immobilized homocysteine-like thiol under investigation.

3.5. Thiol functionalized cryogel as a reducing solid phase: effects of pH on reduction rate of recombinant human growth hormone

A disulfide exchange reaction proceeds by the attack of a nucleophilic thiolate ion on one of the two sulphur atoms of the disulfide. The rate, at which the reaction proceeds, is dependent on the fraction of deprotonated thiols, which in turn depends on the pK_a of the reducing thiol and buffer pH. The pK_a of homocysteine is 9.65 (Keire et al., 1992), and therefore, at physiological pH only a fraction of the thiols will be deprotonated. To investigate if pH has an effect on the reduction rate of the hGHv-cysteamine mixed disulfide, A60 cryogels were incubated with cysteamine capped hGHv at five different pH values spanning the range pH 7–8 (Fig. 6).

Samples were drawn after 1 h and 4 h and analyzed by RP-HPLC. A linear regression analysis of the data indicated, that after 4 h reaction, pH had a significant effect on the reduction rate of hGHv ($p < 0.01$, Fig. 6). However, one replicate sample at pH 8 represented an obvious outlier and when this sample was excluded

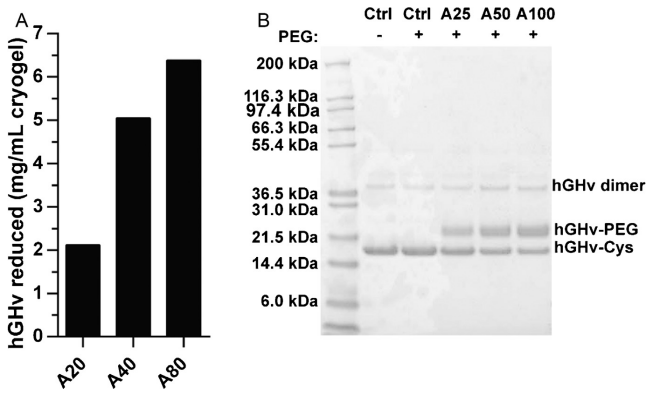

Fig. 5. Reduction of hGHv by thiol-functionalized cryogels. (A) The amount of applied hGHv reduced after 20 h reaction with cryogels with increasing thiol loadings. (B) SDS-PAGE analysis of hGHv-cysteamine reacted with cryogels A20, A40 and A80, respectively. The bands at ≈20 kDa, 22 kDa, 40 kDa are identified as hGHv, hGHv-PEG and hGHv-dimer, respectively. Experiments were performed without replicates.

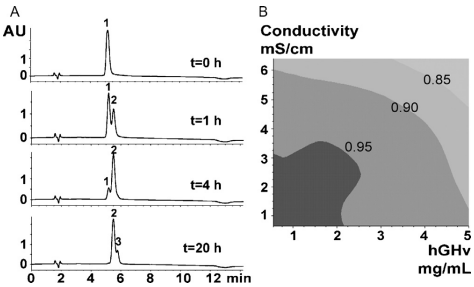

Fig. 7. RP-HPLC and statistical analysis of hGHv reduction elicited by A60 cryogel under varying conditions. (A) Detection by RP-HPLC of non-reduced hGHv (Peak 1), mono-reduced hGHv (Peak 2) and multi-reduced hGHv (Peak 3). Peak 2 and Peak 3 are formed from Peak 1 over time. (B) Contour plot showing the formation of Peak 2 as function of hGHv concentration and buffer conductivity, as calculated from experimental data in corners and centre of plot. The dark area indicate conditions strongly promoting the formation of peak 2.

from the analysis, pH showed to have a clear effect on the reduction rate after 1 h ($p < 0.001$) as well as 4 h ($p < 0.001$), analysis not shown. The results of this experiment indicated, that increasing pH increases the reduction rate of hGHv mixed disulfide. Hence, pH is a parameter of relevance when optimizing the system for an industrial process.

3.6. Thiol functionalized cryogel as a reducing solid phase: effects of protein concentration and buffer conductivity on reduction of hGHv

To further investigate factors that may influence the rate of reaction and state of the reduced product, a 2^2 factorial design experiment was set up at pH 8, using A60 cryogels. The effects of protein concentration and buffer conductivity at three consecutive time points were investigated. The state and composition of reduced protein samples were monitored after 1 h, 4 h and 20 h using RP-HPLC analysis. The analysis revealed three hGHv species in the samples, namely, non-reduced hGHv (Peak 1, Fig. 7A), hGHv mono-reduced on the mixed disulfide (Peak 2, Fig. 7A), and hGHv multi-reduced on mixed disulfide as well as on structural disulfides (Peak 3, Fig. 7A). The composition of the three states of hGHv varied with varying hGHv concentration and buffer conductivity (Table 2).

The results revealed that some fraction of hGHv was reduced in all experimental set points. However, the formation of mono-reduced hGHv was significantly affected by both protein concentration and conductivity (Fig. 7B). The highest yields of mono-reduced hGHv were observed after 20 h, in the sample containing low protein concentration and low conductivity. At higher protein concentrations or at higher conductivity, the formation of multi-reduced hGHv was observed, leading to decrease of the total yield. The calculated statistical model fitted the data very well as evaluated by the Anderson–Darling normality test on standardized residuals ($p = 0.61$, $N = 13$). This experiment shows that hGHv concentration and buffer conductivity are additional optimization parameters of relevance to an industrial process. The overall results of the statistical analysis indicate that the optimum concentration and conductivity conditions, with respect to the formation of mono-reduced product, are to be found at low hGHv concentrations and low conductivity. However, considering that the reduction rate is increased at increasing hGHv concentrations, the actual yield of mono-reduced product is higher and hence, the reaction could be stopped at an earlier time-set, this way securing a high yield and at the same time preventing the formation of multi-reduced hGHv.

3.7. Thiol functionalized cryogel as a reducing solid phase: reduction of hGHv in flow mode

As a final experiment, the capacity of the thiol functionalized cryogels to reduce cysteamine protected hGHv applied in a re-circulating flow mode was investigated. For this experiment, A60 thiol-functionalized cryogel was chosen because it combined the highest thiol loading with the highest elasticity modulus (Table 1), which is preferable when operating in a flow mode. The cryogel was inserted into a glass column and hGHv was re-circulated through it for a total duration of 20 h (Fig. 8A).

Applying hGHv in a flow mode resulted in reduction of 79% of the applied hGHv after 4 h reaction with the cryogel, which translates into a productivity of 0.12 mg mL^{-1} min^{-1}. To analyze the state of the reduced hGHv, samples drawn at the different time points were reacted with PEG-MAL (2 kDa) and subsequently analyzed by SDS-PAGE (Fig. 8B). The results showed that after 4 h reaction with the cryogel by re-circulation flow, a small amount of hGHv had been multi-reduced. This result was confirmed by the presence of peak 3 in the RP-HPLC analysis of the same sample (data not shown). For the sample obtained by batch mode reduction, no peak 3 was apparent after 4 h, which indicates that applying hGHv to the cryogel in batch mode provides a milder treatment compared to the flow

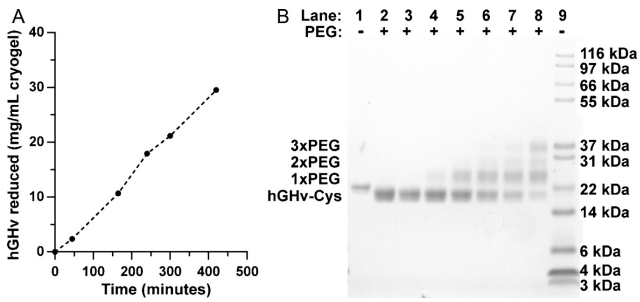

Fig. 8. A60 cryogel's reduction of hGHv-cysteamine performed in column mode. (A) The dotted line is drawn to guide the eye and represents the reduction performed by applying hGHv in a re-circulating flow. Experiments were performed without replicates. (B) SDS-PAGE analysis of time samples from cryogel's reduction of hGHv operated in flow mode. Prior to analysis samples were reacted with PEG-MAL (2 kDa). Lane 1: hGH std, Lane 2: $t = 0$, Lane 3: $t = 30$ min, Lane 4: $t = 45$ min, Lane 5: 165 min, Lane 6: 240 min, Lane 7: 420 min, Lane 8: 1200 min, Lane 9: Protein ladder.

Table 2
Composition of hGHv reduction states analyzed by RP-HPLC after reaction with thiol functionalized cryogel for 1 h, 4 h and 20 h. Each experimental set point was prepared in triplicates (except sample 3 and * labelled sample, prepared in duplicates) and samples were analyzed in random sequences. Values are shown with standard deviations.

Sample name	hGH conc. (mg/mL)	Cond. (mS/cm)	Reaction time (h)	*N*	RP-HPLC area	Fraction hGHv non-reduced (Peak 1)	Fraction hGHv mono-reduced (Peak 2)	Fraction hGHv multi-reduced (Peak 3)
1	5.0	6.4	1	3	39,872 ± 1%	0.63 ± 0.05	0.37 ± 0.05	0.00
			4	3	38,623 ± 1%	0.12 ± 0.03	0.83 ± 0.03	0.04 ± 0.00
			20	3	40,126 ± 2%	0.01 ± 0.00	0.81 ± 0.01	0.18 ± 0.01
2	5.0	0.6	1	3	39,548 ± 1%	0.63 ± 0.05	0.25 ± 0.13	0.00
			4	3	39,918 ± 3%	0.12 ± 0.03	0.85 ± 0.04	0.04 ± 0.01
			20	3	39,486 ± 1%	0.01 ± 0.00	0.90 ± 0.03	0.08 ± 0.03
3	2.9	4.0	1	2	21,257 ± 1%	0.88 ± 0.01	0.12 ± 0.01	0.00
			4	2	20,604 ± 5%	0.27 ± 0.02	0.73 ± 0.02	0.00
			20	2	21,045 ± 3%	0.00 ± 0.01	0.93 ± 0.01	0.07 ± 0.00
4	0.5	6.4	1	3	3771 ± 2%	0.84 ± 0.00	0.16 ± 0.00	0.00
			4	3	3105 ± 5%	0.59 ± 0.07	0.38 ± 0.07	0.03 ± 0.06
			20	2*	2769 ± 16%	0.07 ± 0.01	0.89 ± 0.03	0.04 ± 0.02
5	0.5	0.6	1	3	3665 ± 4%	0.90 ± 0.03	0.10 ± 0.03	0.00
			4	3	3559 ± 8%	0.63 ± 0.02	0.37 ± 0.02	0.00
			20	3	3664 ± 13%	0.02 ± 0.02	0.97 ± 0.03	0.01 ± 0.02

setup. An obvious explanation for this could be that when applying hGHv to the cryogel column through a re-circulating flow, the contact time between hGHv and the cryogel is increased and thus, the possibility of reducing the structural disulfides is increased. However, an additional explanation could be, that forcing hGHv through the cryogel column, by applying pressure, subjects the protein to shear forces by interaction with the pore wall surface, which could distort the structure and hereby expose the otherwise buried, structural disulfides.

Thus, applying hGHv to a 1 mL thiol functionalized cryogel column in a 1 mL/min re-circulating flow resulted in a productivity of 0.12 mg mL^{-1} min^{-1}, corresponding to the reduction of 7.2 mg/h for the present system and conditions. From the results presented in this study, it appears that the reduction rate is dependent on the number of contacts between hGHv and the cryogel and therefore, to increase the reaction rate, and hence the column productivity, one approach could be to increase the surface area of the column. Previous studies describe thiol functionalization of classical poly(glycidyl methacrylate-*co*-ethylene dimethacrylate) monoliths, providing a high density of thiols, comparable to the thiol loadings reported in this study (Preinerstorfer et al., 2004; Lv et al., 2012). The advantage of the classical monolith is its larger surface area, compared to the cryogel, which could probably increase the rate of reduction if it was applied for the reduction of hGHv. However, due to, the more hydrophobic nature of these monoliths there is a risk that interaction with the matrix could result in denaturation of hGHv, leading to increased over-reduction.

In addition, several studies have shown that the porous morphology of cryogels can be controlled by varying the concentration of monomer, initiator/activator and the temperature at which the polymerization proceeds (Plieva et al., 2005, 2006). By increasing the surface area the number of contacts between cryogel and hGHv per volume cryogel would increase, consequently providing an increased productivity of an optimized column. With such an optimization hGHv could be applied to the column at a lower flow-rate, thereby avoiding the harsh conditions of high flow, which presumably contribute to over reduction of hGHv. Another approach to increasing the hGHv-cryogel contact time while maintaining a low flow rate could be to increase the length of the cryogel column. Such an optimization approach would not lead to increased column productivity, but it may be a way to prevent over-reduction, while utilizing the cryogel as a process column step. In terms of increasing hGHv residence time, operating the cryogel in batch mode is an obvious alternative to the column mode. But with regard to scaling up, column mode is preferred as it is more convenient to incorporate into an already existing process. The cryogel column has the advantage of constituting a low pressure system thus imposing fewer demands on pumps and column housings and the monolithic format makes column packing easy. It is thus feasible, that with the right optimizations the thiol functionalized cryogel could constitute a column based processing step inserted immediately before modification of hGHv. The use of such an inexpensive, disposable monolithic column as reducing agent would constitute a considerable improvement to the current use of an expensive, soluble reducing agent, which must be removed after reduction.

4. Conclusion

In this study we have presented a technology that utilizes a thiol functionalized cryogel for the selective reduction of a capped cysteine residue in hGHv. The experiments presented have shown that from a series of co-monomer compositions comprised of an amino functionalized co-monomer and DMAA, the cryogel with 60% amine functionalized co-monomer (A60) had the highest elasticity modulus combined with a high thiol loading and a high reduction capacity towards both GSSG and hGHv. It was further shown that low hGHv concentrations, combined with low buffer conductivity at pH 8, afforded the best results with respect to selectivity of the reduction and yield of the reduced product. Hence, these parameters are of relevance with respect to establishing and optimizing an industrial process based on this technology. The application of a column-mode setup revealed that establishment of an industrial process based on the described technology is feasible, but further optimization with respect to the yield and the purity of product is necessary. The advantage of employing a cryogel based solid phase for this technology resides in the use of an inexpensive material, constituting a low pressure system, which allows for selective reduction of a cysteine residue in an hGH variant and circumvention of the need for removal of a soluble reducing agent following the reducing reaction. Based on the demonstrated application of the thiol functionalized cryogel, it is feasible that such a cryogel, with the proper optimizations, could find use in similar reactions involving other biopharmaceutical proteins.

Author contributions

GRJ designed research, conducted experiments, analyzed the data and wrote the manuscript. FM designed research, conducted

experiments, analyzed data and wrote the manuscript. AKP designed experiments, conducted experiments, analyzed data and wrote the manuscript. HSA designed research and wrote the manuscript. HK designed research and wrote the manuscript. ALN designed research, analyzed data and wrote the manuscript.

Conflicts of interest

GRJ, FM, AKP, HSA, ALN are employees of Novo Nordisk; GRJ, FM, AKP, HSA, ALN are inventors on a patent application covering the findings of this manuscript

Acknowledgements

The Danish Ministry of Science, Innovation and Higher Education is acknowledged for financial support of GRJ through the industrial PhD programme. We would like to thank Connie Vinther for expert technical support with respect to the RP-HPLC analyses.

References

Arvidsson, P., Plieva, F.M., Lozinsky, V.I., Galaev, I.Y., Mattiasson, B., 2003. Direct chromatographic capture of enzyme from crude homogenate using immobilized metal affinity chromatography on a continuous supermacroporous adsorbent. Journal of Chromatography A 986, 275–290.

Bailon, P., Won, C., 2009. PEG-modified biopharmaceuticals. Expert Opinion on Drug Delivery 6, 1–16.

Baumann, G., 2004. Growth hormone (GH). In: Martini, L. (Ed.), Encyclopedia of Endocrine Diseases. Elsevier, New York, pp. 383–389.

Burns, J.A., Butler, J.C., Moran, J., Whitesides, G.M., 1991. Selective reduction of disulfides by tris(2-carboxyethyl)phosphine. Journal of Organic Chemistry 56, 2648–2650.

Cleland, W.W., 1964. Dithiothreitol, a new protective reagent for SH groups. Biochemistry 3 (4), 480–482.

Ellman, G.L., 1958. A colorimetric method for determining low concentrations of mercaptans. Archives of Biochemistry and Biophysics 74, 443–450.

Finn, R., 2009. In: Veronese, F.M. (Ed.), PEGylated Protein Drugs:Basic Science and Clinical Applications. Birkhüser Verlag, Basel Switzerland, pp. 187–205.

Gilbert, H.F., 1995. Thiol/disulfide exchange equilibria and disulfide bond stability. Biothiols, Methods in Enzymology 251, 8–28.

Hahn, R., Jungbauer, A., 2004. Monoliths for fast bioseparation and bioconversion and their applications in biotechnology. Journal of Separation Science 27, 767–778.

Hermanson, G.T., 2008. Bioconjugate Techniques, 2nd ed. Elsevier, United States of America.

Jain, E., Kumar, A., 2013. Disposable polymeric cryogel bioreactor matrix for therapeutic protein production. Nature Protocols 8 (5), 821–835.

Jespersen, G.R., Nielsen, A.L., Matthiesen, F., Andersen, H.S., Kirsebom, H., 2013. Dual application of cryogel as solid support in peptide synthesis and subsequent protein-capture. Journal of Applied Polymer Science, http://dx.doi.org/10.1002/app.39727.

Jevsevar, S., Kunstelj, M., Porekar, V.G., 2010. PEGylation of therapeutic proteins. Biotechnology Journal 5, 113–128.

Keire, D.A., Strauss, E., Guo, W., Noszal, B., Rabenstein, D.L., 1992. Kinetics and equilibria of thiol disulfide interchange reactions of selected biological thiols and related molecules with oxidized glutathione. Journal of Organic Chemistry 57, 123–127.

Kirsebom, H., Topgaard, D., Galaev, I.Y., Mattiasson, B., 2010. Modulating the porosity of cryogels by influencing the nonfrozen liquid phase through the addition of inert solutes. Langmuir 26, 16129–16133.

Lozinsky, V.I., Galaev, I.Y., Plieva, F.M., Savinal, I.N., Jungvid, H., Mattiasson, B., 2003. Polymeric cryogels as promising materials of biotechnological interest. Trends in Biotechnology 21, 445–451.

Lv, Y., Lin, Z., Svec, F., 2012. Thiol-ene click chemistry: a facile and versatile route for the functionalization of porous polymer monoliths. Analyst 137, 4114–4118.

Noel, S., Liberelle, B., Robitaille, L., De Crescenzo, G., 2011. Quantification of primary amine groups available for subsequent biofunctionalization of polymer surfaces. Bioconjugate Chemistry 22, 1690–1699.

Ostergaard, H., Petersen, A.K., 2008. Selective reduction and derivatization of engineered proteins comprising at least one non-native cysteine. United States, Patent Application Publication US 2008/0200651 A1, 1–16.

Plieva, F.M., De Seta, E., Galaev, I.Y., Mattiasson, B., 2009. Macroporous elastic polyacrylamide monolith columns: processing under compression and scale-up. Separation and Purification Technology 65, 110–116.

Plieva, F.M., Galaev, I.Y., Mattiasson, B., 2007. Macroporous gels prepared at subzero temperatures as novel materials for chromatography of particulate-containing fluids and cell culture applications. Journal of Separation Science 30, 1657–1671.

Plieva, F.M., Galaev, I.Y., Noppe, W., Mattiasson, B., 2008. Cryogel applications in microbiology. Trends in Microbiology 16, 543–551.

Plieva, F.M., Karlsson, M., Aguilar, M.-R., Gomez, D., Mikhalovsky, S., Galaev, I.Y., 2005. Pore structure in supermacroporous polyacrylamide based cryogels. Soft Matter 1, 303–309.

Plieva, F.M., Kirsebom, H., Mattiasson, B., 2011. Preparation of macroporous cryostructurated gel monoliths, their characterization and main applications. Journal of Separation Science 34, 2164–2172.

Plieva, F., Xiao, H., Galaev, I.Y., Bergenstahl, B., Mattiasson, B., 2006. Macroporous elastic polyacrylamide gels prepared at subzero temperatures: control of porous structure. Journal of Materials Chemistry 16, 4065–4073.

Preinerstorfer, B., Bicker, W., Lindner, W., Lämmerhofer, M., 2004. Development of reactive thiol-modified monolithic capillaries and in-column surface functionalization by radical addition of a chromatographic ligand for capillary electrochromatography. Journal of Chromatography A 1044, 187–199.

Saggese, G., Ranke, M.B., Saenger, P., Rosenfeld, R.G., Tanaka, T., Chaussain, J.-L., Savage, M.O., 1998. Diagnosis and treatment of growth hormone deficiency in children and adolescents: towards a consensus. Hormone Research in Pediatrics 50, 320–340.

Paper III

Evaluation of a new poly(ether amine) cryogel as a solid support for enzyme bioreactor applications

G.R. Jespersen[a,c]*, J.X. Yun[b], F. Matthiesen[c], A.L. Nielsen[c], H.S. Andersen[c], H. Kirsebom[a]

[a]Department of Chemistry, Division of Biotechnology, Lund University, Getingevägen 60, SE-22100 Lund, Sweden

[b]State Key Laboratory Breeding base of Green Chemistry Synthesis Technology, College of Chemical Engineering, Zhejiang University of Technology, Chaowang Road 18, Hangzhou 310032, Zhejiang Province, China

[c]Novo Nordisk A/S, Biopharmaceutical Research Unit, Novo Nordisk Park 1, DK-2760 Måløv, Denmark

*To whom correspondence should be directed: Gry Ravn Jespersen, gry.jespersen@biotek.lu.se

Abstract:

Poly(ether glycols) are characterized by a high hydrophilicity while being chemically inert. Thus these polymers are potentially suitable for immobilization of macromolecules such as proteins. To develop a macroporous, monolithic solid support suited for the immobilization of enzymes, we prepared two poly(ether amine) based cryogels. Conditions for optimized polymerization yield were identified by a Design-of-Experiments (DoE) approach and cryogels were characterized and compared in terms of selected physico-chemical properties. The amine-functionalized cryogels were aldehyde functionalized through a reaction with *in situ* activated 4-carboxybenzaldehyde. As a model enzyme papain was chosen and successfully immobilized on the material through a reductive amination. Immobilized papain was found to be highly active towards the cleavage of a low molecular weight substrate (L-BAPNA). Moreover, a positive effect of increasing the spacer length between the solid support and the enzyme was confirmed. However, the immobilized papain's activity towards a high molecular substrate (IgG antibody) was found to be reduced, compared to free papain and the cleavage was incomplete. This behaviour was attributed to inaccessibility of papain to the antibody. This activity loss is attributed to the immobilization. The prepared cryogel constitutes a solid support for enzyme immobilizations affording high catalytic activity towards low molecular substrates, however work needs to be done on the optimization of immobilization chemistry to obtain an equally high macromolecular substrate conversions.

1. Introduction

Biocatalysis is widely used in the pharmaceutical industry, as enzymes are often characterized by having very high substrate specificities [1]. Utilization of enzymes immobilized on solid supports offers additional advantages such as circumvention of the need to separate enzyme from the product following the reaction. Moreover, improved enzyme stability and resistance to chemical stresses such as pH and organic solvents as well as offering the possibility of reusability of the immobilized enzyme are attributes of these bioreactor systems [1]. Cryogels are a type of polymeric solid supports categorized as monoliths as they are cast as a single porous blok of material. Noticeable for cryogels is their distinct super-macroporous morphology, which stems from the method of preparation. They are prepared by radical polymerization at sub-zero temperatures where the solvent is frozen into ice crystals [2]. Under these conditions the polymerization proceeds in a non-frozen microphase surrounding the ice crystals, thereby acting as a pore forming agent in the resulting polymeric network [2]. Cryogels are endowed with several features that render them attractive as materials for biotechnological applications involving macromolecules [3-7]. The macropore structure enable mass transport by means of convection, virtually eliminating diffusional limitations and allowing for the application of very high flow rates at concomitant low column back pressures. In addition, cryogels can be prepared from a wide range of monomeric and polymeric precursors, without the use of expensive or harmful organic solvents, rendering them as potentially cheap and costumizable materials. Thus, cryogels are suited as single-use, disposable materials.

Due to their chemical inertness, high hydrophilicity and biocompatibility poly(ethylene glycols) polymers have been utilized in wide range of biotechnological applications [8, 9]. Jeffamines® are a class of poly(ether amines), which combine the attractive features of poly(ether glycols) with the functionality of reactive primary amine end groups. On this basis, Jeffamines® have been utilized as co-monomers for the preparation of polymeric materials within tissue engineering and drug release applications [10-13]. Hence, with respect to the potential use as the basis of a biocatalysis reactor, the combination of the attractive features of a cryogel solid phase with the biocompatibility and reactivity of Jeffamines® could render a matrix very well suited for the immobilization of reactive biomacromolecules.

on the basis of these considerations, we aimed at preparing cryogels utilizing acrylamide derivatized Jeffamine® macromonomers with two different polymer chain lengths. To the best of our knowledge, the preparation of cryogels from poly(ether amine) macromonomers has not been described and therefore initially, the conditions for free radical cryopolymerization were optimized

with respect to temperature, monomer- and initiator/activator concentration and the resulting cryogels were evaluated in terms of selected physico-chemical parameters. In order to evaluate the cryogels' applicability as solid phase for enzyme immobilizations, papain was chosen as a model enzyme and was immobilized on aldehyde functionalized Jeffamine® cryogels. Subsequently, immobilized papain activity was evaluated in order to determine effect of immobilization, spacer length and substrate molecular size.

2. Experimental

2.1 Chemicals

Jeffamine® ED-2003-acrylamide (JEFF-2.0) and Jeffamine® ED-900-acrylamide (JEFF-0.9) were purchased from Bimax inc., *N, N, N' N'* –tetramethylethylenedimamine (TEMED) (ultra-pure grade) was purchased from Amresco inc.. Ammonium persulfate (98%, APS), 4-(2-hydroxy-1-naphthylazo)benzenesulfonic acid sodium salt (Orange II), L-cysteine (97%), sodium chloride (99.5%), 4-carboxybenzaldehyde, *N,N'*-diisopropylethylamine (DIPEA), sodium cyanoborohydride (95%), *N*-benzoyl-L-arginine-4-nitroanilide hydrochloride (L-BAPNA) were all purchased from Sigma-Aldrich. Ethylenediaminetetracetic acid disodium salt dehydrate (EDTA) (electrophoresis purity) was purchased from BIO-RAD, 5,5'-dithiobis-(2-nitrobenzoic acid) (DTNB) was purchased from Thermo Scientific, *O*-(benzotriazol-1-yl)-*N,N,N'N'*-tetramethylurionum tetrafluoroborate (TBTU) was purchased from IRIS Biotech, , 1M hydrochloric acid and 1M sodium hydroxide were purchased from VWR. Papain (EC 3.4.22.2) and N-methylpyrrolidone (NMP) were purchased from Merck. Fuming hydrochloric acid (37%, 12.3M), disodium hydrogenphosphate, sodium dihydrogenphosphate, disodium carbonate, sodium hydrogencarbonate were all of analytical grade and were purchased from Merck. Human IgG4 antibody was supplied by Novo Nordisk A/S.

2.2 Cryogel preparation – investigation of synthesis parameters by 2^4 factorial design of experiment

To prepare cryogels from JEFF-0.9 and JEFF-2.0 acrylamide macromonomers four different solutions were prepared, containing varying concentrations of monomers and APS/TEMED as listed in Table 1.

Tabel 1: Monomer solutions prepared for 2^4 factorial experiment investigating the effect of monomer- and , initiator/activator concentrations, reaction temperature and -time

Solution no.	**1**	**2**	**3**	**4**
Monomer (% w/w)	6	6	12	12
APS/TEMED (mM)	7.9/15.5	2.6/15.5	15.8/31.0	5.2/31.0

The TEMED concentration corresponded to 3% (w/w) of monomers and the APS concentrations corresponded to 1% and 3% (w/w) of monomers, respectively. The solutions were prepared by dissolving the monomers in Milli-Q purified water (MQ water), followed by addition of TEMED. The solutions were degassed for 15 min with N_2 before being cooled on ice for 30 min. The solutions were added APS, stirred briefly, and immediately hereafter 1 mL was transferred to glass tubes (10 mm diameter), plugged at one end with a rubber stopper. The glass tubes were transferred to a Jalubo, F34-EH refrigerated circulator bath (Jalubo GmbH, Germany), which was pre-cooled to -12°C or -20°C, and they were left for either 24 or 48 h. After the reaction, the glass tubes were removed from the cooling bath and the cryogels were thawed at r.t. The cryogels were washed extensively with MQ water before they were removed from the glass tube and lyophilized overnight (Christ Gamma 1-16 LCS freeze dryer, Martin Christ GmbH) to obtain their dry weights.
The cryogel polymerization yields were calculated from the recorded dry weights by use of the following equation:

$$Y_{polym.} = \frac{m_{lyophil.}}{m_{theoret.}} \times 100\% \qquad (1)$$

where, $m_{\text{lyophil.}}$ is the average dry weight of the cryogels and $m_{\text{theoret.}}$ is the theoretical dry weight at 100% polymerization yield.
To determine the cryogels's gravity flow, they were left in the glass column in which they were cast. To the glass column was added water to aheight of 2 cm above the gel and the level was maintained by continuous addition of water while the water was collected at the bottom of the cryogel for 10 min. The water fraction eluted through the cryogel was weighed to obtain the exact volume. All cryogels were prepared in duplicates and dry weights and gravity flows were obtained in arbitrary sequences. Data were evaluated by use of statistical software MiniTab version 14 (Minitab, Inc.)

2.3 Determination of cryogel porosity

Porosity of the macropores was determined by the use of the following equation:

$$P = \frac{m_{wet} - m_{drain}}{m_{wet}} \times 100\% \qquad (2)$$

where P is the mass of water contained in the cryogel macropores, m_{wet} is the mass of the swollen cryogel and m_{drain} is the weight of the cryogel, which had been squeezed to drain the macropores. Measures of macropore porosity were performed in triplicates.

2.4 Cryogel texture analysis

The elasticity of the unmodified cryogels was determined by use of a texture analyser (XTPlus, Stable Micro Systems, England) with a 5 kg weight load and a cylindrical probe with a diameter of 25 mm. The cryogels were placed on a metal plate and the weight was applied at a speed of 0.1 mm/s. During the test samples were compressed to 60% of their original height and the applied force was calculated using Exponent TEE32, version 4 software (Stable Micro Systems, England). All experiments were performed at r.t. and the linear range elasticity moduli of the samples were calculated at the point of 60% of the original sample height, using the Young's modulus equation:

$$E = \frac{{}^{F}/_{A_0}}{{}^{\Delta l}/_{L_0}} \qquad (3)$$

where E is the Young's elasticity modulus (Pa), F is the force applied (N), A_0 is the cross sectional area (m^2), Δl is the change in sample height during the compression (m) and L_0 is the sample's original height.

2.5 Scanning electron microscopy (SEM)

To visualize the pore morphology, thin discs were cut from the middle part of each sample.

The cryogel discs were fixed with 2.5% (v/v) glutaraldehyde in phosphate buffer (100 mM, pH 7.0) overnight. Then they were post-fixed with 1% OsO4 in phosphate buffer (100 mM, pH 7.0) for 1.5 h followed by three washes with the phosphate buffer. The fixed cryogel discs were then dehydrated by graded series of ethanol before they were transferred to iso-amyl acetate, in which they were kept for two days, before they were critical point dried using CO_2 (Hitachi HCP-2). The dry, fixed

cryogel discs were coated with gold-palladium and inspected by SEM (Hitachi TM-1000). Mean pore diameter was determined by measuring 40 pores, identified as surface pores, using ImageJ software version 1.46.r (http//imagej.nih.gov./).

2.6 Determination of cryogel primary amine loading

To determine the cryogel primary amine loading a procedure described elsewhere was applied [14]. Three replicate cryogels (volume 0.2 mL, diameter 5 mm) were washed once with acidic solution (MQ water adjusted with HCl to pH 3) before they were each added 3 mL of dye solution (40 mM Orange II sodium salt in MQ water, pH adjusted to 3 with HCl). The cryogels were incubated with this for 3 hrs at r.t. with mixing. The cryogels were drained and washed extensively with acidic solution to remove any unbound dye, and were then added 4 mL alkaline solution (MQ water, pH adjusted to 12 with NaOH), which they were incubated with for 30 min at r.t. with mixing. The pH of the eluted dye was then adjusted to 3 by addition of 1% (v/v) 12 M HCl and the absorbance at 412 nm of the dye solution was recorded using a SpectraMax M2e multimode microplate reader (Molecular Devices, United States). The UV measurements were converted to concentrations using an Orange II standard curve.

2.7 Determination of cryogel permeability

To determine the permeability the cryogels (volume 1 mL, diameter 1 mm) were inserted in a column (10 mm diameter) which was firmly adapted at the bottom of a 100 cm measuring tube. The flow at different water column heights above the cryogel was recorded and the hydraulic permeability was determined from Darcy's law equation:

$$k_w = \frac{Q_w \mu_w L}{\Delta p_w A} \qquad (4)$$

where, Q_w is the flow of water through the column, μ_w is the viscosity of water, L is the length of the cryogel column, A is the cryogel column cross sectional area, and Δp_w is the pressure drop.

2.8 p-Formylbenzoate derivation of cryogel

To introduce *p*-formylbenzoate functional groups onto Jeffamine®-acrylamide cryogels, dry samples were swollen directly in a mixture of 4-caboxybenzaldehyde (3 molar equivalents excess to cryogel primary amines), TBTU (3.3 molar equivalents), DIPEA (3.3 molar equivalents) in NMP. The cryogels were reacted with this for 24 hrs at r.t. To ensure that the reaction had gone to completion, a ninhydrin test was performed following the procedure described elsewhere [15].

2.9 Immobilization of papain and determination of papain loading on cryogel

To immobilize papain onto *p*-formylbenzoate-modified cryogels, a solution consisting of 1 mg/mL papain, 0.27 mg/mL sodium cyanoborohydride in phosphate buffer (0.1 M sodium phosphate, 5 mM EDTA, pH 7) was prepared and 4 mL of this was added to each cryogel (volume 1 mL, diameter 10 mm). The cryogel was reacted with this, with mixing for 24 hrs at r.t. Then the cryogel was washed according to the following scheme; three times with MQ water, three times with buffer (0.1 M sodium phosphate, 1 M NaCl, 5 mM EDTA, pH 7); three times with buffer (0.1 M sodium phosphate, 5 mM EDTA, pH 7) to remove any unreacted papain. Cryogels with immobilized papain were used immediately after immobilization or stored at 4°C.

The papain content in the immobilization buffer before and after reaction with the cryogel was analyzed by use of SE-HPLC on a Bio Sep-SEC–S3000 column (Phenomenex, Denmark) connected to a Waters Alliance HPLCsystem (Waters, Denmark). Running buffer (200 mM sodium phosphate, 300 mM NaCl, 10% 2-propanol (v/v), pH 6.9), flow rate 1 mL/min, column temperature 30°C. To determine the papain concentration, the papain peak before and after immobilization was compared and the percentage decrease was converted into mg. Average papain loadings were determined based on three replicate samples.

2.10 Cryogel with immobilized papain - hydrolysis of L-BAPNA substrate

A cryogel with immobilized papain was inserted into a glass column (10 mm diameter), which was connected to a peristaltic table pump (Watson-Marlow 403U/VM3, Watson-Marlow Flexicon A/S) and the flow was adjusted to 1 mL/min. The cryogel was calibrated with cysteine buffer (0.1 M sodium phosphate, 5 mM EDTA, 20 mM cysteine, pH 7) for 30 min and then 10 mL of 200 mM L-BAPNA (0.1 M sodium phosphate, 5 mM EDTA, 20 mM cysteine, pH 7) was re-circulated through the cryogel column for 21 hrs. Samples were drawn at consecutive time points and analyzed by UV-detection at 410 nm using a SpectraMax M2e multimode microplate reader (Molecular Devices,

United States). The concentration of hydrolyzed product was calculated from the molar absorptivity ε=8800 $M^{-1}cm^{-1}$ [16].

For investigation of the effect of flow rate, prior to each applied flow rate the cryogel column was calibrated with cysteine buffer as described above. Then 10 mL of freshly prepared 200 µM L-BAPNA (0.1 M sodium phosphate, 5 mM EDTA, 20 mM cysteine, pH 7) was re-circulated through the column at each flow rate and when 90 mL had been passed through the column, a sample was drawn and analyzed as described above. Flow rates 0.7 and 1.0 mL/min were tested on three replicate samples.

2.11 Cryogel with immobilized papain - cleavage of antibody

A cryogel (volume 0.2 mL, diameter 5 mm) with immobilized papain was incubated with cysteine buffer (PBS, 20 mM cysteine, pH 7.4) for 30 minutes. The cryogel was drained and then added 2 mL of a solution consisting of 1 mg/mL antibody in cysteine buffer (PBS, 20 mM cysteine, pH 7.4), and the system was incubated with for 24 hrs at 37°C with gentle mixing. This experiment was tested on five replicate samples. As a control experiment solubilized papain was activated in cysteine buffer (PBS, 20 mM cysteine, pH 7.4) for 30 minutes and then antibody was added rendering a solution of 2 mL consisting of 1 µM papain, 1 mg/mL antibody in cysteine buffer. The solution was incubated at 37°C for 24 hrs with gentle mixing.

2.12 Analysis of digested antibody

To quantify the amount of Fab fragment generated, the papain cleavages of antibody were analyzed by SE-HPLC on a Bio Sep-SEC–S3000 column (Phenomenex, Denmark) connected to a Waters Alliance HPLC-system (Waters, Denmark). Running buffer (200 mM sodium phosphate, 300 mM NaCl, 10% 2-propanol (v/v), pH 6.9), flow rate 1 mL/min, column temperature 30°C. The peak area was compared to an antibody standard sample of known concentration and the Fab concentration was determined using the molar extinction coefficient, ε = 1500 $cm^{-1}M^{-1}$.

To analyze the mass composition of the crude cleavage mixtures an Agilent 6224 TOF LC/MS with a desalting column (MassPrep Micro Desalting Column, Waters Denmark) was used. The column was operated at 0.4 mL/min, 20°C applying a gradient of buffer B (0.1% formic acid v/v in acetonitrile) in buffer A (0.1% formic acid v/v in water).

To isolate the product resulting from the immobilized papain cleavage of antibody, 40 µL of the crude cleavage mixture was applied to a Bio Sep SEC S3000, connected to an analytical HPLC-

system (Agilent Technologies.) equipped with a fraction collector (Agilent Technologies). The peak containing the cleavage product was collected and susequently analyzed by mass spectrometry on a Waters Acquity UPLC with a Waters Acquity UPLC BEH, C-4, 1.7 µm, 2.1 mm x 50 mm column and a Waters (Micromass) LCT Premier XE detector.

3. Results and Discussion

3.1 Optimization of synthesis conditions for the preparation of Jeffamine-acrylate cryogels

It is well known that hydrogels formed from poly(ethylene glycol) (PEG) macromonomers can be regarded as biocompatible materials based on their high water content and chemical inertness [8, 17]. Furthermore, studies have shown that the use of PEG-based spacers in the immobilization of proteins onto solid supports is favourable with respect to increasing the immobilized protein's availability towards molecular interactions [18, 19]. In this study we used a commercially available poly(ether amine), which had been acrylamide derivatized at its primary amine end groups, constituting a mixture of mono- and diacrylated monomers in a 20:1 ratio. Two Jeffamine® monomers with different polymer chain lengths were selected , namely ED-900 (JEFF-0.9) and ED-2003 (JEFF-2.0) respectively constituting 0.9 kDa and 2.0 kDa (Fig. 1). Polymers with these chain lengths are within a range reported suitable as spacers for immobilization of proteins [18].

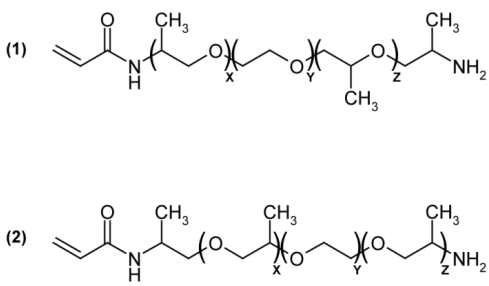

Figure 1: Structural presentation of Jeffamine®-acrylamide macromonomers. 1: JEFF-0.9, Y ≈ 12.5, (X+Z) ≈ 6. **2:** JEFF-2.0, Y ≈ 39, (X+Z) ≈ 6 acrylated at one primary amine.

Studies of cryogels have shown that reaction temperature and -time as well as monomer- and initiator/activator concentration are parameters governing the polymerization yield and porosity [20, 21]. Thus, we designed experiments to elucidate how these parameters affect the formation of cryogels prepared from JEFF-0.9 by performing a 2^4 factorial design of experiments (DoE) (Table 2).

Table 2: Factors influencing cryopolymerization yield, investigated by DoE 2^x factorial experiments

Monomer type	**A** Temperature (˚C)	**B** Monomer concentration (%)	**C** APS/TEMED (% of monomers)	**D** Reaction time (hours)	Response
JEFF-0.9	-12 -20	6 12	1 3	24 48	Yield
JEFF-2.0	-12	6 12	1 3	24 48	Yield

A one-way analysis of variance (ANOVA) of the data revealed that the initiator/activator concentration did not have any effect on the cryogel yield of polymerization, whereas both temperature, time and monomer concentration all significantly affected the reaction yield. It was found that, if the reaction was complete after 24 hrs, the high temperature setting (-12°C) afforded a higher yield of reaction than the low setting (-20°C). At -12°C the low monomer setting (6% w/w) yielded higher than the high setting (12% w/w), contrary at -20°C the high monomer setting was the highest yielding. Based on the overall results of the analysis, it was found that after 24 hrs reaction, cryogels prepared from 6% w/w monomers at -12°C gave the highest overall polymerization yield (Figure 2.A).

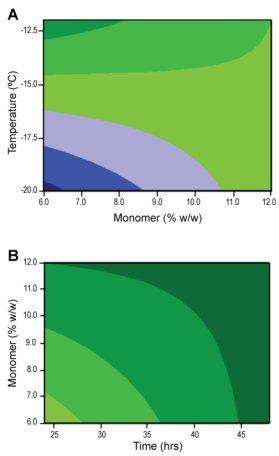

Figure 2: Contour plots of selected parameters' effect on cryo-polymerization yield. A: Effect of monomer concentration and temperature on cryo-polymerization yield of JEFF-0.9. Dark green colour indicates area of high yield, dark blue colour indicates area of low yield. **B:** Effect of reaction time and monomer concentration on cryopolymerization yield of JEFF-2.0. Dark green indicates area of high yield, light green indicates area of low yield.

If the cryo-polymerization was extended to 48 hrs none of the investigated factors had a significant impact on the yield (data not shown). Previous work has shown that upon freezing a radical polymerization solution, a lag phase is introduced, delaying the onset of polymerization [22]. This observation is explained by a slower formation of radicals, thus delaying the activation of the acrylamide groups in the monomer mixture. Similarly, the present observation, that lowering the temperature negatively affects the polymerization yield at 24 hrs reaction, can probably be attributed to the fact that, at low temperatures molecular movement is reduced and hence the reaction kinetics of the system is slowed down. After 48 hrs, this effect of temperature is no longer significant, which can be interpreted in the sense that at this time point, the reaction has reached its end for all factor combinations.

In a study by Kirsebom *et al.* it was shown that the initial monomer concentration affected the rate of cryopolymerization of dimethylacrylamide/PEG-diacrylate and that a high monomer concentration (12% w/w) exhibited the fastest reaction kinetics due to a high diffusion constant of the monomers [23]. Thus, it was surprisingly found that after 24 hrs reaction and -12°C, the high monomer setting (12% w/w) afforded the lowest yield of polymerization and thus, exhibiting the slowest reaction rate. An explanation for this discrepancy between the two studies could reside in the difference in size of the monomers under study. As the molecular weight of JEFF-0.9 (≈900 g/mol) exceeds dimethylacrylamide (99 g/mol) by 10-fold it is likely that the diffusivity of the former is much slower, potentially rendering this factor becomes less important for the reaction rate. Another factor which influences the polymerization rate is the concentration of initiator/activator and this may in fact explain the results of this study. Furthermore, it has been shown that, independent of the initial monomer concentration, the monomer concentration in the unfrozen liquid microphase, where polymerization proceeds, is constant at a fixed temperature [23]. Given that this is the case, the concentration of initiator/activator in the unfrozen microphase of the high monomer setting (12% w/w) of our study will be twice as large as for the low monomer setting (6% w/w) thus, promoting a faster reaction rate of the polymerization solution containing a high initial monomer concentration.

On the other hand, though generally affording a lower yield compared to -12°C, at -20°C, the low monomer setting (6% w/w) afforded the lowest polymerization yield. An additional observation to this end was that all cryogels, prepared at the lowest temperature, had impaired flow characteristics and that the high monomer setting cryogels exhibited virtually no gravity flow through the gel, indicating that they contained either no pores or only closed end pores. This phenomenon can be

explained by the freezing regime at low temperatures, which seems to favour the formation of more, but smaller ice crystals resulting in an increased number of small pores of the cryogel [23, 24]. Due to the poor polymerization yields and flow properties of cryogels prepared at -20°C, this temperature setting was regarded as suboptimal for this study.

To investigate if the same factor effects were seen for cryo-polymerization of JEFF-2.0, a similar 2^3 factorial design experiment, investigating the effect of monomer concentration initiator/activator concentration and reaction time on the polymerization yield of this monomer, was performed (Table 2).

Table 2: Factors influencing cryopolymerization yield, investigated by DoE 2^x factorial experiments

Monomer type	**A** Temperature (˚C)	**B** Monomer concentration (%)	**C** APS/TEMED (% of monomers)	**D** Reaction time (hours)	Response
JEFF-0.9	-12	6	1	24	Yield
	-20	12	3	48	
JEFF-2.0	-12	6	1	24	Yield
		12	3	48	

The results revealed that, like for JEFF-0.9, monomer concentration and reaction time both had a significant effect, whereas initiator/activator concentration had no effect (Figure 2.B). After 24 hrs reaction at -12°C the low monomer setting (6% w/w) afforded the lowest yield, whereas after 48 hrs low and high monomer setting yielded the same. It is interesting to note, that cryopolymerization of JEFF-2.0 at -12°C exhibits the same result as JEFF-0.9 polymerized at -20°C, namely that 6% w/w polymerizes to a lower yield than 12% w/w. Common to these cryogels was that they all exhibited varying degrees of impaired flow compared to JEFF-2.0 cryogels prepared at -12°C. This indicates the presence of smaller pores, possibly surrounded by thicker pore walls. This can be explained by the fact that the swelling ratio, and thus the fraction of water closely associated with a poly(ether) such as the Jeffamine® macromonomer, is dependent on and increases with the molecular weight of the polymer [25]. Thus, during cryopolymerization, the volume of the unfrozen microphase will be increased for JEFF-2.0 monomer and possibly to a volume large enough for the monomers to diffuse faster, thereby the diffusion constant of the monomer could potentially govern the reaction rate. [23]. As control experiments to the cryo-polymerizations, reactions were also performed at r.t. and interestingly, it was found that only 12% (w/w) JEFF-0.9 polymerized to its gel point at this temperature. This observation indicates that both monomers have relatively low reactivity and must

be concentrated beyond a certain level before polymerization to the extent of their gel point is achieved.

3.2 Physical characterization of cryogels

The cryogels prepared from JEFF-0.9 and JEFF-2.0 were characterized with respect to polymerization yield, primary amine loading, porosity, elasticity and mean pore diamenter (Table 3). Despite the conducted optimization study, the yields of the polymerizations were found to be fairly low for both monomers (Table 3). These low yields could be attributed to the relatively low reactivity of the macromonomers, as is also observed by the inability of the monomers to polymerize to the point of gelation at room temperature.

Table 3: Physical characterization of Jeffamine® cryogels

Monomer type	**Polymerization yield (%)**	**Amine loading (µmol/g dry cryogel)**	**Porosity of macropores (%)**	**Young's modulus (kPa)**	***Mean pore diameter (µm)**
JEFF-0.9	65±2	484±85	84.2±2.6	6.4	62±21
JEFF-2.0	63±0.6	139±28	78.8±1.7	3.1	41±21

*JEFF-0.9 min. 33 µm max. 110 µm, JEFF-2.0 min. 12 µm max. 117 µm.

The primary amine loadings were determined by the use of the anionic dye Orange II and it was measured to 484±85 µmol/g and 139±28 µmol/g dry cryogel for JEFF-0.9 and JEFF-2.0 cryogels, respectively. The estimated primary amine loadings reflect the fact that the JEFF-0.9 cryogel contains approx. 2.2 times molar excess of monomer over the JEFF-2.0 cryogel as the cryogels are prepared from weight concentrations.

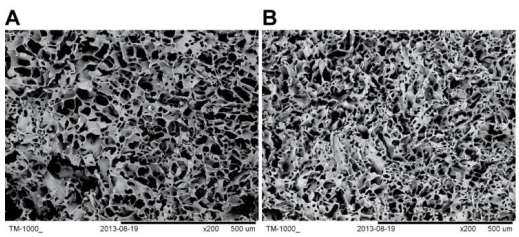

Figure 3: SEM images of the cryogels's porous morphology: A: Cryogel prepared from JEFF-0.9 at 200 times magnification. **B:** Cryogel prepared from JEFF-2.0 at 200 times magnification.

To visualize the porous structure scanning electromicroscopy (SEM) was employed, and both cryogels where confirmed to possess the distinct super-macroporous morphology attributed to cryogels (Figure 3). From the SEM images, the mean pore diameters of the two cryogels were estimated to 62±21 μm and 41±21 μm for JEFF-0.9 and JEFF-2.0, respectively. This result further confirms that JEFF-2.0 cryogel contains smaller pores than JEFF-0.9, which is in line with our discussion of factors affecting polymerization yield and porosity in section 3.1. Moreover, the texture analysis of the two cryogels revealed that the elasticity modulus of JEFF-2.0 cryogel was approximately half of that of JEFF-0.9 cryogel. This observation can be directly related to the respective monomer sizes as the cryogels are prepared from equal weight concentrations. The JEFF-2.0 cryogel contains half the molar amount of monomers and thus, half the amount of stabilizing connecting chemical bonds. This impact of the connecting chemical bonds was also observed in the permeability testing, where both cryogels were found to compress at a certain flow and the JEFF-2.0 cryogel compressed at lower flow rates than the JEFF-0.9 cryogel (Figure 4). The permeabilities of the two cryogels were calculated to $9.9*10^{-13}$ m^2 and $6.5*10^{-13}$ m^2 for JEFF-0.9 and JEFF-2.0, respectively, reflecting the smaller mean pore size of the JEFF-2.0 cryogel. Finally, the porosity of the JEFF-2.0 cryogel was lower than for the JEFF-0.9 gel, consistent with the smaller mean pore diameter of this cryogel.

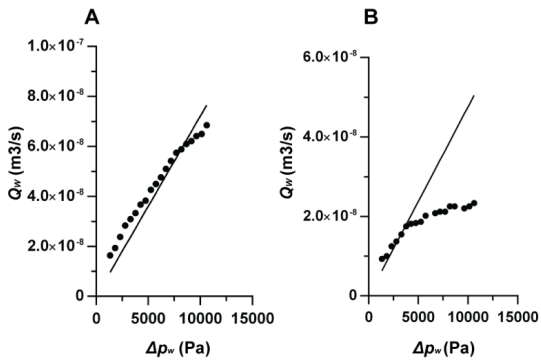

Figure 4: Experimental and fitted flow rates as a function of the pressure drop generated by increasing water column heights: A: Cryogel prepared from JEFF-0.9. **B:** Cryogel prepared from JEFF-2.0.

3.3 Modification of cryogels

The aim of the work was to evaluate the polyetheramine based cryogel as a carrier for immobilized enzyme. For this purpose, papain was chosen as a model enzyme, because it is an industrially relevant well characterized enzyme and his has been reported that papain can be immobilized on a solid support and maintain enzymatic activity [26-29].

Papain has a cysteine residue in its active site, which must remain free for papain to maintain its activity and due to this, it was crucial to select a coupling chemistry, which was not thiol reactive. For most proteins, obvious reactive anchoring points are the primary amines of lysines or the N-terminal of the polypeptide chain, which can react with a suitable electrophile on the solid support. Aldehydes are electrophiles which are virtually unreactive towards thiols, but will react readily with primary amines to form imines, which in turn can be converted into an amide bond between the carbonyl and the amine through a reductive amination [30].

Glutaraldehyde has been one reagent of choice for introducing aldehyde groups onto solid supports, however,this short homo-bifunctional linker tends to cross bind matrix primary amines and studies on papain immobilization have shown this reagent to give low immobilization yields and low immobilized enzyme activities [31, 32]. Hence, an alternative aldehyde is *p*-benzaldehyde, which can be coupled to primary amines in its active ester form as succinimidyl *p*-formylbenzoate (SFB) was chosen [30]. As SFB is an expensive reagent with a short shelf-life once opened, we opted to introduce *p*-benzaldehyde directly onto the cryogel matrix through the *in situ* activation of 4-carboxybenzaldehyde by TBTU, followed by reaction with matrix primary amine (scheme 1). This strategy showed to be highly efficient as all cryogel primary amines were converted, as evaluated by a Kaiser test for the detection of primary amines [33].

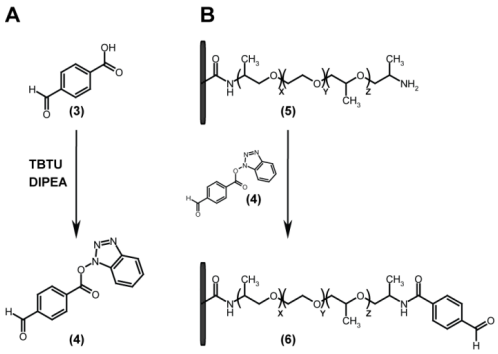

Scheme 1: Benzaldehyde functionalization of JEFF-0.9 cryogel: The reaction proceeds in two steps. Step A: Activation of 4-carboxybenzaldehyde (3) by TBTU. Step B: Reaction of cryogel primary amine (5) with active ester intermediate (4) resulting in the formation of SFB-activated cryogel (6).

Subsequently, papain was immobilized on the cryogels through a reductive amination involding the aldehyde functionalities on the solid support and primary amines on papain. The resulting papain loading of the cryogels was determined to 0.20±0.03 mg papain/g dry cryogel and 0.08±0.07 mg papain/g dry cryogel for JEFF-0.9 and JEFF-2.0 cryogels, respectively. This was equivalent to approx 0.05% utilization of aldehydes for both cryogels. The loadings were determined for triplicate samples by SE-HPLC analysis of the papain concentration in the immobilization solution before and after reaction, taking into account the dilution factor of adding the swollen cryogel to the solution. The large standard deviation of the JEFF-2.0 cryogel is due to one sample, which accounted for a high papain loading, nonetheless the observed variation could reflect a somewhat inhomogeneous material.

3.4 Cryogels with immobilized papain: Activity towards cleavage of low molecular substrate; L-BAPNA

To test the immobilized papain activity towards hydrolysis of L-BAPNA in a continuous flow mode, the cryogel was inserted in a glass column which was connected to a peristaltic table pump and a solution of 200 μM L-BAPNA in 20mM cysteine buffer was re-circulated through the column at 1 mL/min for the duration of 20 hrs. The results showed that immobilized papain on both JEFF-0.9 and JEFF-2.0 cryogel had maintained activity, and that the apparent overall enzymatic activity of the two cryogels was in the same range. However, taking into account the average amount of enzyme immobilized on each type of cryogel, enzyme immobilized on JEFF-2.0 generated considerably more product than when immobilized on JEFF-0.9 (Figure 5.A). After 20 hrs,

approximately half of the applied L-BAPNA had been hydrolyzed by the immobilized papain, which was twice as much as obtained in the corresponding experiment with solubilized papain (2 mL of 1 μM papain, approx. equivalent to papain loading on JEFF-0.9 cryogel) under the same conditions. These findings suggest that immobilization onto Jeffamine®-acrylamide cryogels does not introduce restrictions on the enzyme's flexibility, which could impede its activity towards hydrolysis of L-BAPNA compared to free papain. The fact that immobilized catalytic activity was found to be higher than solubilized could in this case probably be due to the difference in operation mode, i.e. solution vs. column. Several studies on the immobilization of papain onto solid supports have shown that the insertion of spacers of varying length between the polymer matrix and papain increases the enzyme's activity [31, 34, 35] and in a specific study on immobilization of papain on cross-linked polymer supports Ganapathy *et al.* report of finding immobilized papain activities similar to free papain upon the insertion of a spacer [27]. Interestingly, in this study the enzymatic activity of papain immobilized on JEFF-2.0 was found to be higher than when immobilized on JEFF-0.9. This finding may be regarded as a direct effect of the increased flexibility and distance away from the polymeric backbone introduced by the longer spacer arm of JEFF-2.0. For low molecular substrate, *N*-benzyl-L-arginine ethyl ester (BAEE), it has been shown that introducing a glycine spacer with up to three glycine units increased papain activity, but beyond this length there was no additional gain [36].

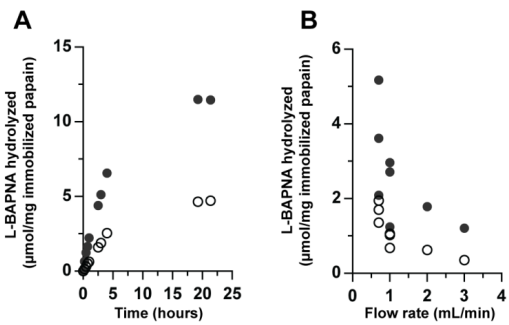

Figure 5: L-BAPNA hydrolysis by papain immobilized on cryogels prepared from JEFF-0.9 (open circles) and JEFF-2.0 (gray dots), operated in continuous flow mode: A: L-BAPNA hydrolyzed product resulting from re-circulating L-BAPNA through the cryogel column for 20 hrs. **B:** L-BAPNA hydrolyzed product resulting from re-circulating L-BAPNA through the cryogel column at different flow rates.

The fact that our results show a gain in papain activity by increasing a very long spacer from 900 g/mol to 2000 g/mol could lie in the operational mode employed in this study. In the present work,

the cryogels were operated in a flow-mode, where the unrestricted availability of enzyme becomes even more significant.

As a next step we wanted to investigate the effect of flow rate on the hydrolysis of L-BAPNA and to do this 10 mL of 200 μM L-BAPNA in 20mM cysteine buffer was re-circulated through the cryogel column at increasing flow rates. When increasing the flow rate above 1 mL/min we experienced that the cryogels compressed due to their relatively low mechanical stability. Therefore we only had one successful test of flow rates of 2.0 and 3.0 mL/min, respectively, whereas flow rates of 0.7 and 1.0 mL/min were tested on triplicate samples. The results showed that by increasing the flow rate the amount of hydrolyzed L-BAPNA decreased (Figure 5.B). This finding is in line with other reported work on characterization of a papain-agarose bioreactor [29] and is not surprising as papain and L-BAPNA must have a certain contact time for the hydrolysis to proceed. By increasing the flow rate of the system, this contact time is decreased with the consequence that the overall L-BAPNA hydrolysis progresses less effectively. Looking at the reproducibility of results between the triplicate samples, there appears to be a large variation especially in the case of JEFF-2.0 cryogels (Figure 5B). This is probably a reflection of the fact that the cryogels prepared from Jeffamine-acrylamides are rather inhomogeneous, which is also seen by large variation observed with regard to papain loading as discussed in section 3.3.

3.5 Cryogels with immobilized papain: Activity towards cleavage of high molecular substrate; an IgG antibody

To obtain a record of the immobilized papain's activity towards a high molecular substrate we used a human IgG4 antibody. In previous studies, casein has been utilized as a model of a high molecular protein substrate for papain cleavage. Hoever, to investigate the effect of spacer length we opted for an antibody due to its large size (≈150 kDa). The papain activity was tested in a batch mode set-up, where the antibody was incubated with the cryogels for the duration of 24 hrs with gentle shaking. The amount of cleaved antibody was then determined by SE-HPLC (Figure 6) and showed that JEFF-0.9 and JEFF-2.0 accounted for 0.70±0.1 and 0.55±0.01 mg/mL cryogel equivalent to 7.0% and 5.5% conversion of applied antibody, respectively. In comparison to these results, free papain cleaved all the applied antibody under the same conditions and within the same time span. It is thus concluded that for a large substrate, such as an antibody, the apparent enzyme activity is seriously impaired by immobilization onto the Jeffamine®-acrylamide cryogels.

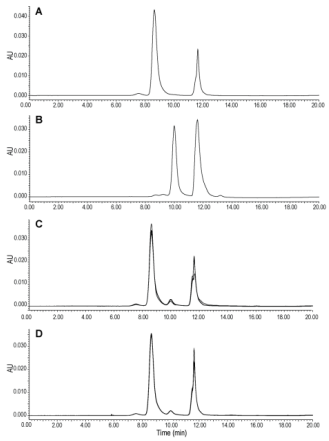

Figure 6: SE-HPLC analysis of papain cleavage of antibody. A: Antibody incubated in cysteine buffer at 37°C for 24 hrs, **B:** Antibody incubated with 1µM papain in cysteine buffer at 37°C for 24 hrs, **C:** Overlay of chromatograms from five replicate samples of antibody in cysteine buffer incubated with JEFF-0.9 cryogel with immobilized papain at 37°C for 24 hrs, **D:** Overlay of chromatograms from five replicate samples of antibody in cysteine buffer incubated with JEFF-2.0 cryogel with immobilized papain at 37°C for 24 hrs.

To obtain an additional qualitative record of the cleavage product, it was analyzed by LC-MS (Figure 7) and by this an interesting result emerged. Antibody cleaved by immobilized papain revealed one single specific mass equivalent to a Fab' fragment (49462 Da) and comparably the antibody cleaved by free papain rendered a series of fragments in the mass range of 48.1-49.3 kDa corresponding to Fab and Fc fragments. We did not pursue this finding any further as it outside the scope of this particular study. It is, however, worth mentioning that it has been reported that papain under certain conditions will cleave antibodies into $F(ab')_2$ fragments [37, 38] and that this has been attributed to steric conditions preventing the complete cleavage rendering the Fab fragments [39].

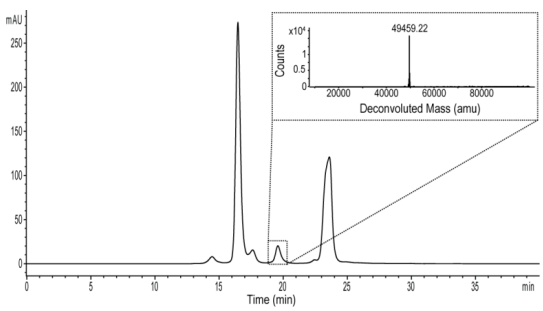

Figure 7: SE-HPLC and LC-MS displaying antibody fragment generated by incubation with papain immobilized on cryogel: The peak isolated from SE-HPLC at approx. 19.5 min was analyzed on LC-MS revealing one specific mass of 49459 Da.

The effect of spacer length was not pronounced with regard to yield of cleavage and the qualitative product obtained was identical between JEFF-0.9 and JEFF-2.0 cryogels. The reason for this can most likely be attributed to the fact that immobilization of papain renders it partly inaccesible and sterically confined with regard to interaction with the antibody.

4. Conclusion

In the present study poly(ether amine) macronmonomers were successfully cryopolymerized, rendering amine functionalized cryogels with two different spacer lengths. Conditions for cryopolymerization were optimized by a DoE approach and resulting cryogels were characterized according to their primary amine loading, porosity, elasticity modulus, mean pore diameter and permeability. The cryogels were found to posses relatively low elasticity moduli but high primary amine functional loadings. Aldehyde activation of matrix was performed by introducing *p*-formylbenzoate functional groups by an efficient route rendering full conversion of matrix primary amines. Subsequently, papain was successfully immobilized and its activity towards a low molecular (L-BAPNA) and high molecular (IgG antibody) substrate was evaluated against the performance of free papain. Evaluated in a column mode, immobilized papain exhibited activity towards cleavage of L-BAPNA, higher than that of free papain and with an indication of increased activity of papain immobilized onto the longer spacer. Evaluated in batch mode, papain exhibited decreased activity towards cleavage of antibody, which was cleaved into a $F(ab')_2$ fragment. This finding could be attributed to inaccessibility of immobilized papain to the antibody.

The poly(ether amine) cryogels prepared in this study afford a hydrophilic, macroporous matrix containing active primary amine functional groups. These were proven highly effective with respect to chemical derivatization.

The use of a cryogel as solid support in enzyme immobilizations is highly relevant as it holds the advantages of convective flow properties, hydrophilic and biocompatible polymeric matrix, as well as being an inexpenssive and environmentally friendly alternative to traditional monoliths. The immobilization chemistry presented in this study should be optimized in order of achieving an immobilized papain with a spatial orientation more accessible to macromolecular interactions and improvements of the mechanical stability of the cryogel should be performed. With such

optimizations undertaken it is feasible that this poly(ether amine) cryogel could be utilized as an alternative solid phase in papain- as well as other enzyme reactor applications.

Acknowledgements

The author Junxian Yun gratefully acknowledge the financial supports partially by the International Science & Technology Cooperation Program between China and Europe Country's Governments from the Ministry of Science and Technology of China (No. 1017 with S2010GR0616) and the National Natural Science Foundation of China (Nos. 21036005). The authors also acknowledge Dr. Songhong Zhang and Xiuhong Cheng for their assistance in the texture and SEM tests.

References

[1] R. DiCosimo, J. McAuliffe, A.J. Poulose, G. Bohlmann, Chem. Soc. Rev. 42 (2013) 6437.

[2] H. Kirsebom, B. Mattiasson, Polymer Chemistry 2 (2011) 1059.

[3] V.I. Lozinsky, F.M. Plieva, I.Y. Galaev, B. Mattiasson, Bioseparation 10 (2001) 163.

[4] P. Arvidsson, F.M. Plieva, V.I. Lozinsky, I.Y. Galaev, B. Mattiasson, Journal of Chromatography A 986 (2003) 275.

[5] F.M. Plieva, I.N. Savina, S. Deraz, J. Andersson, I.Y. Galaev, B. Mattiasson, Journal of Chromatography B-Analytical Technologies in the Biomedical and Life Sciences 807 (2004) 129.

[6] A. Hanora, F.M. Plieva, M. Hedstrom, I.Y. Galaev, B. Mattiasson, J. Biotechnol. 118 (2005) 421.

[7] S. Sun, Y. Tang, Q. Fu, X. Liu, W. Du, L. Guo, Y. Zhao, Journal of Separation Science 35 (2012) 893.

[8] J.M. Harris (Editor), Poly(ethylene glycol) Chemistry: Biotechnical and Biomedical Applications. Plenum Press, New York, United States of America, 1992, p. 1-14.

[9] N.A. Peppas, K.B. Keys, M. Torres-Lugo, A.M. Lowman, J. Controlled Release 62 (1999) 81.

[10] D.J. Overstreet, R. Huynh, K. Jarbo, R.Y. McLemore, B.L. Vernon, Journal of Biomedical Materials Research Part A 101A (2013) 1437.

[11] D.J. Overstreet, R.Y. McLemore, B.D. Doan, A. Farag, B.L. Vernon, Soft Materials 11 (2013) 294.

[12] C. Lin, I. Gitsov, Macromolecules 43 (2010) 10017.

[13] J. Zimmermann, K. Bittner, B. Stark, R. Mulhaupt, Biomaterials 23 (2002) 2127.

[14] S. Noel, B. Liberelle, L. Robitaille, G. De Crescenzo, Bioconjug. Chem. 22 (2011) 1690.

[15] E. Kaiser, Colescot.Rl, Bossinge.Cd, P.I. Cook, Anal. Biochem. 34 (1970) 595.
[16] B.F. Erlanger, W. Cohen, N. Kokowsky, Arch. Biochem. Biophys. 95 (1961) 271.
[17] J.M. Goddard, J.H. Hotchkiss, Progress in Polymer Science 32 (2007) 698.
[18] P.J. Soltys, M.R. Etzel, Biomaterials 21 (2000) 37.
[19] B.C. Weimer, M.K. Walsh, X.W. Wang, J. Biochem. Biophys. Methods 45 (2000) 211.
[20] F.M. Plieva, M. Karlsson, M.R. Aguilar, D. Gomez, S. Mikhalovsky, I.Y. Galaev', Soft Matter 1 (2005) 303.
[21] F. Plieva, H. Xiao, I.Y. Galaev, B. Bergenstahl, B. Mattiasson, Journal of Materials Chemistry 16 (2006) 4065.
[22] H. Kirsebom, G. Rata, D. Topgaard, B. Mattiasson, I.Y. Galaev, Polymer 49 (2008) 3855.
[23] H. Kirsebom, G. Rata, D. Topgaard, B. Mattiasson, I.Y. Galaev, Macromolecules 42, 14 (2009) 5208-5214.
[24] F. Plieva, H. Xiao, I.Y. Galaev, B. Bergenstahl, B. Mattiasson, Journal of Materials Chemistry 16 (2006) 4065.
[25] C.Y. Won, M.D. Bentley, J.M. Harris, J Appl Polym Sci 74 (1999) 913.
[26] E. Amri, F. Mamboya, American Journal of Biochemistry and Biotechnology 8 (2012) 99.
[27] S. Ganapathi, D.A. Butterfield, D. Bhattacharyya, Journal of Chemical Technology and Biotechnology 64 (1995) 157.
[28] R. Ganapathy, S. Manolache, M. Sarmadi, F. Denes, Journal of Biomaterials Science-Polymer Edition 12 (2001) 1027.
[29] L.A.A. Sluyterman, J. Wijdenes, Biotechnol. Bioeng. 23 (1981) 1977.
[30] G.T. Hermanson, Bioconjugate Techniques, 2nd Edition. 2008, .
[31] P. Zhuang, D.A. Butterfield, J Appl Polym Sci 47 (1993) 1329.
[32] H.H. Weetall, R.D. Mason, Biotechnol. Bioeng. 15 (1973) 455.
[33] E. Kaiser, Colescot.Rl, Bossinge.Cd, P.I. Cook, Anal. Biochem. 34 (1970) 595.
[34] A. Bhardwaj, J.B. Lee, K. Glauner, S. Ganapathi, D. Bhattacharyya, D.A. Butterfield, J. Membr. Sci. 119 (1996) 241.
[35] V.G. Jayakumari, V.N.R. Pillai, J Appl Polym Sci 42 (1991) 583.
[36] T. Hayashi, Y. Ikada, Biotechnol. Bioeng. 35 (1990) 518.
[37] S.J. Boguslawski, D.J. Ledden, R.A. Fredrickson, J. Immunol. Methods 120 (1989) 51.
[38] P. Parham, M.J. Androlewicz, F.M. Brodsky, N.J. Holmes, J.P. Ways, J. Immunol. Methods 53 (1982) 133.

[39] M. Adamczyk, J.C. Gebler, J. Wu, J. Immunol. Methods 237 (2000) 95.

Paper IV

Journal of Chromatography A, 1218 (2011) 5487–5497

Contents lists available at ScienceDirect

Journal of Chromatography A

journal homepage: www.elsevier.com/locate/chroma

An improved capillary model for describing the microstructure characteristics, fluid hydrodynamics and breakthrough performance of proteins in cryogel beds

Junxian Yun[a,b,*], Gry Ravn Jespersen[a,c], Harald Kirsebom[a], Per-Erik Gustavsson[c], Bo Mattiasson[a], Igor Yu Galaev[a,d,1]

[a] Department of Biotechnology, Lund University, P.O. Box 124, SE-22100 Lund, Sweden
[b] State Key Laboratory Breeding Base of Green Chemistry Synthesis Technology, College of Chemical Engineering and Materials Science, Zhejiang University of Technology, Chaowang Road 18, Hangzhou 310032, Zhejiang Province, China
[c] Department of Biopharm Chemistry, Novo Nordisk A/S, DK-2760 Måloev, Denmark
[d] DSM Food Specialties B.V., P.O. Box 1, 2600 MA Delft, The Netherlands

ARTICLE INFO

Article history:
Received 31 January 2011
Received in revised form 19 May 2011
Accepted 9 June 2011
Available online 22 June 2011

Keywords:
Cryogel
Mathematical model
Pore size distribution
Tortuosity
Skeleton thickness
Protein

ABSTRACT

A capillary-based model modified for characterization of monolithic cryogels is presented with key parameters like the pore size distribution, the tortuosity and the skeleton thickness employed for describing the porous structure characteristics of a cryogel matrix. Laminar flow, liquid dispersion and mass transfer in each capillary are considered and the model is solved numerically by the finite difference method. As examples, two poly(hydroxyethyl methacrylate) (pHEMA) based cryogel beds have been prepared by radical cryo-copolymerization of monomers and used to test the model. The axial dispersion behaviors, the pressure drop vs. flow rate performance as well as the non-adsorption breakthrough curves of different proteins, i.e., lysozyme, bovine serum albumin (BSA) and concanavalin A (Con A), at various flow velocities in the cryogel beds are measured experimentally. The lumped parameters in the model are determined by matching the model prediction with the experimental data. The results showed that for a given cryogel column, by using the model based on the physical properties of the cryogel (i.e., diameter, length, porosity, and permeability) together with the protein breakthrough curves one can obtain a reasonable estimate and detailed characterization of the porous structure properties of cryogel matrix, particularly regarding the number of capillaries, the capillary tortuousness, the pore size distribution and the skeleton thickness. The model is also effective with regards to predicting the flow performance and the non-adsorption breakthrough profiles of proteins at different flow velocities. It is thus expected to be applicable for characterizing the properties of cryogels and predicting the chromatographic performance under a given set of operating conditions.

1. Introduction

Monolithic cryogels have recently been proposed as a new class of chromatographic supports for separation of biomolecules in downstream processes [1–3]. Numerous studies have been carried out on the preparation of cryogels [4–14], graft polymerization and modification of the cryogel matrix [15–21], characterization of the cryogel properties and adsorption behaviors [6,7,22–25], as well as cryogel applications in capturing various target biomolecules, cells and viruses from crude feedstocks or suspensions [5,26–35]. Cryogel beds could be prepared with a wide variety of different pore size distributions, microstructures, binding capacities, permeabilities and behaviors of hydrodynamic dispersion, breakthrough and elution. The essential part of the preparation of cryogels is freezing of the reaction mixture, which is a stochastic process. Hence each cryogel sample is somewhat unique and has its own physical properties, and thus, specific hydrodynamic and chromatographic behavior towards a given target feedstock. Non-destructive methods for characterization of the sample porosity are of crucial importance for a development of reproducibly performing commercial product. Modeling of fluid flow and mass transfer within cryogel beds as well as characterization of the matrix are of great relevance and fundamental to unraveling of the properties of cryogels. Such insights will promote development of new cryogels and thus expand the applications of the monolithic format in chromatographic separations. Due to the complexity of the pore network system within cryogels, it is still a challenging task to develop a detailed model for characterizing the porous properties of a cryogel

* Corresponding author at: College of Chemical Engineering and Materials Science, Zhejiang University of Technology, Chaowang Road 18, Hangzhou 310032, China Tel.: +86 571 88320951; fax: +86 571 88033331.
E-mail addresses: yunjx@zjut.edu.cn (J.X. Yun), Igor.galaev@dsm.com (I.Y. Galaev).
[1] Present address: DSM Food Specialties B.V., P.O. Box 1, 2600 MA Delft, Alexander Fleminglaan 1, 2613 AX Delft, The Netherlands. Tel.: +31 15 2793771; fax: +31 15 2794110.

0021-9673/$ – see front matter © 2011 Elsevier B.V. All rights reserved.
doi:10.1016/j.chroma.2011.06.056

matrix and describing the chromatographic adsorption and breakthrough behaviors of macromolecules such as proteins.

Numerous mathematical models have been developed to describe the fluid flow and mass transfer characteristics in fixed beds and monoliths in the past years, for instance [36–49]. Some well-validated models in packed beds, such as the equilibrium-dispersive model, the lumped pore diffusion model and the classical random-walk model of Giddings [50], were also employed to investigate the adsorption–desorption and mass transfer kinetics and breakthrough profiles in monolith columns [51,52]. However, the chromatographic and transport characteristics between the monoliths and packed beds are very different due to their different microstructures and these models are needed to be modified. Actually, the fluid hydrodynamics and mass transfer behaviors in monolith beds depend strongly on the micro-structural properties of pores and skeletons. Several approaches have been proposed by considering the detailed structural properties of monoliths in literatures [37,38,50–70], also as reviewed recently in Refs. [71–73]. The Kozeny–Carman approach derived from packed beds has been suggested to calculate the hydraulic permeability and the dispersion behaviors in monolith columns [53–58]. In this approach the porous structure of a monolith was assumed to be made up of uniform spheres together with the interstitial void spaces between these spheres. Unfortunately, incorrect results could be obtained by direct using the Kozeny–Carman equation to characterize monolith beds. For monolith beds, parameters such as the equivalent sphere diameter, the domain size or the equivalent dispersion particle diameter, were proposed alternatively to replace the particle diameter in Kozeny–Carman equation. Due to the complicated and tortuous morphology of pores and skeletons existing in monoliths, this method found its applications limited mainly in silica monolith rods. Meyers and Liapis [37] developed an approach by employing a pore network model to investigate the liquid flow, solute diffusion and breakthrough dynamic behaviors in monoliths. In their model the porous structure of interconnected pores was represented by a regular cubic lattice including pore bonds and nodes [38]. As one knows that huge numbers of pores exist in an actual monolithic column and it is in some cases difficult to construct a network close to a real monolith. Furthermore, the pore structures and shapes of monoliths are so complicated that it is still a challenge to accurately determine the key parameters such as pore connectivity in network models. Miyabe and Guiochon [59] suggested a model by considering the monolith as continuous porous unit structure consisting of cylindrical skeletons surrounded by through-macropores. The bed was assumed homogeneous and thus the general kinetic model could be solved to analyze peak broadening, dispersion and mass transfer kinetics [60,61]. By combining the homogeneous cylindrical unit model and the network model, Gritti et al. [62] developed the parallel pore and pore network models to predict exclusion curves for inverse size-exclusion chromatography. In recent years, the morphology reconstruction approach combining Computational Fluid Dynamics (CFD) and imaging techniques have also been introduced in monolith modeling by several groups [63–69]. The so-called tetrahedral skeleton model was proposed to reconstruct more complicated geometrical structure close to the internal structures of monoliths. This interest model has been demonstrated to be useful and effective in the simulation of the mobile phase transport and hydrodynamics in silica monoliths. However, numerical calculation of concentration fields in such a complicated model for an actual monolith is a challenging task. Recently, Trilisky et al. [70] developed a model by constructing the monolith based on the 2D electron images of pore geometry. The protein breakthrough curves and binding capacities were calculated by considering the pore size distributions.

Common to these monoliths or particulate adsorbents is, that they all have pore diameters which are close to or below micron scale, and thus, primarily diffusional transport occurs within these small pores, although in some macropores of monoliths or interstitial voids of particulate packed beds convective transport also exists during the procedure of chromatography. Polymer-based or silica-based monoliths even have porous structures with both small mesopores and large through-pores, and consequently complex transport behaviors within these wide-scale bimodal pores [56,71–73]. However, the sizes of pores in cryogels are in the range from a few to hundreds of microns [1–5,9,26], which is much larger than that within the conventional monolithic beds. Due to the cryo-polymerization under frozen conditions during the formation of cryogels, the monomers were concentrated by the formation of ice crystals. The polymerization was then achieved at high local-concentration conditions and very dense and thin skeleton was produced. In this skeleton of high polymer concentration very few mesopores exists or very few of them are available for chromatography at low column pressures (much lower than those in conventional monoliths like silica monoliths). Therefore, the microstructures of pores and skeleton within cryogels are much different as those in conventional monoliths having multi-scale pores. In cryogel beds, supermacropores are predominate and the contributions of small skeleton mesopores to the liquid flow and transport of macromolecules like proteins are very limited and thus could be neglected. Within those supermacropores, convective laminar flow is expected to be the dominating means of transport.

Capillary model is a simplification approach of porous media with macropores like the packed beds of perfusive adsorbents and the macroporous silica monoliths, in which the bed was assumed to consist of a bundle of capillaries [41,42,44,45,50,74]. Zabka et al. [41,42] developed a capillary model for silica-based monoliths by assuming the bed as equal parallel capillaries with silica skeletons. In their model, both the diffusion mass transfer within the skeleton and the laminar flow, the parabolic velocity profile, as well as the axial and radial diffusion in capillaries were considered. Actually, the morphology of supermacropores in cryogels is close to the distorted cannular shape and the skeletons are very thin, thereby making the capillary model a simple and easy but interest and effective representation approach for actual cryogels. Persson et al. have proposed a capillary-based model for the characterization of properties and the description of mass transfer and chromatographic adsorption within cryogel beds [22]. In the model, the cryogel was assumed to be made up of several groups of capillaries. These capillaries had equal length as that of the cryogel itself and the skeleton thickness was neglected. The model was demonstrated to be effective in describing protein adsorption performance in a 10 mm diameter cryogel column. Based on this work, we have recently developed a model for the description of protein adsorption and mass transfer behaviors by considering the overall axial dispersion [75].

In this work, we present an improved model by considering the actual detailed properties of the cryogel microstructure, e.g., the tortuosities of pores and the skeleton thickness and consequently a numerical method for solving the differential equations in the model is proposed. Experimental data of proteins from two pHEMA cryogel beds under non-adsorption conditions are matched and compared to the model prediction. The corresponding lumped parameters in the model are determined and the overall results and applicability of the model are discussed.

2. Model

A cryogel is made up of dense polymer skeletons with varying thickness and many pores of different sizes. The skeletons provide the mechanical support and the sites of functional groups for the adsorption of target biomolecules, while the pores permit the flow

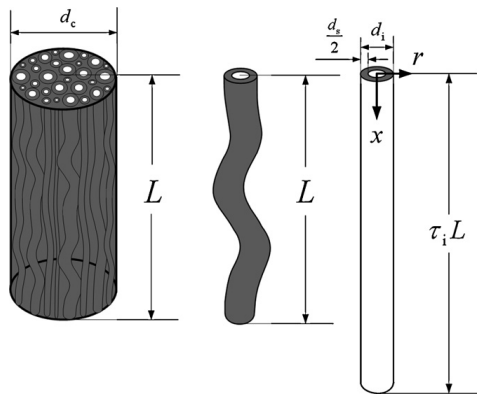

Fig. 1. The schematic diagram of a cryogel made up of tortuous capillaries.

of liquids through the gel. These pores are interconnected and form a complicated network system for the liquid fluid flow and mass transfer of target molecules.

In the present model, the cryogel is assumed to be made up of capillaries with a given size distribution, similar to those in references [22,41,42,44,50,74]. Here, however, we assumed these capillaries are not straight but tortuous. The interconnectivity among capillaries was ignored because the skeleton is thin and the pore sizes are large. The inlets of capillaries are all located at the cryogel inlet surface and their outlets are located at the cryogel outlet surface. They have different lengths and tortuosities. In order to simplify the model, the polymer skeleton outside each capillary is assumed to have a constant thickness, i.e., half of the skeleton thickness d_s.

2.1. Cryogel microstructure and porosity

Fig. 1 displays schematically a cryogel structure made up of capillaries with different length and tortuosities.

For a given capillary i, the tortuosity τ_i is defined as

$$\tau_i = \frac{L_i}{L} \tag{1}$$

where L_i is the capillary length and L the length of the cryogel, respectively.

The porosity of the cryogel bed φ is determined by the total volume of capillaries and the bed volume:

$$\varphi = \frac{\pi}{4A}\sum_{i=1}^{N_g} n_i d_i^2 \tau_i \tag{2}$$

where A ($= \pi d_c^2/4$, d_c is the cryogel diameter) is the cross-area of the cryogel bed, N_g the total number of capillary groups with the same diameter, d_i the capillary diameter and n_i the number of capillaries in group i, respectively. It is assumed that capillaries in a given group have the same diameter, length, tortuosity and skeleton thickness.

The total volume of capillaries and skeleton walls is equal to the bed volume, thus

$$\frac{\pi}{4A}\sum_{i=1}^{N_g} n_i (d_i + d_s)^2 \tau_i = 1 \tag{3}$$

2.2. Fluid flow within a capillary and permeability of the cryogel

In most practical cases, liquid flow in these capillaries is laminar due to the low Reynolds number. The flow rate in a capillary i can then be calculated by the Hagen-Poiseuille equation, as described in [22,74]:

$$Q_i = \frac{\pi d_i^4 \Delta p_i}{128 \mu_L L_i} \tag{4a}$$

where μ_L is the liquid viscosity, Q_i the flow rate and Δp_i the pressure drop between the inlet and outlet of the capillary i, respectively.

The pressure drop of each capillary is equal to that of the whole cryogel Δp. Then, Eq. (4a) is re-written as

$$Q_i = \frac{\pi d_i^4 \Delta p}{128 \mu_L \tau_i L} \tag{4b}$$

The total flow rate in the cryogel bed Q is given by

$$Q = \frac{\pi \Delta p}{128 \mu_L L}\sum_{i=1}^{N_g} \frac{n_i d_i^4}{\tau_i} \tag{5}$$

At a given pressure drop, the flow rate in the cryogel bed can also be calculated by Darcy's equation

$$Q = \frac{kA\Delta p}{\mu_L L} \tag{6}$$

where k is the fluid permeability of the cryogel bed.

Combining Eqs. (5) and (6) one can obtain

$$\frac{\pi}{128kA}\sum_{i=1}^{N_g} \frac{n_i d_i^4}{\tau_i} = 1 \tag{7}$$

A size distribution of capillary diameters with a probability density function $f_1(d_i)$ is assumed. Since the capillary diameters are in the range from the minimum pore diameter d_{min} to the maximum pore diameter d_{max} within cryogels, the actual probability density function for the capillary diameter distribution $f(d_i)$ can be expressed as (similarly as that in expanded beds by Yun et al. [76])

$$f(d_i) = \frac{f_1(d_i)}{1 - \int_{-\infty}^{d_{min}} f_1(d_i)\delta d_i - \int_{d_{max}}^{+\infty} f_1(d_i)\delta d_i} \tag{8a}$$

For a normal distribution, the probability density function for capillary diameters is given by

$$f(d_i) = \frac{(1/\sqrt{2\pi}\sigma)\exp[-(d_i - d_m)^2/2\sigma^2]}{1 - \int_{-\infty}^{d_{min}} (1/\sqrt{2\pi}\sigma)\exp[-((d_i - d_m)^2/2\sigma^2)]\delta d_i - \int_{d_{max}}^{+\infty} (1/\sqrt{2\pi}\sigma)\exp[-((d_i - d_m)^2/2\sigma^2)]\delta d_i} \tag{8b}$$

where σ is the standard deviation and d_m the mean diameter of capillaries in the cryogel column.

2.3. Mass transfer and dispersion in the mobile fluid phase

For a cryogel without ligands, biomolecules would pass through the pores freely and no adsorption would occur. Therefore, under

this non-adsorption condition the differential mass balance equation of biomolecules in the mobile fluid phase of the tortuose capillary i can be written as following by modifying the axial dispersed mass balance equation for plug flow [22,49,74]

$$\frac{\partial C_{\mathrm{Di}}(x_{\mathrm{D}}, t_{\mathrm{Di}})}{\partial t_{\mathrm{Di}}} = \frac{1}{Pe_{\mathrm{i}}} \frac{\partial^2 C_{\mathrm{Di}}(x_{\mathrm{D}}, t_{\mathrm{Di}})}{\partial x_{\mathrm{D}}^2} - \frac{\partial C_{\mathrm{Di}}(x_{\mathrm{D}}, t_{\mathrm{Di}})}{\partial x_{\mathrm{D}}} \tag{9a}$$

The initial and the boundary conditions are expressed as

$$C_{\mathrm{Di}}(x_{\mathrm{D}}, t_{\mathrm{Di}})\big|_{t_{\mathrm{Di}}=0, x_{\mathrm{D}}>0} = 0 \tag{9b}$$

$$C_{\mathrm{Di}}(x_{\mathrm{D}}, t_{\mathrm{Di}})\big|_{x_{\mathrm{D}}=0} = 1 \tag{9c}$$

$$\left.\frac{\partial C_{\mathrm{Di}}(x_{\mathrm{D}}, t_{\mathrm{Di}})}{\partial x_{\mathrm{D}}}\right|_{x_{\mathrm{D}}=1} = 0 \tag{9d}$$

where $C_{\mathrm{Di}}(x_{\mathrm{D}}, t_{\mathrm{Di}})$ ($=C_{\mathrm{i}}(x,t)/C_0$, $C_{\mathrm{i}}(x,t)$ is the bulk-phase concentration and C_0 the inlet concentration) is the dimensionless bulk-phase concentration of biomolecules in the capillary i, x_{D} ($=x/\tau_{\mathrm{i}}L$, x is the distance) the dimensionless distance from the inlet along the capillary length, t_{Di} ($=tU_{\mathrm{i}}/\tau_{\mathrm{i}}L$, where the velocity $U_{\mathrm{i}} = U_{\mathrm{L}}d_{\mathrm{i}}^2/32k\tau_{\mathrm{i}}$, t is the time and $U_{\mathrm{L}} = Q/A$ is the liquid flow velocity in the cryogel bed) the dimensionless time, Pe_{i} ($=\tau_{\mathrm{i}}LU_{\mathrm{i}}/D_{\mathrm{axi}}$, D_{axi} is the axial liquid dispersion coefficient) the axial Peclet number, respectively.

For laminar flow in a straight tube, the axial dispersion coefficient can be estimated by Taylor–Aris correlation [77–81], which was based on the work originally by Taylor in 1950s [82]:

$$D_{\mathrm{axi}} = D_{\mathrm{AB}} + \frac{U_{\mathrm{i}}^2 d_{\mathrm{i}}^2}{192 D_{\mathrm{AB}}} \tag{10a}$$

where D_{AB} is the molecular diffusion coefficient of biomolecules. In the present case, however, the capillary is tortuous. In comparison with the straight tube the axial dispersion in a tortuous tube is more complicated because the tortuosity could induce the local secondary flow and variation of residence time across the flow, as those observed in coiled tubes or helical channels [83,84]. Basically, the axial dispersion coefficient in a curved tube is influenced by several factors, such as the flow velocity profile, the fluid properties, the tube diameter and tortuosity, and even the alternating curvatures. All these factors could contribute to the longitudinal molecular diffusion and the radial mass transfer and thus, the changing of the axial dispersion coefficient in comparison with that for straight tubes. For laminar flow in the present tortuous capillary, there is a lack of precise correlations for the axial dispersion coefficient. Recently, Gutsche and Bunke [45] obtained a modified correlation of the axial dispersion coefficient in fixed beds. In their correlation, the contributions of the bed tortuosity and the bed skeleton (i.e., adsorbents) to the axial dispersion were included and the deviations from the ideal flow and mixing behavior were described by using a dimensionless parameter, which was determined according to the experimental measurements. Based on the correlation suggested by Gutsche and Bunke [45], we use the following correlation to estimate D_{axi} in the present tortuous capillary

$$D_{\mathrm{axi}} = \frac{D_{\mathrm{AB}}}{\tau_{\mathrm{i}}} + \frac{1}{\psi} \frac{U_{\mathrm{i}}^2 d_{\mathrm{i}}^2}{192 D_{\mathrm{AB}}} \tag{10b}$$

The parameter $\psi = \zeta Pe_{\mathrm{AB}}^{0.775}$ in a fixed bed and the constant ζ depends on the adsorbents used ($\zeta = 0.011$ and 0.018 for regular and irregular adsorbents, respectively [45]). For a tortuous capillary in a cryogel bed, ζ should depend on the shape and thickness of the skeletons and thus can also be assumed to be a constant. The molecule Peclet number in capillary i can be expressed as $Pe_{\mathrm{ABi}} = d_{\mathrm{i}}U_{\mathrm{i}}/D_{\mathrm{AB}}$ and then $\psi = \zeta Pe_{\mathrm{ABi}}^{0.775}$. In this model, the correlation by Gutsche and Bunke [45] is used for each capillary, i.e., $\psi = 0.018 Pe_{\mathrm{ABi}}^{0.775}$.

2.4. Tortuosity of capillaries

In the above model, it is necessary to determine the unknown parameter τ_{i}. As can be seen from Eq. (4b), at a given pressure drop the time for fluid flow through a capillary with larger diameter and smaller tortuosity could be much shorter than that for a small one with larger tortuosity. In such case, the broad residence time distribution (RTDs) for fluid through could occur in a cryogel bed with the wide size distribution of capillaries, which implies that strong dispersion could always be observed. However, the axial dispersion in many real cryogels with pore diameters in the range from 10 to 200 μm is not strong but weak (the axial dispersion coefficient 10^{-6} to 10^{-8} m^2/s) and the RTD curves are not broad either [9–11,20,21,32]. This reveals that the larger capillaries might be longer or more tortuous than that of the smaller ones, which could result in the narrow RTDs and weak axial dispersion. Therefore, in this work we assume the following linear function for describing the variation of τ_{i} vs. the capillary diameter:

$$\tau_{\mathrm{i}} = \tau_{d\,\mathrm{min}} + \varpi\,(d_{\mathrm{i}} - d_{\mathrm{min}}) \tag{11a}$$

where $\tau_{d\mathrm{min}}$ (≥ 1) is the tortuosity of the capillary with diameter d_{min} and the parameter ϖ is the line slope of the tortuosity vs. capillary diameter.

Actually, the tortuosity $\tau_{d\mathrm{max}}$ of the capillary with diameter d_{max} can be determined from the RTDs or breakthrough curves using a non-adsorbent tracer. The time for the tracer passing through the largest capillary within the cryogel bed is expressed as

$$t_{d\,\mathrm{max}} = \frac{\tau_{d\,\mathrm{max}} L}{U_{d\,\mathrm{max}}} = \frac{\tau_{d\,\mathrm{max}} L}{U_L d_{\mathrm{max}}^2} 32k\tau_{d\,\mathrm{max}} \tag{11b}$$

where $U_{d\mathrm{max}}$ is the liquid velocity within the capillary with the diameter d_{max}. Then, ϖ is determined and Eq. (11a) can be rewritten as

$$\tau_{\mathrm{i}} = \tau_{d\ \mathrm{min}} + \frac{(d_{\mathrm{i}} - d_{\mathrm{min}})}{(d_{\mathrm{max}} - d_{\mathrm{min}})} \left(\sqrt{\frac{t_{d\ \mathrm{max}} U_L}{32kL}} d_{\mathrm{max}} - \tau_{d\ \mathrm{min}} \right) \tag{11c}$$

In most practical cases, however, it is difficult to determine $\tau_{d\mathrm{min}}$ directly from the RTDs or breakthrough curves due to the extended tails of these curves. The parameter can then be determined by fitting the permeability and porosity as well as the protein breakthrough data of the cryogel bed.

3. Numerical methods

For a given cryogel bed, the unknown parameters $\tau_{d\mathrm{min}}$, d_{s}, σ, d_{m} and the total number of capillaries M ($= \sum_{i=1}^{N_{\mathrm{g}}} n_{\mathrm{i}}$) in the model were estimated by fitting Eqs. (2), (3), (7) and (9a) together with the experimental data and restricting d_{s} and M in certain limits.

For a typical class of cryogels prepared under similar conditions, the skeleton thickness varies in a relatively narrow range as observed in experiments [2–11,22], e.g., 4–24 μm for the polyacrylamide-based cryogels prepared by Persson et al. [22] and Yao et al. [20]. Therefore, in this model the value of d_{s} is restrained in a given range. The range of M was estimated by considering different situations. In the case that all the capillaries have the same diameter of d_{min}, the maximum number of capillaries M_{max} can be obtained by regarding the total volume of these capillaries as equal to the cryogel bed and from Eq. (4a)

$$\frac{M_{\mathrm{max}} \pi (d_{\mathrm{min}} + d_{\mathrm{s}})^2 \tau_{d\ \mathrm{min}} L}{4} = \frac{\pi d_{\mathrm{c}}^2 L}{4} \tag{12a}$$

In the case that all the capillaries have the same diameter of d_{max}, the minimum value M_{min} can also be achieved in a similar way and we get

$$\frac{M_{max}\pi(d_{min}+d_s)^2\tau_{d\ max}L}{4}=\frac{\pi d_c^2 L}{4} \tag{12b}$$

Then,

$$M_{max,1}=\frac{d_c^2}{(d_{min}+d_s)^2\tau_{d\ min}} \tag{12c}$$

$$M_{min,1}=\frac{d_c^2}{(d_{max}+d_s)^2\tau_{d\ max}} \tag{12d}$$

On the other hand, M_{max} or M_{min} are obtained by regarding the cross-section areas of these capillaries equal to the cross-area of the cryogel bed due to the fact that all the inlets of capillaries (along each of the capillary axis) should be distributed on the surface of the cryogel bed inlet.

$$M_{max,2}=\frac{d_c^2}{(d_{min}+d_s)^2} \tag{12e}$$

$$M_{min,2}=\frac{d_c^2}{(d_{max}+d_s)^2} \tag{12f}$$

Therefore, for an actual cryogel the possible value of M should be in the following range

$$\mathrm{Max}(M_{min,1}, M_{min,2}) \le M \le \mathrm{Min}(M_{max,1}, M_{max,2}) \tag{13a}$$

i.e.,

$$M_{min,2} \le M \le M_{max,1} \tag{13b}$$

Eq. (13b) was employed as one constrained condition and the possible value of M was then determined by matching the model calculation with the experimental data.

The finite difference method was then employed to solve the mass balance equation in the model, as that reported in [22]. The discrete procedure is also similar as that reported by Özdural et al. [40] and Yun et al. [76]. The mass balance equation was discretized by the central difference approximation for $\partial C_{Di}/\partial x_D$ and $\partial^2 C_{Di}/\partial x_D^2$ and the implicit scheme of finite difference with the backward difference approximation for $\partial C_{Di}/\partial t_{Di}$. The concentration at the out let of the cryogel bed was obtained by averaging the concentrations in capillaries based on their flow rates and written as

$$C=\frac{\sum_{i}^{N_g} C_i n_i Q_i}{Q} \tag{14}$$

The deviations of the model predictions from the experimental data of the porosity, permeability, the bed volume as well as the protein breakthrough were estimated by calculating the differences between the predicted (subscript symbol is "cal") and experimental data (subscript symbol is "exp"). The relative difference of the porosity is given by

$$\delta_\phi=\frac{|\varphi_{cal}-\varphi_{exp}|}{\varphi_{exp}} \tag{15a}$$

The relative difference of the permeability is expressed as

$$\delta_k=\frac{|k_{cal}-k_{exp}|}{k_{exp}} \tag{15b}$$

The relative difference of the bed volume is defined as

$$\delta_V=\frac{|V_{cal}-V_{exp}|}{V_{exp}} \tag{15c}$$

where V_{cal} and V_{exp} are the predicted and experimental volumes of the cryogel, respectively.

The mean dimensionless difference of the breakthrough data is expressed as

$$\delta_C=\frac{\sum_{j=1}^{N_j}|C_{cal,j}-C_{exp,j}|}{N_j C_0} \tag{15d}$$

where N_j is the total data number of the experimental breakthrough.

4. Experimental

4.1. Materials

Hydroxyethyl methacrylate (HEMA, 96%), was purchased from Acros Organics. Allyl glycidyl ether (AGE, 99%), poly(ethyleneglycol) diacrylate (PEGDA, 99%, $M_n \sim 258$ g/mol), iminodiacetic acid (IDA, 98%), *N,N,N′,N′*-tetramethylethylenediamine (TEMED, 99%), ammonium persulfate (APS) and, lysozyme from chicken egg white and Con A were all purchased from Sigma–Aldrich. BSA (98%) was from Amresco (Ohio, USA). PBS buffer tablets were purchased from Medicago AB. Other chemicals used were analytical grade. All reagents were used as received.

4.2. Preparation of pHEMA cryogels

Two pHEMA cryogels were produced by free radical cryocopolymerization of monomers initiated by TEMED and APS in glass columns with the inner diameters of 5 mm and 10 mm, respectively. For the preparation of cryogel in the column of 5 mm diameter (Cryogel-1), monomers (1.53 g of HEMA, 0.46 g of PEGDA and 0.27 g AGE) were dissolved in 11 ml of deionized water and the mixture was degassed with nitrogen gas for 10 min. The mixture was then cooled to 0 °C and 0.02 g of TEMED (dissolved in 1 ml of deionized water) and 0.02 g of APS (dissolved in 1 ml of deionized water) were added to the mixture to give a total volume of 15 ml and a monomer concentration of 15% (w/v). The gelation mixture was then briefly stirred and 0.8 ml was quickly added to a glass column and frozen at −12 °C for 24 h. The resulting cryogel was thawed at room temperature and washed by pumping 100 ml of deionized water through it to remove unreacted monomers. 100 ml of 0.5 M Na_2CO_3 was then pumped through the cryogel followed by 100 ml of 0.5 M IDA in 1.0 M Na_2CO_3 which was applied in a recycling mode for 18 h at room temperature. Thereafter, the cryogel was washed with 100 ml of 0.5 M Na_2CO_3 and then with water until neutral pH. The height of the obtained water swollen cryogel column was 4.8 cm. For the preparation of cryogel in the column of 10 mm diameter (Cryogel-2), the solution containing monomers with the same concentrations as those used in the preparation of Cryogel-1 was added into the glass column, which was then sealed and immersed into ethanol contained in a freezing system and frozen at −15 °C for 24 h. The obtained cryogel was thawed at room temperature and washed by deionized water for further measurements. The height of Cryogel-2 was 6.5 cm.

4.3. Measurement of breakthrough curves of proteins and characterization of cryogels

The column of Cryogel-1 was connected to an ÄKTA Explorer Chromatographic System and the extra-volume of this system was determined by measuring the time for an input tracer pulse (1%, v/v, acetone solution, UV_{280}) flowing through the system, bypassing the

column at a known flow-rate. For the breakthrough experiments, a lysozyme solution of 0.5 mg/ml in PBS buffer (pH 7.4) was employed and passed through the column under non-binding conditions, i.e., the protein molecules were non-retained or not bound in the cryogel. A sample of 3 ml was loaded for each run at a different flow velocity and the process was monitored at UV 280 nm. The column was washed by buffer between each run.

For the column of Cryogel-2, residence time distributions (RTDs) and breakthrough of proteins were measured at various flow velocities in a chromatographic system with a peristaltic pump, a switching valve and an on-line flow-through UV spectrometer, as used previously [9–11,20,21,23,32–34]. RTDs were investigated by the tracer pulse method and 150 μL of 0.5 mg/ml BSA and 0.5 mg/ml lysozyme solution were applied as the tracers in each run, respectively. The obtained response signals were then used to evaluate the axial dispersion performance within the column. The axial dispersion coefficients at different liquid flow velocities were determined by the variance and the mean residence time of the corresponding RTD curve under close-vessel boundary [10]. In the breakthrough curve measurements, the protein solution of 0.5 mg/ml of lysozyme in 20 mM PBS buffer (pH 7.4) was passed through the column at various flow velocities. The loaded sample was 15 ml for each run and the process was also monitored at UV 280 nm. The column was washed using 2 M NaCl in 20 mM PBS buffer (pH 7.4) between each run. The breakthrough curves of BSA and Con A at the same conditions were also measured.

The relationships between the pressure vs. flow rate through the cryogels were measured by passing deionized water through the columns at different hydrostatic pressure drops (i.e., using different heights of water-columns) and the cryogel permeabilities were determined by fitting the experimental data with Eq. (6). Porosities of Cryogel-1 and Cryogel-2 were determined by measuring the content of free water and the cryogel volume of a given sample as previously described in [5,6,10], and the microstructure of the cryogel was visualized and determined by scanning electron microscope (SEM), according to the procedure described by [6,7,13].

5. Results and discussion

Experimental values of the cryogel diameter, length, porosity and permeability, as well as the liquid properties, were used as the known inputs for the model. In the model calculation, viscosities and densities of the present aqueous dilute solution of lysozyme, BSA or Con A at the test concentration and temperatures were estimated using the equations reported by Monkos [85,86], as similar as in Ref. [76]. The diffusion coefficients of BSA and Con A in PBS buffer were estimated using the correlation suggested by Young et al. [87] and the diffusion coefficient of lysozyme was calculated by the equation proposed by Tyn and Gusek [88], respectively. These correlations were found to fit well with experimental data as demonstrated by He and Niemeyer [89]. Basic parameter values used in the model are summarized in Table 1.

The physical parameters of the capillaries and skeletons in the model were determined by fitting the model calculation in a manual manner with the experimental results of the cryogel size, porosity, permeability together with the protein breakthrough curves at a given flow velocity. For a typical fitting, the value of $t_{d\max}$ at a certain liquid velocity was obtained from the breakthrough curve for Cryogel-1 or the RTD curve for Cryogel-2 and the range of d_s was set as from 1 to 12 μm in this work because the skeletons of the present cryogels were very thin. Firstly, the initial values of d_m, σ, d_s and $\tau_{d\min}$ were given and the range of M was calculated by Eq. (13b). For each M, the number of capillary groups was estimated by setting the diameter step as 1 μm and the number of capillary in each group was determined by integrating Eq. (8b) between the group intervals. Then, the porosity, the permeability and the total bed volume were calculated by Eqs. (2), (3) and (7). The obtained values were compared with the corresponding experimental values and their relative errors were calculated. The allowable maximum relative error between the calculated and experimental values was set below 2% for porosity and permeability, and 1% (Cryogel-1) or 1.8% (Cryogel-2) for the total bed volume, respectively. If the obtained relative errors were larger than the allowable values, new values of these unknown parameters were generated and the calculation of the porosity, the permeability and the total bed volume was repeated again. The iterative step of $\tau_{d\min}$ was set as 0.005, which was sufficient to give a good accuracy to achieve the fitting. In order to improve the fitting efficiency and decrease the calculation time, the manual procedure for generating new values of d_m, σ and d_s was employed here, which was achieved by using iterative steps of 1, 0.1 and 0.5 μm at each new calculation, respectively. This procedure was repeated until the obtained relative errors were within the allowable values. Generally, there could be different sets of parameters in the model which can match well with the experimental values. But only those fitting well with the experimental breakthrough curve at a given flow velocity were considered as the reasonable parameters and used in the calculation. The model was solved numerically and the dispersion coefficients and breakthrough profiles of proteins under non-adsorption conditions at different flow velocities were predicted. The relative differences of the porosity, the permeability and the bed volume as well as the mean difference of the breakthrough data between the model predictions and the experimental values were calculated and listed in Table 2. These values are low, indicating satisfied predictions by the present model.

5.1. The total number and tortuosities of capillaries in the model

The total number of capillaries and the tortuosities are two crucial parameters needed to be determined by the model. From SEM images of the pHEMA cryogels shown in Fig. 2(a) and (b), the pore diameters are in the range from about 10 to 100 μm for Cryogel-1 and 10 to 110 μm for Cryogel-2. We roughly set $d_{\min} = 10$ μm for both cryogels and $d_{\max} = 100$ μm for Cryogel-1 and $d_{\max} = 110$ μm for Cryogel-2 in the calculation. For Cryogel-1, $t_{d\max}$ of 25.4 s was observed from the experimental breakthrough of lysozyme under non-adsorption conditions at the liquid flow velocity of 8.49×10^{-4} m/s, and this value was employed to determine $t_{d\max}$. For Cryogel-2, $t_{d\max}$ of 245 s was obtained from the RTD curve at the liquid flow velocity of 1.65×10^{-4} m/s. The tortuosities of different capillaries were determined using Eq. (11b) together by considering Eq. (13b), and the total number of capillaries is likely to be within the range of $2289 \le M \le 50{,}491$ for Cryogel-1 or $7763 \le M \le 261{,}284$ for Cryogel-2. A satisfactory number of 2306 capillaries for Cryogel-1 or 7791 for Cryogel-2 was obtained by fitting the model prediction with the experimental data, and this value was then employed in the following calculation. The obtained tortuosities of capillaries increased from 2.36 to 4.08 with the increase of capillary diameter from 10 to 100 μm for Cryogel-1, while from 2.10 to 6.49 with the increase of capillary diameter from 10 to 110 μm for Cryogel-2, as shown in Fig. 3.

5.2. Diameter distribution and skeleton thickness of capillaries in the model

Pore sizes and wall thickness distribution in cryogels can be assessed by imaging processing method using software like NIH ImageJ, as demonstrated recently by Dainiak et al. [90]. However, the uncertain results of image analysis may be influenced by both the image quality and the method of image processing, especially

Table 1
Basic parameters used in the model.

Column	Protein	d_c (m)	L (m)	φ (–)	k (m^2)	μ_L (Pa s)	ρ_L (kg/m^3)	D_{AB} (m^2/s)
Cryogel-1	Lysozyme	5×10^{-3}	4.8×10^{-2}	0.847	8.45×10^{-12}	1.0×10^{-3}	1002	1.18×10^{-10}
Cryogel-2	Lysozyme	10×10^{-3}	6.5×10^{-2}	0.886	5.58×10^{-12}	8.0×10^{-4}	1000	1.43×10^{-10}
Cryogel-2	BSA	10×10^{-3}	6.5×10^{-2}	0.886	5.58×10^{-12}	7.8×10^{-4}	1000	7.98×10^{-11}
Cryogel-2	Con A	10×10^{-3}	6.5×10^{-2}	0.886	5.58×10^{-12}	8.4×10^{-4}	1000	6.38×10^{-11}

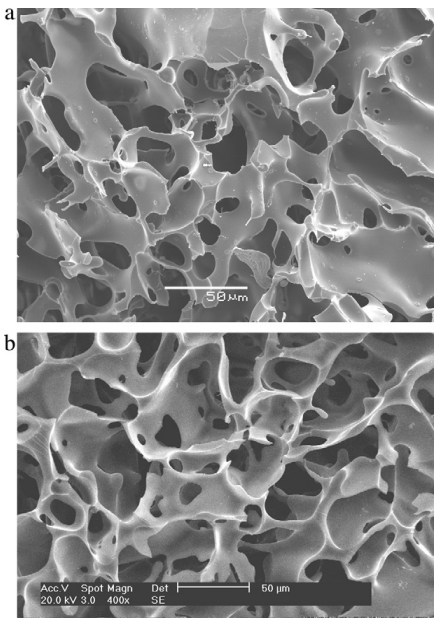

Fig. 2. Scanning electron microscope photographs of the poly(hydroxyethyl methacrylate) cryogels. (a) Cryogel-1 and (b) Cryogel-2.

the choice of threshold magnitude for the segmentation of pores and skeletons and even the pore structure heterogeneity. In the present work, we determine the unknown physical parameters of the capillaries d_s, d_m and σ by simultaneously fitting the model calculation with the experimental data of permeability, porosity, bed volume as well as the protein breakthrough curve at a given velocity. For Cryogel-1 a good agreement between the calculated and experimental data was observed for $d_m = 51$ μm, $\sigma = 13.0$ μm and $d_s = 4.5$ μm, while for Cryogel-2 the obtained values were $d_m = 46$ μm, $\sigma = 19.7$ μm and $d_s = 3.5$ μm. It should be noted that the skeleton thickness is comparable to those for pDMAA (*N*,*N*-dimethylacrylamide) cryogels reported by Persson et al. [22] and gelatin–fibrinogen cryogels by Dainiak et al. [90]. It is also seen that Cryogel-2 has a wider pore size distribution that that for Cryogel-1. The reason is that the small column diameter (5 mm diameter) gave more uniform microstructures or pores than the larger column (10 mm diameter) for the monomer solution with the same concentration under the similar freezing conditions. Based on these parameters, the calculated porosities by the model were 0.849 for Cryogel-1 and 0.882 for Cryogel-2, while the permeabilities by the model were 8.43×10^{-12} m^2 and 5.48×10^{-12} m^2, respectively. These values are very close to the experimental values listed in Table 1.

Fig. 4 shows the capillary diameter distributions in the cryogel beds given by the model. As can be seen, for Cryogel-1 the effective capillary diameters are in the range from 11 to 92 μm (correspondingly the actual tortuoses of these capillaries increased linearly from 2.37 to 3.92) and for Cryogel-2 the effective capillary diameters are in the range from 10 to 110 μm. For Cryogel-1 the contribution of capillaries with $d_i < 11$ μm and $d_i > 92$ μm was neglected. Therefore, it is expected that the actual pores could be in the range of diameters from 11 to 92 μm with the mean diameter of 51 μm in Cryogel-1 and 10 to 110 μm with the mean diameter of 46 μm in Cryogel-2, both with the normal size distribution.

In this model, we assumed a constant skeleton thickness for each cryogel. In reality, it is difficult to determine the accurate value of this parameter even from the SEM images, because the skeleton observed by SEM is not uniform (varied from about 1 to 12 μm, as shown in Fig. 2) and may be either deformed by the sample preparation process or enlarged by a change in observational position or direction. The present value of $d_s = 4.5$ μm for Cryogel-1 or $d_s = 3.5$ μm for Cryogel-2 can thus be considered as an approximate but satisfactory description of the actual skeleton thickness due to

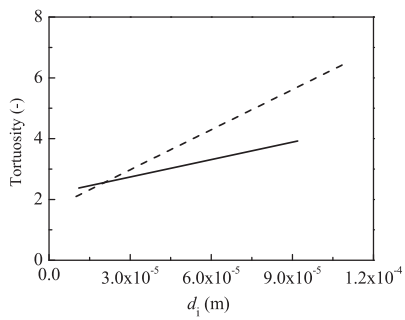

Fig. 3. Tortuosities of capillaries in the poly(hydroxyethyl methacrylate) cryogel beds in the model. (–) Cryogel-1 and (- - -) Cryogel-2.

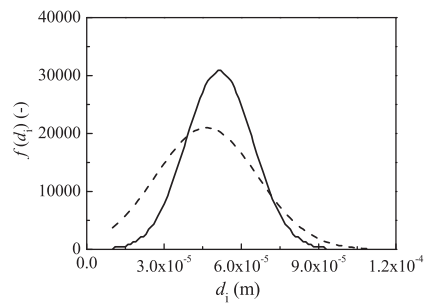

Fig. 4. Diameter distribution of capillaries in the model. (–) Cryogel-1 and (- - -) Cryogel-2.

Table 2
Deviations of the model predictions from the experimental data at various flow velocities.

Column	Protein	δ_φ	δ_k	δ_V	δ_C at different flow velocities											
					8.25 $\times 10^{-5}$ m/s	8.49 $\times 10^{-5}$ m/s	1.65 $\times 10^{-4}$ m/s	1.70 $\times 10^{-4}$ m/s	2.48 $\times 10^{-4}$ m/s	2.55 $\times 10^{-4}$ m/s	3.48 $\times 10^{-4}$ m/s	5.10 $\times 10^{-4}$ m/s	8.41 $\times 10^{-4}$ m/s	8.49 $\times 10^{-4}$ m/s	1.70 $\times 10^{-3}$ m/s	2.55 $\times 10^{-3}$ m/s
Cryogel-1	Lysozyme	0.002	0.002	0.007	–	0.043	–	0.028	–	0.028	–	–	–	0.019	0.020	0.028
Cryogel-2	Lysozyme	0.005	0.018	0.008	0.024	–	0.015	–	0.011	–	0.019	0.020	0.042	–	–	–
Cryogel-2	BSA	0.005	0.018	0.008	0.016	–	0.015	–	0.008	–	0.006	0.020	0.014	–	–	–
Cryogel-2	Con A	0.005	0.018	0.008	0.017	–	0.016	–	0.013	–	0.014	0.013	0.016	–	–	–

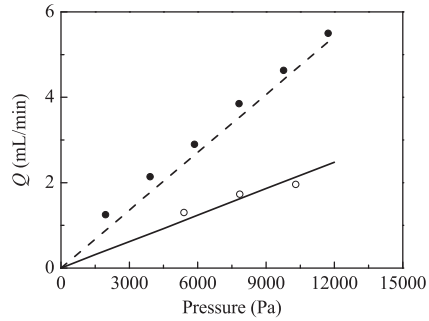

Fig. 5. Comparison of the experimental values of flow rate vs. pressure drop with the data calculated by the model in the poly(hydroxyethyl methacrylate) cryogel beds. (○) experimental in Cryogel-1, (●) experimental in Cryogel-2, (–) predicted in Cryogel-1, and (- - -) predicted in Cryogel-2.

the good agreement between the calculated and experimental data of porosity, permeability and bed volume. These parameters represent suitable values and the presented model itself could thus be regarded as successful in giving a good description of the actual pHEMA cryogel bed.

5.3. Flow rate vs. pressure and axial dispersion

The permeabilities of the cryogels obtained by fitting the experimental data of flow rate vs. pressure drop with Darcy's equation are 8.45×10^{-12} m^2 for Cryogel-1 (the correlation coefficient $R = 0.984$) and 5.58×10^{-12} m^2 for Cryogel-2 ($R = 0.986$), respectively. Fig. 5 displays the comparisons between the experimental values and the calculated data of flow rate vs. pressure drop by the model in the cryogel beds. As can be seen, the agreement between the calculated data by the model and the experimental values is good within the range of flow rates considered.

The axial dispersion coefficients of lysozyme within different capillaries in Cryogel-1 were calculated by Eqs. (10a) and (10b) in the model and shown in Fig. 6. As can be seen, the values of D_{axi} increase both with the increase of capillary diameter and flow velocity. These values are for most capillaries much higher than the molecular diffusion coefficient of lysozyme. Similar results were observed in Cryogel-2 (data not shown here).

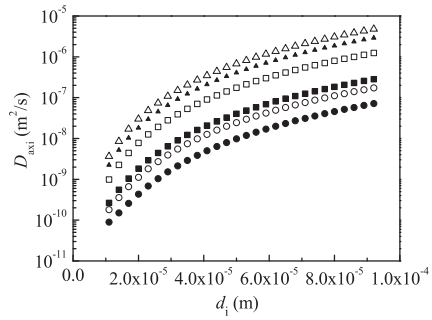

Fig. 6. Variation of axial dispersion coefficients with capillary diameter in Cryogel-1 at liquid flow velocities of 8.49×10^{-5} (●), 1.70×10^{-4} (○), 2.55×10^{-4} (■), 8.49×10^{-4} (□), 1.70×10^{-3} (▲) and 2.55×10^{-3} (Δ) m/s, respectively.

In reality, it is very difficult to obtain the experimental data of axial dispersion coefficients in each supermacropore within an actual cryogel bed and thus, we cannot compare the calculated dispersion directly with experimental data in each capillary. Alternatively, the mean axial dispersion coefficient in all these capillaries according to their flow rates was considered as the calculated dispersion coefficient by the model, which can be determined by the equation expressed as

$$D_{ax} = \frac{\sum_{i}^{N_g} D_{axi} n_i Q_i}{Q} \quad (16)$$

The axial dispersion coefficients in Cryogel-2 at the flow velocities of 8.25×10^{-5}, 1.65×10^{-4}, 2.48×10^{-4}, 3.48×10^{-4}, 5.10×10^{-4}, and 8.41×10^{-4} m/s were determined by RTDs using BSA and lysozyme as tracers, respectively. The obtained results are shown in Fig. 7. It is seen that the dispersion coefficients increased from 6.59×10^{-8} to 5.00×10^{-7} m^2/s for lysozyme and 4.66×10^{-8} to 5.12×10^{-7} m^2/s for BSA with the increase of flow velocity from 8.25×10^{-5} to 8.41×10^{-4} m/s. The mean axial dispersion coefficients were also calculated by the model at the same flow velocities and the obtained values were compared with the experimental, as also shown in Fig. 7. It can be seen that the agreement between the calculated and experimental data is good, indicating that Eq. (10b) is valid in the estimation of axial dispersion coefficients and could be employed in describing the axial dispersion within capillaries in these cryogel beds.

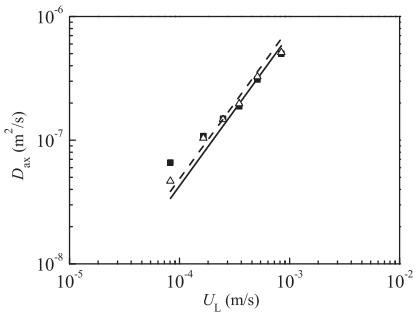

Fig. 7. Comparison of the predicted and experimental mean axial dispersion coefficients at various liquid velocities in Cryogel-2. (■) lysozyme, experimental, (Δ) bovine serum albumin, experimental, (–) lysozyme, predicted and (- - -) bovine serum albumin, predicted.

5.4. Breakthrough curves of proteins under non-adsorption condition

In this work, three different proteins, i.e., lysozyme, BSA and Con A, were employed as the model proteins to test the model under non-adsorption conditions. Molecular weights of these proteins are 14.3, 67 and 102 kDa, respectively. For Cryogel-1, breakthrough curves of lysozyme at the liquid velocities of 8.49×10^{-5}, 1.70×10^{-4}, 2.55×10^{-4}, 8.49×10^{-4}, 1.70×10^{-3} and 2.55×10^{-3} m/s were obtained. It was observed that in these runs the binding capacity of protein molecules due to the possible IDA functional groups was very low (below 0.006 mg/ml cryogel)

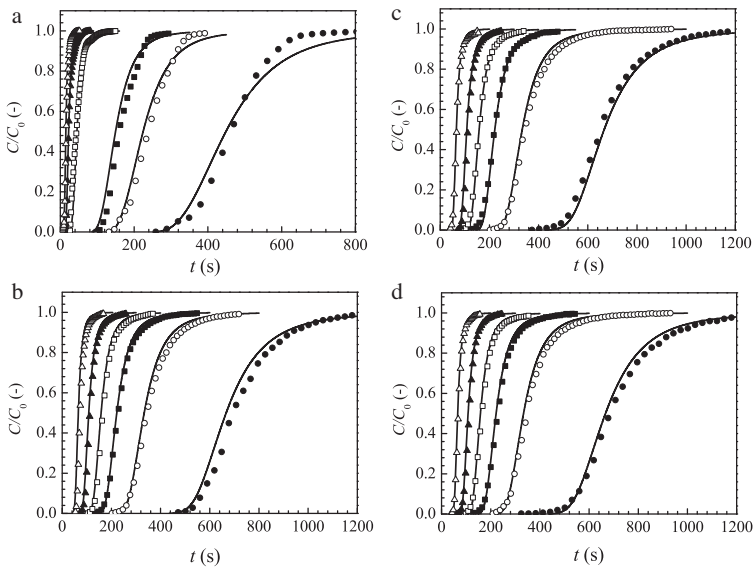

Fig. 8. Comparison of the predicted and experimental breakthrough curves of proteins under non-adsorption condition at various liquid velocities. (a) Lysozyme in Cryogel-1, (b) lysozyme in Cryogel-2, (c) bovine serum albumin in Cryogel-2 and (d) concanavalin A in Cryogel-2. The liquid velocities in Cryogel-1 are 8.49×10^{-5} (●), 1.70×10^{-4} (○), 2.55×10^{-4} (■), 8.49×10^{-4} (□), 1.70×10^{-3} (▲) and 2.55×10^{-3} (Δ) m/s, respectively. The liquid velocities in Cryogel-2 are 8.25×10^{-5} (●), 1.65×10^{-4} (○), 2.48×10^{-4} (■), 3.48×10^{-4} (□), 5.10×10^{-4} (▲) and 8.41×10^{-4} (Δ) m/s, respectively. The solid lines represent the calculation results by the model.

and thus was neglected. For Cryogel-2, breakthrough curves of lysozyme, BSA and Con A are measured at the liquid velocities of 8.25×10^{-5}, 1.65×10^{-4}, 2.48×10^{-4}, 3.48×10^{-4}, 5.10×10^{-4}, and 8.41×10^{-4} m/s, respectively. No binding of proteins was observed. Therefore, in both cryogels the non-binding assumption was valid and protein molecules passed through the pores of the cryogels freely without being bound. Under non-adsorption conditions, the mass balance equation was solved by the finite difference method and the breakthrough profiles were calculated by the model at the corresponding flow velocities as the experiments. In the solving process, each capillary was divided into 50 cells and time steps of 0.1 s were used in the calculation. There was no obvious improvement of accuracy connected with further decreasing the time step or distance interval step.

Fig. 8 shows the comparisons of the calculated results of breakthrough of the considered proteins with the experimental data (expressed as the symbols) at various velocities in Cryogel-1 and Cryogel-2. As it is seen the model predictions are in good agreement with the experimental data, though when varying the values of the different parameters, other likely fittings with the experimental data could be obtained. Therefore, further optimizations based on the precise experimental determination of the parameters are worthy of being investigated in future as it seems that the accuracy of these parameters is very important for the model prediction.

6. Conclusions

The presented model has been shown to be effective in characterizing the microstructure of a cryogel bed and in describing the liquid flow and mass transfer behaviors within supermacropores. The pore tortuosity and the skeleton thickness are considered in this model, and this gives a more detailed model description of an actual cryogel. The parameters of capillaries in the model can be determined by fitting experimental data of permeability, porosity, cryogel bed volume and breakthrough curve under the non-adsorption condition. Once these parameters are determined, the model can then be used to predict the behaviors of protein breakthrough profiles at different flow velocities. Based on the model predictions we have found that the effective pore sizes of the considered pHEMA cryogels are likely be in the range of 10–90 μm for Cryogel-1 and 10–110 μm for Cryogel-2. The mean pore diameters for these two cryogels are likely to be around 51 and 46 μm, and both these calculated predictions show to be close to the actual values of the pores observed from the SEM image. The next step in the development of a comprehensive model of chromatographic performance of cryogels would be the study of breakthrough profiles under the binding conditions. This was the motivation behind the synthesis and study both the plain and IDA-containing pHEMA cryogels, which are the basic matrix for further preparation of ion exchange, hydrophobic and immobilized metal ion affinity cryogels, albeit the IDA-functionality has not been exploited further in the present work.

Acknowledgements

This work was supported by Swedish Research Council. Junxian Yun acknowleges the financial support by the State Scholarship from the China Scholarship Council, the Science and Technology Cooperation Project between China-Europe Country's Governments from the Ministry of Science and Technology of China (Grant No. 1017), the National Natural Science Foundation of China (Nos. 20876145, 21036005) and the Zhejiang Provincial Natural Science Foundation of China (No. Y4080326). The authors also thank Dongjiao Zhou for cryogel measurements.

References

[1] V.I. Lozinsky, F.M. Plieva, I.Y. Galaev, B. Mattiasson, Bioseparation 10 (2002) 163.
[2] V.I. Lozinsky, I.Y. Galaev, F.M. Plieva, I.N. Savina, H. Jungvid, B. Mattiasson, Trends Biotechnol. 21 (2003) 445.
[3] F.M. Plieva, I.Y. Galaev, B. Mattiasson, J. Sep. Sci. 30 (2007) 1657.
[4] V.I. Lozinsky, Russ. Chem. Rev. 71 (2002) 489.
[5] P. Arvidsson, F.M. Plieva, V.I. Lozinsky, I.Y. Galaev, B. Mattiasson, J. Chromatogr. A 986 (2003) 275.
[6] F.M. Plieva, I.N. Savina, S. Deraz, J. Andersson, I.Y. Galaev, B. Mattiasson, J. Chromatogr. B 807 (2004) 129.
[7] F.M. Plieva, J. Andersson, I.Y. Galaev, B. Mattiasson, J. Sep. Sci. 27 (2004) 828.
[8] F.M. Plieva, M. Karlsson, M.R. Aguilar, D. Gomez, S. Mikhalovsky, I.Y. Galaev, B. Mattiasson, J. Appl. Polym. Sci. 100 (2006) 1057.
[9] K.J. Yao, S.C. Shen, J.X. Yun, L.H. Wang, X.J. He, X.M. Yu, Chem. Eng. Sci. 61 (2006) 6701.
[10] K.J. Yao, J.X. Yun, S.C. Shen, L.H. Wang, X.J. He, X.M. Yu, J. Chromatogr. A 1109 (2006) 103.
[11] X.J. He, K.J. Yao, S.C. Shen, J.X. Yun, Chem. Eng. Sci. 62 (2007) 1334.
[12] R.V. Ivanov, V.I. Lozinsky, S.K. Noh, S.S. Han, W.S. Lyoo, J. Appl. Polym. Sci. 106 (2007) 1470.
[13] H. Kirsebom, G. Rata, D. Topgaard, B. Mattiasson, I.Y. Galaev, Polymer 49 (2008) 3855.
[14] G. Baydemir, N. Bereli, M. Andaç, R. Say, I.Y. Galaev, A. Denizli, Funct. Polym. 69 (2009) 36.
[15] I.N. Savina, I.Y. Galaev, B. Mattiasson, J. Chromatogr. A 1092 (2005) 199.
[16] I.N. Savina, B. Mattiasson, I.Y. Galaev, Polymer 46 (2005) 9596.
[17] I.N. Savina, I.Y. Galaev, B. Mattiasson, J. Mol. Recogn. 19 (2006) 313.
[18] I.N. Savina, B. Mattiasson, I.Y. Galaev, J. Polym. Sci. Part A: Polym. Chem. 44 (2006) 1952.
[19] F.M. Plieva, B. Bober, M. Dainiak, I.Y. Galaev, B. Mattiasson, J. Mol. Recogn. 19 (2006) 305.
[20] K.J. Yao, J.X. Yun, S.C. Shen, F. Chen, J. Chromatogr. A 1157 (2007) 246.
[21] F. Chen, K.J. Yao, J.X. Yun, S.C. Shen, Chem. Eng. Sci. 63 (2008) 71.
[22] P. Persson, O. Baybak, F.M. Plieva, I.Y. Galaev, B. Mattiasson, B. Nilsson, A. Axelsson, Biotechnol. Bioeng. 88 (2004) 224.
[23] K.J. Yao, S.C. Shen, J.X. Yun, L.H. Wang, F. Chen, X.M. Yu, Biochem. Eng. J. 36 (2007) 139.
[24] F. Yılmaz, N. Bereli, H. Yavuz, A. Denizli, Biochem. Eng. J. 43 (2009) 272.
[25] F.M. Plieva, E.D. Seta, I.Y. Galaev, B. Mattiasson, Sep. Purif. Technol. 65 (2009) 110.
[26] P. Arvidsson, F.M. Plieva, I.N. Savina, V.I. Lozinsky, S. Fexby, L. Bulow, I.Y. Galaev, B. Mattiasson, J. Chromatogr. A 977 (2002) 27.
[27] M.B. Dainiak, A. Kumara, F.M. Plieva, I.Y. Galaev, B. Mattiasson, J. Chromatogr. A 1045 (2004) 93.
[28] A. Hanora, F.M. Plieva, M. Hedström, I.Y. Galaev, B. Mattiasson, J. Biotechnol. 118 (2005) 421.
[29] A. Kumar, V. Bansal, K.S. Nandakumar, I.Y. Galaev, P.K. Roychoudhury, R. Holmdah, B. Mattiasson, Biotechnol. Bioeng. 93 (2006) 636.
[30] A. Hanora, I.N. Savina, F.M. Plieva, V.A. Izumrudov, B. Mattiasson, I.Y. Galaev, J. Biotechnol. 123 (2006) 343.
[31] S. Deraz, F.M. Plieva, I.Y. Galaev, E.N. Karlsson, B. Mattiasson, Enzyme Microb. Technol. 40 (2007) 786.
[32] J.X. Yun, S.C. Shen, F. Chen, K.J. Yao, J. Chromatogr. B 860 (2007) 57.
[33] L.H. Wang, S.C. Shen, J.X. Yun, K.J. Yao, S.J. Yao, J. Sep. Sci. 31 (2008) 689.
[34] Y. Chen, S.C. Shen, J.X. Yun, K.J. Yao, J. Sep. Sci. 31 (2008) 3879.
[35] F.M. Plieva, I.Y. Galaev, W. Noppe, B. Mattiasson, Trends Microbiol. 16 (2008) 543.
[36] J.J. Meyers, A.I. Liapis, J. Chromatogr. A 827 (1998) 197.
[37] J.J. Meyers, A.I. Liapis, J. Chromatogr. A 852 (1999) 3.
[38] A.I. Liapis, J.J. Meyers, O.K. Crosser, J. Chromatogr. A 865 (1999) 13.
[39] K. Kaczmarski, D. Antos, H. Sajonz, P. Sajonz, G. Guiochon, J. Chromatogr. A 925 (2001) 1.
[40] A.R. Özdural, A. Alkan, P.J.A.M. Kerkhof, J. Chromatogr. A 1041 (2004) 77.
[41] W. Li, Y. Li, Y. Sun, Chem. Eng. Sci. 60 (2005) 4780.
[42] M. Zabka, M. Minceva, A.E. Rodrigues, Chem. Eng. Process. 45 (2006) 150.
[43] M.A. Hashim, K.H. Chu, Sep. Purif. Technol. 53 (2007) 189.
[44] M. Zabka, M. Minceva, A.E. Rodrigues, J. Biochem. Biophys. Methods 70 (2007) 95.
[45] R. Gutsche, G. Bunke, Chem. Eng. Sci. 63 (2008) 4203.
[46] L. Melter, A. Butté, M. Morbidelli, J. Chromatogr. A 1200 (2008) 156.
[47] N. Forrer, A. Butté, M. Morbidelli, J. Chromatogr. A 1214 (2008) 71.
[48] F. Augier, C. Laroche, E. Brehon, Sep. Purif. Technol. 63 (2008) 466.
[49] G. Guiochon, A. Felinger, D.G. Shirazi, A.M. Katti, Fundamentals of Preparative and Nonlinear Chromatography, 2nd ed., Elsevier, Amsterdam, The Netherlands, 2006.
[50] J.C. Giddings, Dynamics of Chromatography, Part I, Principles and Theory, Marcel Dekker, New York, 1965.
[51] F. Gritti, W. Piatkowski, G. Guiochon, J. Chromatogr. A 978 (2002) 81.
[52] F. Gritti, W. Piatkowski, G. Guiochon, J. Chromatogr. A 983 (2003) 51.
[53] H. Minakuchi, K. Nakanishi, N. Soga, N. Ishizuka, N. Tanaka, J. Chromatogr. A 762 (1997) 135.
[54] H. Minakuchi, K. Nakanischi, N. Soga, N. Ishizuka, N. Tanaka, J. Chromatogr. A 797 (1998) 121.
[55] R. Hahn, A. Jungbauer, Anal. Chem. 72 (2000) 4853.

[56] F.C. Leinweber, D. Lubda, K. Cabrera, U. Tallarek, Anal. Chem. 74 (2002) 2470.
[57] U. Tallarek, F.C. Leinweber, A. Seidel-Morgenstern, Chem. Eng. Technol. 25 (2002) 12.
[58] R. Skudas, B.A. Grimes, M. Thommes, K.K. Unger, J. Chromatogr. A 1216 (2009) 2625.
[59] K. Miyabe, G. Guiochon, J. Phys. Chem. B 106 (2002) 8898.
[60] K. Miyabe, A. Cavazzini, F. Gritti, M. Kele, G. Guiochon, Anal. Chem. 75 (2003) 6975.
[61] K. Miyabe, G. Guiochon, J. Sep. Sci. 27 (2004) 853.
[62] F. Gritti, R. Skudas, K.K. Unger, D. Lubda, J. Chromatogr. A 1144 (2007) 14.
[63] N. Vervoort, P. Gzil, G.V. Baron, G. Desmet, Anal. Chem. 75 (2003) 843.
[64] N. Vervoort, H. Saito, K. Nakanishi, G. Desmet, Anal. Chem. 77 (2005) 3986.
[65] P. Gzil, N. Vervoort, G.V. Baron, G. Desmet, J. Sep. Sci. 27 (2004) 887.
[66] P. Gzil, J.D. Smet, G. Desmet, J. Sep. Sci. 29 (2006) 1675.
[67] F. Detobel, P. Gzil, G. Desmet, J. Sep. Sci. 32 (2009) 2707.
[68] D. Hlushkou, S. Bruns, U. Tallarek, J. Chromatogr. A 1217 (2010) 3674.
[69] D. Hlushkou, S. Bruns, A. Höltzel, U. Tallarek, Anal. Chem. 82 (2010) 7150.
[70] E.I. Trilisky, H. Kokua, K.J. Czymmek, A.M. Lenhoff, J. Chromatogr. A 1216 (2009) 6365.
[71] G. Guiochon, J. Chromatogr. A 1168 (2007) 101.
[72] K.K. Unger, R. Skudas, M.M. Schulte, J. Chromatogr. A 1184 (2008) 393.
[73] A. Jungbauer, R. Hahn, J. Chromatogr. A 1184 (2008) 62.
[74] J.C. Giddings, Unified Separation Science, Wiley, New York, 1991.
[75] J.X. Yun, H. Kirsebom, I.Y. Galaev, B. Mattiasson, J. Sep. Sci. 32 (2009) 2601.
[76] J.X. Yun, D.Q. Lin, S.J. Yao, J. Chromatogr. A 1095 (2005) 16.
[77] R. Aris, Proc. R. Soc. A 235 (1956) 67.
[78] O. Levenspiel, Ind. Eng. Chem. 50 (1958) 343.
[79] K.B. Bischoff, O. Levenspiel, Chem. Eng. Sci. 17 (1962) 245.
[80] J. Dayan, O. Levenspiel, Ind. Eng. Chem. Fund. 8 (1969) 840.
[81] O. Levenspiel, Chemical Reaction Engineering, 3rd ed., Wiley, New York, 1999.
[82] G. Taylor, Proc. R. Soc. A 219 (1953) 186.
[83] R.J. Nunge, T.-S. Lin, W.N. Gill, J. Fluid Mech. 51 (1972) 363.
[84] C.B. Minnich, F. Sipeer, L. Greiner, M.A. Liauw, Ind. Eng. Chem. Res. 49 (2010) 5530.
[85] K. Monkos, Int. J. Biol. Macromol. 18 (1996) 61.
[86] K. Monkos, Biochim. Biophys. Acta 1339 (1997) 304.
[87] M.E. Young, P.A. Carroad, R.L. Bell, Biotechnol. Bioeng. 22 (1980) 947.
[88] M.T. Tyn, T.W. Gusek, Biotechnol. Bioeng. 35 (1990) 327.
[89] L.Z. He, B. Niemeyer, Biotechnol. Prog. 19 (2003) 544.
[90] M.B. Dainiak, I.U. Allan, I.N. Savina, L. Cornelio, E.S. James, S.L. James, S.V. Mikhalovsky, H. Jungvid, I.Y. Galaev, Biomaterials 31 (2010) 67.